A closer look at long-established drugs: enantioselective protein binding and stability studies

Dissertation zur Erlangung des naturwissenschaftlichen Doktorgrades der

Julius-Maximilians-Universität Würzburg

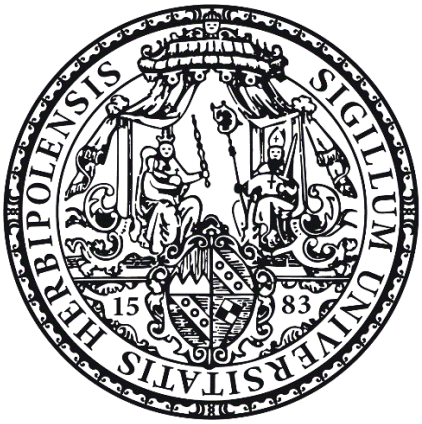

vorgelegt von

Sebastian Schmidt

aus

Lauf a. d. Pegnitz

Würzburg 2023

Eingereicht bei der Fakultät für Chemie und Pharmazie am

_____

Gutachter der schriftlichen Arbeit

1. Gutachter: _____

2. Gutachter: _____

Prüfer des öffentlichen Promotionskolloquiums

1. Prüfer: _____

2. Prüfer: _____

3. Prüfer: _____

Datum des öffentlichen Promotionskolloquiums

_____

Doktorurkunde ausgehändigt am

_____

“Only the disciplined ones are free in life. If you are undisciplined, you are a slave to your moods and your passions.”

Eliud Kipchoge, 1st man to run a marathon under two hours

Für meine Eltern

DANKSAGUNG

Die vorliegende Arbeit wurde auf Anregung und unter Anleitung von

Frau Prof. Dr. Ulrike Holzgrabe

am Lehrstuhl für Pharmazeutische und Medizinische Chemie des Instituts für Pharmazie und Lebensmittelchemie der Julius-Maximilians-Universität Würzburg angefertigt.

Ich möchte mich an dieser Stelle bei ihr für die Möglichkeit der Promotion kurz vor ihrem Ende der Professorenlaufbahn, ihren Anregungen und Ideen sowie für das in mich gesetzte Vertrauen bedanken, welches mir das selbstständige und eigenverantwortliche Anfertigen dieser Arbeit ermöglichte.

Außerdem möchte ich mich bei Ihr bedanken, dass ich während der Promotion die Weiterbildung zum Fachapotheker für Pharmazeutische Analytik und Technologie durchführen konnte und dass ich als Betreuer beim „pharmacon“ - Kongress in Schladming mitreisen durfte, da ich sonst Alice nie kennengelernt hätte.

Vielen Dank an alle Mitglieder des AK Holzgrabe, sowie weiteren AK des Instituts für Pharmazie:

Luki, Laura, Therry, Sylvia, Rasmus, Ruben, Klaus, Adrian, Nic, Niclas, Antonio, Joshi, Flo, Paul, Alex, Nina, Jonas W, Jonas U., Nelson, Markus, Emilie, Curd, Cristian, Bettina, Theresa H., Christine, Jasmin, Maria, Christian, Liling, Carina, Max, Mohammed, Lina, Lena, Jens, Lu, Simon, Thomas, Sophie und Zimbo

Besonders hervorzuheben sind dabei:

Dr. Curd Schollmayer und Markus Zehe für die Hilfe bei den NMR-Messungen und deren Auswertung, Jonas U., der mir die Basics und Tücken der CE-Anlagen beigebracht hat, Laura und Lukas für die Hilfe bei den MS-Messungen in Heroldsberg, Lena und Simon des AK Meinel für die Hilfe bei den ITC und XRPD-Experimenten, Therry für die Unterstützung bei meiner Synthese und Klaus, der mich als Wahlpflichtpraktikant bei sich aufgenommen hat und dort die Basis für die Promotion gelegt hat.

Vielen Dank an Jens und Lu für jegliche Unterstützung während der gesamten Promotion sowie Prof. Dr. Oliver Scherf-Clavel für jegliche Hilfe bei Fragen analytischer Art.

Vielen Dank an Prof. Dr. Fritz Sörgel und Dr. Martina Kinzig für die Unterstützung bei den massenspektrometrischen Messungen in Heroldsberg beim IBMP sowie Dr. Michael Limmert für die Kooperation bei dem „Ketamin-Stabilität“ Projekt.

Herzlichen Dank an Dr. Thorben Link und Dr. Eva Stockwald, die die CE-Anlagen so lange am Leben erhalten haben, bis ich die Promotion beendet hatte.

Vielen Dank an die Assistenten des 6. und 8. Semesters für die äußerst spaßige und kreuzworträtselintensive Zeit während der Praktikumsbetreuung sowie an Eva-Maria, Renate und Silke für die gute Zusammenarbeit mit der Analysenausgabe.

Vielen Dank an Christoph, Matthias und Karl aus der institutseigenen Werkstatt sowie Frau Möhler, Frau Weidinger und Frau Schneider aus dem Sekretariat für Hilfe jeglicher Art.

Vielen Dank bei meinen Wahlpflichtpraktikanten Jonas H., Karlo, Hannah, Dominik, Annika, Lars und Pascal für ihr Engagement während ihres Praktikums.

In besonderem Maße danke ich:

Rasmus für all seine Unterstützung während der Promotion und dass er, ohne es zu beabsichtigen, meine Liebe für den Ausdauersport entfacht hat!

Laura für all ihre Unterstützung, Motivation und Gespräche, sowohl fachlich als auch menschlich, während der Promotion!

Meiner Familie und Freunden, die mir immer Rückhalt geben.

Alice, die ich erst am Ende der Promotion kennengelernt habe, aber sie seitdem mein Fels in der Brandung ist! ⋆

TABLE OF CONTENTS

LIST OF ABBREVIATIONS

AGP	alpha-1-acid glycoprotein
ANOVA	analysis of variance
API	active pharmaceutical ingredient
BGE	background electrolyte
CCC	circumscribed central composite
CE	capillary electrophoresis
CM-β-CD	carboxymethyl-β-cyclodextrin sodium salt
CPMG	Carr-Purcell-Meiboom-Gill
DoE	design of experiments
DUF	discontinuous ultrafiltration
E	ephedrine
EOF	electroosmotic flow
ESI	electrospray ionization
FCCC	face-centered central composite
GUCS	general unknown comparative screening
HDAS-β-CD	heptakis-(2,3-di-O-acetyl-6-sulfo)-β-cyclodextrin
HPLC	high performance liquid chromatography
HRMS	high-resolution mass spectrometry
HSA	human serum albumin
ICH	International Council for Harmonization of Technical Requirements for Pharmaceutical for Human Use
IDA	information dependent acquisition
ITC	isothermal titration calorimetry
K_a respectively pK_a	acidity constant
K_{aff} respectively pK_{aff}	affinity constant
K_D	dissociation constant
LC	liquid chromatography
LLE	liquid-liquid extraction
LOQ	limit of quantification
ME	methylephedrine

MS	mass spectrometry
m/z	mass-to-charge-ratio
NE	norephedrine
NMR	nuclear magnetic resonance
NOE	nuclear overhauser enhancement
NSAID	non-steroidal anti-inflammatory drug
PE	pseudoephedrine
PhEur	European pharmacopoeia
QbD	Quality by design
RDB	ring and double bond equivalents
SPE	solid phase extraction
STD	saturation transfer difference
TM-β-CD	heptakis-(2,3,6-tri-O-methyl)-β-cyclodextrin
TRIS	tris-(hydroxymethyl)-aminomethane
UF	ultrafiltration
UHPLC	ultra high-performance liquid chromatography
UV/Vis	ultraviolet/visible
XIC	extracted ion chromatogram
XRPD	X-ray powder diffraction

1. INTRODUCTION

The application of a drug lead to many processes and interactions with the organism. These interactions are summarized under the term pharmacokinetics. They are based on the ADME principle: **A**bsorption, **D**istribution, **M**etabolism, and **E**xcretion [1]. The model can be extended to include liberation from the dosage form – although this is a pharmaceutics aspect [2]. All these processes have an influence on the success of drug therapy. For example, toxic or longer-acting metabolites may be formed, which may pose a risk to the patient [3]. One important pharmacokinetic parameter is indirectly covered by this model via distribution – plasma protein binding [4, 5], which will be discussed in the next paragraph.

The physiological purpose of plasma protein binding is the transport of exogenous and endogenous substances in the organism [6]. Lipophilic substances, which would be too poorly soluble in water for distribution in the blood, can be transported by binding to the plasma proteins to their desired target. Depending on the properties of a drug, it may bind or not to plasma proteins. Knowledge of the binding properties of a drug is of immense importance for successful drug therapy, as it has a decisive influence on the dose that can exert its effect at the site of action, because only the free unbound fraction of the drug can unfold its pharmacological effect [7]. However, not every protein that occurs in plasma also binds drugs. An overview of selected plasma proteins according to their electrophoretic fraction are detailed in Table 1 [8, 9]. The two proteins that bind the most drugs are albumin and alpha-1-acid glycoprotein (AGP) [10]. If several drugs bind to the same protein, it can be displaced from the binding pocket and consequently change drug concentration in plasma [11]. On the one hand, changing plasma levels can cause overdoses with undesirable effects, and on the other hand, underdoses and thus no therapeutic effect is achieved [12, 13]. This is critical with drugs with a narrow therapeutic range and a high protein binding.

Table 1: Overview of selected plasma proteins according to their electrophoretic fraction

fraction	protein	molecular weight [kDa]	average concentration in plasma		function
			[g/l]	[µmol/l]	
albumin (60%)	transthyretin	61	0.3	5.0	binding of thyroxine
	albumin	66	40.0	580.0	colloid osmotic pressure, vehicle
α_1-globulins (4%)	**α_1-acid glycoprotein**	44	0.8	18.0	acute phase protein
	α_1-lipoprotein (high density lipoproteins)	200	3.5	17	lipide transport (mainly phospholipids)
	α_1-antitrypsin	52	1.5	28.8	protease inhibitor
α_2-globulins (8%)	caeruloplasmin	160	0.3	2.0	oxidase activity, binding of cooper
	α_2-macroglobulin	820	2.5	3.0	plasmin/protease inhibition
	α_2-haptoglobin	85	3.0	12.0	binding of haemoglobin
	plasminogen	92	0.2	2.2	blood coagulation
	α_2-antithrombin	58	0.1	1.1	blood coagulation, protease inhibition
β-globulins (12%)	transferrin	75-80	3.0	33.0	transport of iron
	β-lipoprotein (low density lipoproteins)	3-20	5.5	1.0	lipide transport (cholesterine)
	fibrinogen	340	3.0	9.0	blood coagulation
γ-globulins (16%)	IgG	156	12.0	77.0	immune defence
	IgA	15	2.4	16.0	immune defence
	IgM	960	1.2	1.0	agglutinins

1.1. Albumin

At about 60%, albumin accounts for the largest proportion of plasma proteins and is synthesized in the liver. It consists of 585 amino acids, is not glycosylated, and has a molecular weight of 66 kDa. The most important functions of albumin are the carrier function of endogenous and exogenous substances, as well as the regulation of the colloid osmotic pressure of the blood. Due to its various functions, albumin continues to be used as a biomarker to monitor the function of the liver and kidneys [14]. Cirrhosis of the liver, for example, is characterized by hypoalbuminemia. Due to the lack of albumin, the body is no longer able to maintain the colloid osmotic pressure of the blood. As a result, oedema is formed [15]. The reduced plasma concentration can also lead to a change in the protein binding of drugs [16]. To compensate for the albumin deficiency, an albumin solution is administered intravenously.

The protein has many ionizable amino acid residues and has a negative net charge at the physiological pH value. This results in good solubility in water. In addition, it has 35 cysteine residues that form 17 disulfide bridges to stabilize the conformation of the protein. Cys34 has a free thiol group that acts as radical scavenger and, thus, albumin has additionally an antioxidant function. The secondary structure consists mainly of α-helices, which arrange the protein into three homologous domains (I-III), each with two subdomains (A, B) [14]. Drugs are mainly bound to two binding sites. One of them is in the subdomain IIA (Sudlow`s site I), the other in subdomain IIIA (Sudlow`s site II) [17, 18]. They differ fundamentally in their structure. Sudlow`s site I is more suitable for larger ligands. It is characterized by two apolar regions and has a polar region in the center. Typical ligands are drugs with large heterocycles with a centrally located negative charge. Sudlow`s site II, on the other hand, is largely apolar and has a polar group directly at the entrance to the binding site. Due to the clear “separation” into two different areas, ligands that have a clearly defined aromatic lipophilic part, separated of a negative charge, bind mainly to this binding site [14]. Albumin preferentially binds acidic and neutral drugs, but basic ones if uncharged can also be bound. Sudlow`s site II is smaller than Sudlow`s site I, which is why smaller ligands are better bound to this binding site. Since albumin is the most important transporter protein in plasma, it binds fatty acids, metals, bilirubin, and other endogenous and exogenous substances at many other binding sites outside of Sudlow`s site I and II [19].

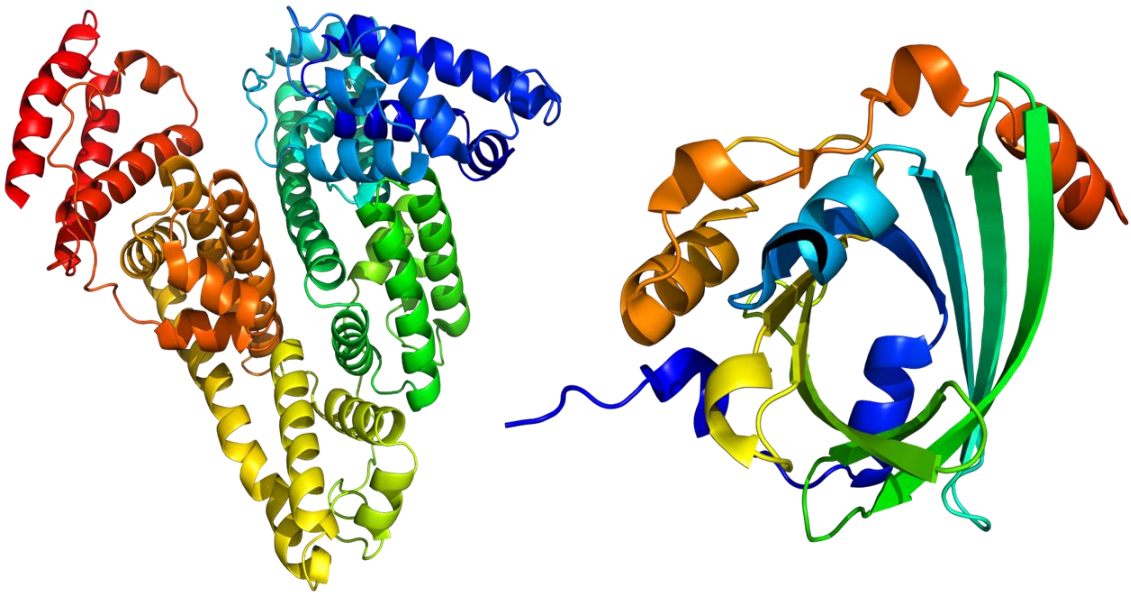

Fig. 1: left: human albumin (PDB: 1AO6); right: human AGP (PDB: 3KQ0)

1.2. Alpha-1-acid glycoprotein

Besides albumin, AGP is the second most important plasma protein that binds mainly basic drugs. It is also synthesized in the liver and, in contrast to albumin, is very strongly glycosylated with a carbohydrate content of 45% [20]. At 42 kDa, it is significantly smaller than albumin and accounts for about 3% of the total amount of plasma proteins. AGP, also known as orosomucoid, is an acute phase protein and is ideally suited as a biomarker for immunologically induced inflammatory processes such as Crohn´s disease. As an acute phase protein, it has mainly immunomodulatory and anti-inflammatory properties [21]. The binding behaviour is not yet fully understood. On the one hand, it is described in the literature as a dominant, high-affinity main binding site with several low-affinity binding sites. On the other hand, two main binding sites with the same affinity for acidic and basic drugs are postulated [22]. In 2008, Schönfeld et al. characterized the crystal structure of non-glycosylated AGP and described a major binding site [23]. This binding site is split/funnel shaped with three areas inside: I, II, and III. I is centrally located and completely nonpolar and thus offers hydrophobic substances a way to bind. II and III are respectively on the sides of I and are negatively charged. II is particularly deep in the binding pocket and can interact well with charged basic drugs [23]

1.3. Methods for the determination of the extent of plasma protein binding, structural moieties involved, and binding properties

The extent of plasma protein binding and binding properties can be characterized using versatile methods. Not all methods are presented, the focus is on the most used ones.

1.3.1. Separating methods

Separating methods are the gold standard for the determination of the extent of protein binding. They are all based on the same principle: the drug is incubated with the protein until an equilibrium is reached. Then the formed drug-protein complex is separated, and the free unbound drug is quantified with a suitable analytical method. By knowing the initial concentration of the drug, it is possible to calculate back to the percentage binding [24-26]. In ultrafiltration, the protein and the drug-protein complex are retained by a semipermeable membrane, whose cut-off has to be chosen regarding that only the free unbound drug passes through, which can be quantified thereafter [27-36]. Ultracentrifugation does not require a membrane. The protein and the resulting drug-protein complex have a much higher molecular weight than the free unbound drug. Due to the centrifugal force applied by centrifugation, the heavier protein as well as the complex is deposited at the bottom of the centrifuge tube. The free unbound drug is in the supernatant and can be further analyzed [37-40]. A combination of these two methods is also possible. In a unified ultracentrifugation cell, the incubation solution is filtered through a semipermeable membrane while its centrifugated [29, 41-46]. A scheme of this experimental setup is presented in Fig. 2.

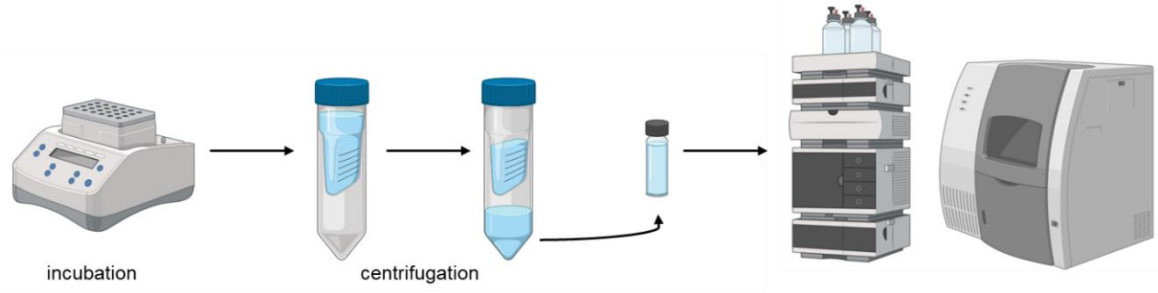

Fig. 2 Scheme of the combined ultrafiltration and centrifugation

The third option is equilibrium dialysis. Protein and drugs are incubated in a cell separated by a semipermeable membrane from a second cell containing only medium solution. The unbound drug diffuses through the membrane, so that an equilibrium between incubation cell and the medium cell is established. The free unbound drug in both cells is determined [47-57].

1.3.2. Spectroscopic methods

1.3.2.1. Nuclear magnetic resonance spectroscopy

Nuclear magnetic resonance (NMR)-spectroscopy offers great possibilities in the screening of possible ligands to their respective targets. These methods can also be used to determine the binding properties of drugs to proteins. A major advantage is that structural moieties involved in binding can be identified. This can be achieved via saturation transfer difference-NMR (STD-NMR), waterLOGSY, and Carr-Purcell-Meiboom-Gill (CPMG)-NMR experiments as well as the determination of changes in the chemical shift upon binding [58, 59].

STD-NMR experiments are based on the nuclear overhauser enhancement (NOE) effect. The protons of a protein can be specifically saturated using a radiofrequency pulse. If there is an interaction between a protein and a bound ligand, the saturation is transferred from the protein to the ligand. As a result, the signals of the ligand are attenuated. For each protein, the appropriate saturation pulse must be found. It is important that the ligand itself is not saturated by the pulse. This can be ensured by prior experiments, where the ligand is exposed to the saturation pulse without any protein. In Fig. 3a, the principle of an STD-NMR measurement is detailed. Two spectra are recorded: 1) spectrum without saturation pulse (off-resonance spectrum) 2) spectrum with saturation pulse (on-resonance spectrum). The difference spectrum is obtained by subtracting both spectra from each other. Signals in the difference spectrum are protons which are involved in binding to the protein [60-66].

WaterLOGSY is also based on the NOE. The difference to STD-NMR is that not the protein is saturated, but the bulk water. This can be done in several ways (cf. Fig. 3b): 1. Saturation is transferred directly to the bound ligand by water molecules located in the binding site II. Water molecules on the protein surface become saturated and saturation is transferred to the ligand via the protein 3. Exchange between water and protons attached to heteroatoms such as in hydroxyl or amine groups. The problem here is that the water can also transfer the saturation directly to the ligand although it is not bound to a protein. Therefore, it is essential to perform reference measurements of the ligand in the absence of protein.

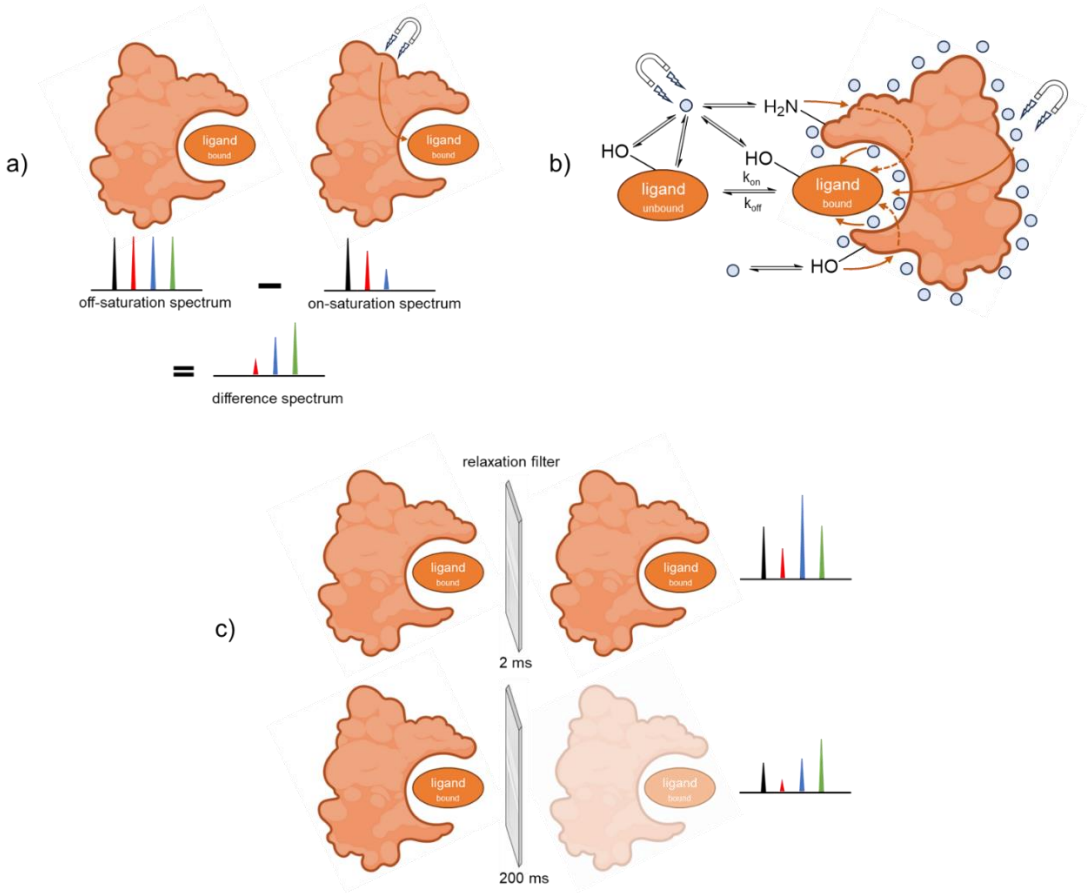

Fig. 3 Schemes of a) STD-NMR spectroscopy b) waterLOGSY-NMR spectroscopy c) CPMG-NMR spectroscopy

By transferring saturation, the signals of the bound ligand are attenuated to such an extent that they can turn negative [64-70].

CPMG-NMR uses a different principle for the characterization of binding properties. Large molecules relax faster than small molecules. By using suitable T2 relaxation time filters, the signal of the protein can be reduced until it is no longer visible in the spectrum. Signals from the usually much smaller ligand remain unaffected. Nevertheless, a reference sample of the ligand in absence of the protein must be performed to ensure that the ligand is not also filtered out. If a ligand binds to a protein, the signals of the ligand involved in binding are also attenuated when the protein is expose to a relaxation filter [64, 71-73].

Ligand-protein interactions can also be studied by differences in the chemical shift or width of signals upon binding. The signal in NMR spectroscopy is depending on the magnetic field experienced by the respective nucleus. Inductive and mesomere effects within a structure lead to locally different electron densities, which shield the nuclei from the magnetic field in different ways und thus, changes of the chemical shifts are seen. Binding to a protein that is very bulky compared to the ligand results in a large change in the magnetic field experienced by the ligand. If the exchange between bound and free ligand

is very fast, only one signal per nucleus is visible in the spectrum. However, if the exchange is very slow, the signal of both the free ligand and bound ligand are visible. As a result, the signals of bound nuclei shift due to the change of the electric field compared to the pure ligand. In addition, there is a broadening of the signal. Due to fast exchange between ligand and protein, the ligand maintains the relaxation properties of the protein. The measured signal is the average between the free and unbound form and therefore broadened [64]. These effects can be exploited by measuring different ligand-protein ratios. The data obtained can be fitted by various plots to determine the dissociation constant K_D [59, 66, 74].

1.3.2.2. Fluorescence and UV/Vis spectroscopy

Fluorescence spectroscopy is a widely used method for investigating the protein binding of drug to albumin. Human albumin has exactly one fluorescent tryptophan residue in domain IIA in the region of the Sudlow`s site I. This can be selectively excited at a wavelength of 295-300 nm. The principle of the measurement is based on the fluorescence quenching. In case of binding by a ligand, the tryptophan residue is shielded and the intensity of the fluorescence decreases. The ligand does not automatically have to be a Sudlow`s site I ligand. Bonds at other binding sites of the protein can also cause a fluorescence quenching effect by means of conformational changes. An increase in the concentration of the ligand usually enhances the fluorescence quenching effect. By measuring different drug-protein ratios, the dissociation constant can be determined using the Stern-Volmer equation [75-82].

UV/Vis (ultraviolet/visible) spectroscopy plays a less important role in the methodology for determining protein binding. It is mainly used to confirm observations with an orthogonal method. Different ligand-protein ratios are compared with a sample of pure protein. There is a shift in the absorption maximum and a change in the signal intensity when the ligand binds to the protein. This can be explained by the formation of the drug-protein complex. A prerequisite for a successful measurement is that the ligand has its absorption maximum in the area where the protein itself does not absorb [78, 82, 83].

1.3.3. Thermal methods

Among the thermal methods, isothermal titration calorimetry (ITC) stands out above all. Due to the use of small sample volumes, it proves to be extremely resource-efficient, which is a significant factor when investigating expensive proteins. Energy is converted when the ligand-protein complex is formed. This can be both an exothermic and an endothermic process, leading to an increase in temperature or decrease, respectively. To a protein solution, ligand solution is titrated at certain time intervals. It is also possible the other way

round, but most of the time the amount of protein available is the limiting factor. The temperature in the sample cell is compared to the temperature in a reference cell that contains medium only. Based on the data curves obtained, statements about the affinity of the ligand to the protein can be made. A major advantage of ITC is that, in addition to binding properties such as K_D, thermodynamic properties, and stoichiometry can be determined. However, since the temperature differences are very small, the extremely sensitive method is unfortunately very susceptible to disturbances and no information is gained about the structural moiety involved in binding [84-88].

1.3.4. Affinity chromatography and capillary electrophoresis

Another method to determine the affinity of a ligand to a protein is affinity chromatography and capillary electrophoresis. Using chromatography, the protein is immobilized at a stationary phase. This can be an analytical column in high performance liquid chromatography (HPLC) or a modified silica gel in column chromatography. The stronger the affinity of an analyte to the stationary phase, the longer it is retained, and its net retention time is extended [89-96]. In the case of affinity capillary electrophoresis, the protein is not immobilized at the capillary surface, but added to the background electrolyte as an additive. The analyte migrates faster or slower depending on the charge of the protein and the polarity of the electrodes at a high affinity. This is reflected in the net migration time. By reference measurements of substances with known plasma protein binding, it is possible to determine the extent of plasma protein binding [97-102].

1.4. Enantioselective plasma protein binding

Enantiomers behave like image and mirror image of each other. They have the same chemical and physical properties unless they are in a chiral environment. Receptors can be such a chiral environment. Due to different affinities to the receptors, enantiomers can develop different pharmacological effects. The saddest example of such a difference in effect is the thalidomide scandal of the late 1950s. Thalidomide was marketed in racemic form for sleep disorders in pregnancy [103]. In drug therapy, the more active enantiomer with the desired pharmacological effect is referred to as the eutomer, while the less-active enantiomer is called the distomer [104]. While the *R*-enantiomer as eutomer produced this advertised effect, the *S*-enantiomer showed a teratogenic effect that caused malformations in the unborn children [105].

Enantiomers can bind not only stereoselectively to receptors, but also to plasma proteins. For example, the *S*-enantiomer of propranolol binds with a higher affinity to AGP, whereas the *R*-enantiomer prefers to be bound by albumin [106]. The consequences of stereoselective protein binding primarily affect pharmacokinetic parameters such as

clearance. Particularly in the case of drugs that are very strongly bound, fluctuations in the unbound fraction are of greater influence. E.g., in the case of the non-steroidal anti-inflammatory drug (NSAID) ketorolac, it was observed that the plasma clearance of *S*-ketorolac increased twofold due to stereoselective binding to albumin [107]. Factors for enantioselective binding include small openings at binding sites that form a steric barrier. Thus, the stereoselective potential for the Sudlow`s site II binding site of albumin is increased, since the entrance to the binding site is significantly smaller than that of Sudlow`s site I.

1.5. Capillary electrophoresis

1.5.1. Classic capillary electrophoresis

In contrast to liquid chromatography (LC), separation in capillary electrophoresis (CE) is not based on the different distribution between mobile and stationary phases, but on the movement in an electric field. The typical setup of a capillary electrophoresis is displayed in Fig. 4.

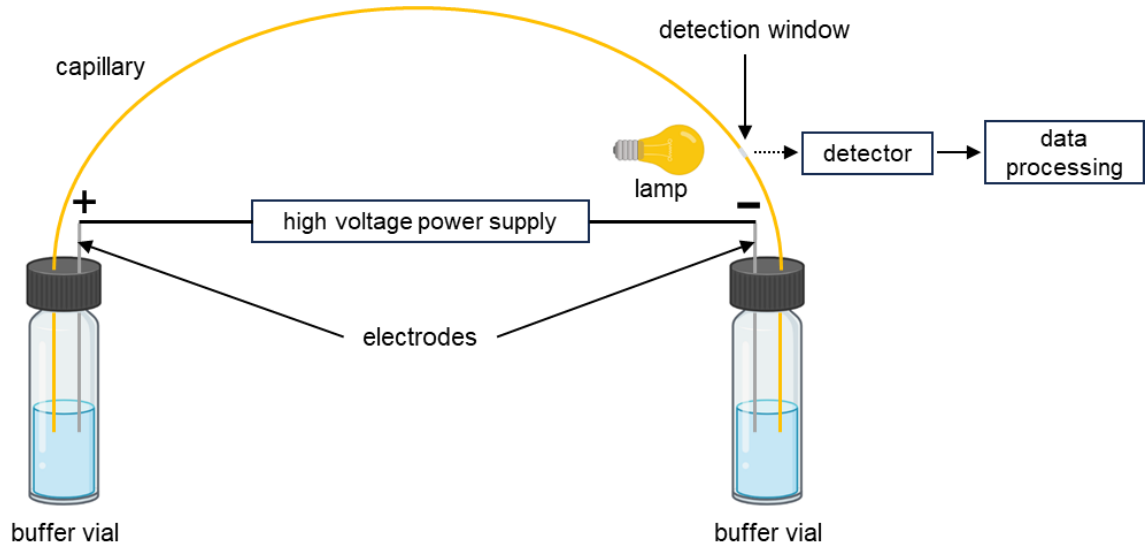

Fig. 4 Instrumental structure of a capillary electrophoresis

In the classic CE, the capillary used is made mainly of fused silica. A polyimide layer covers the silica inner layer to make it flexible and less susceptible to mechanical stress. Depending on the type of detection used, the polyimide layer may need to be removed for a detection window, as is the case when using a UV/Vis detector. The capillary protrudes into two vials filled with the separation buffer or background electrolyte (BGE). In each of these vials there is a platinum electrode connected to a high voltage power supply. If a high voltage is applied, the outlet electrode becomes the cathode (plus pole) and the inlet electrode the anode (minus pole) under normal polarity. Depending on the charge, size and effective shape of the analyte, the type of separation buffer used and the applied field

strength, the analytes migrate at different rates. The overall migration of substances is superimposed by the electroosmotic flow (EOF). It is so powerful that, in addition to cations, neutral substances and anions, which would otherwise not move to the cathode, migrate, and can be detected on the cathodic side. At a pH of 2-2.5 or higher, the silanol groups of the silica layer on the inside of the capillary start to deprotonate. This negative surface attracts cations from the BGE and two positively charged layers are formed – the rigid inner layer also called the Helmholtz layer, and a more mobile outer layer called Debuye Hückel layer. The cations of the mobile layer migrate to the cathode and entrain the entire BGE via their solvate shells, and thus also neutral substances and anions. The EOF does not contribute to the separation of analytes, as it is the same for all. However, not only buffer cations attach to the negative surface of the capillary, but also protonated bases. This can lead to peak fronting and tailing, which makes the analysis of basic components challenging [108-110].

1.5.2. Chiral capillary electrophoresis

The analysis of enantiomers is challenging due to the same chemical and physical properties in a non-chiral environment. However, there are ways to create a chiral environment chromatographically and electrophoretically. In high-performance liquid chromatography, this is done by immobilizing a chiral selector such as AGP, albumin or cellulose on the column [96]. Unfortunately, this modification makes the columns very expensive. Capillary electrophoresis offers a cost-effective way of separating enantiomers by adding a chiral selector to the separation buffer, thus saving resources. Enantiomers can interact with the chiral selectors to form different diastereomeric complexes that differ in their chemical and physical properties and the analytes can therefore be separated. The most used are cyclodextrins, but crown ethers and proteins, as in affinity capillary electrophoresis, are also applied [92, 111]. Cyclodextrins are annular glucose oligomers that natively consist of 6 (α), 7 (β) and 8 (γ) units. Due to the arrangement, they form a toroid structure with a hydrophobic cavity and a polar exterior. Enantiomers can be deposited differently in the cavity and thus different diastereomeric complexes can be formed. The hydroxyl groups of the individual glucose monomers are ideally suited for chemical modification. They can be mixed with neutral alkyl chains, but also amines or acids. For a successful separation, it is crucial that either the analyte or the cyclodextrin must be charged. Fig. 5 details different applications of modified cyclodextrins under normal polarity. An advantage is the wide range of possible combinations between the type of cyclodextrin and the degree of protonation of the analyte that are available [112-115].

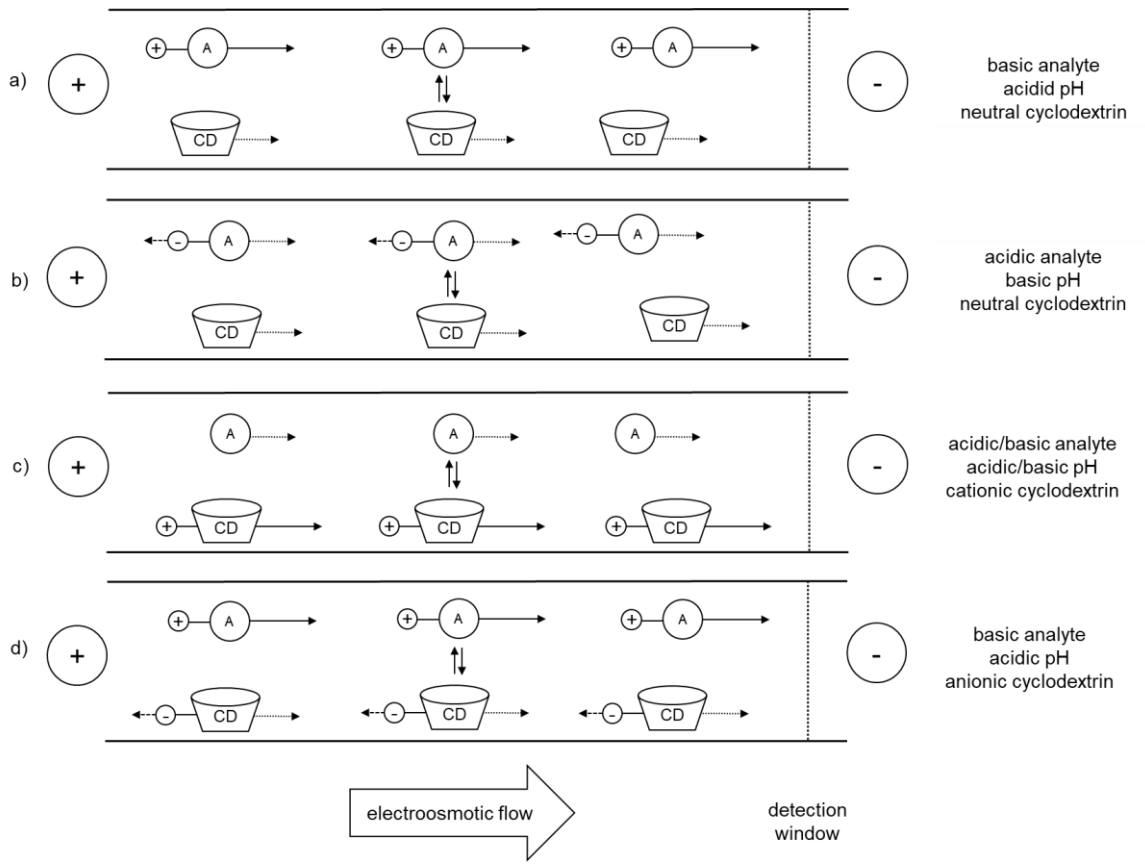

Fig. 5 Different applications of modified cyclodextrins under normal polarity: a) basic analyte, acidic pH, neutral cyclodextrin; b) acidic analyte, basic pH, neutral cyclodextrin; c) acidic/basic analyte, acidic/basic pH, cationic cyclodextrin; d) basic analyte, acidic pH, anionic cyclodextrin; dotted arrow: migration with the EOF; dashed arrow: migration against the EOF; solid arrow: migration through attraction of the cathode

1.6. Stability of active pharmaceutical ingredients and drug products

Drug therapy has undergone a tremendous development. There are many different types of drug dosage forms available for a wide variety of applications [116]. From the classic tablet to technologically sophisticated vehicles such as liposomes, therapy can be very individualized. In addition, to the “common” dosage forms presented in Fig. 6, there are further innovations [117].

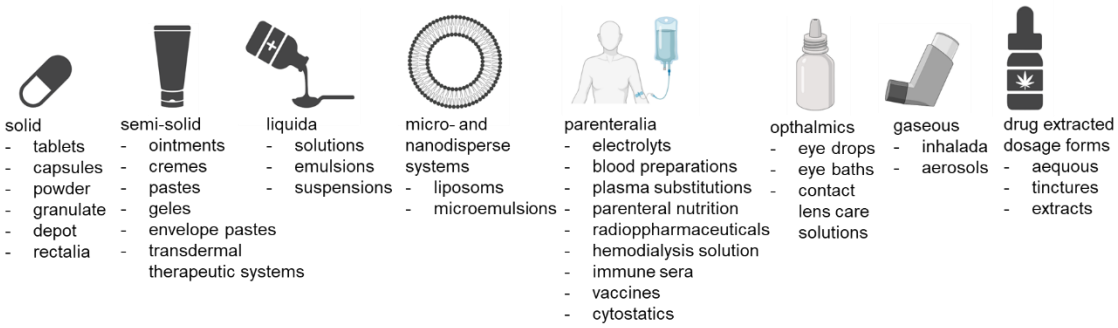

Fig. 6 Common dosage forms of drug products

In the development of drug substances and dosage forms, the stability of the active pharmaceutical ingredient (API) and the drug product requires special attention. A distinction must be made between chemical, physical, microbial, toxicological, and therapeutic stability [118, 119]. However, a boundary cannot often be drawn, and the individual areas overlap. Table 2 shows the classification, sources, effects, possible solutions and examples. However, the table only refers to individual substances. If several substances interact with each other, incompatibilities may occur in a drug product [120]. These can be visually recognizable or larvalized and have a major impact on the quality of the drug product. The market authorization holder must ensure that a drug product and the API are stable and compatible over specified periods of time and storage conditions. For this purpose, stability studies are carried out that extend beyond the period of market launch. There are discussed in more detail in chapter “Stability assessment: ketamine”. In the best case, these studies are carried out within the framework of quality by design. This is an approach to drug development and manufacturing that uses statistical and risk-based methods. Possible impurities, stability problems, etc. are already considered during development to bring the safest product possible onto the market and to safeguard it using statistical methods [121-123].

Table 2: Overview over different types of stability their origin, effects, possible solutions and examples

type of stability	sources	effect	solution	examples
chemical	solvolysis (mainly hydrolysis), oxidation, photolysis, dehydration, racemization epimerization	degradation of API	suitable pH. antioxidants, oxygen exclusion, dry storage protected from light	hydrolysis of acetylsalicylic acid [124], photodegradation of nifedipine [125] racemization of chlorthalidone enantiomers [126] epimerization of tetracycline [127]
physical	crystallization (crystallization of amorphous drugs, formation, and growth of crystals), moisture adsorption, vaporizing,	solubility changes, reactivity, hydrolysis, degradation of API, precipitates, dissolution changes	control of storage temperature, and humidity, adding non-volatile fixing agents	loss of water in cremes result in dryness, and to separation of phases in emulsions, loss of stable crystal form of chloramphenicol [128], precipitation of protein formulations [129]
microbial	air, water as sources for microbial contamination	loss of sterility	aseptic production (e.g., sterile filtration), preservatives	no sterile filtration for ophthalmic preparations [130]
toxicological	degradation to toxic products	health risk for the patient	toxicological studies of degradation products, setting limits	formation of a toxic catabolite of zidovudine [131]
therapeutical	loss of the effective form of the API due to degradation	therapeutic dosage is not reached	extensive studies of physical and chemical properties of the drug	protein aggregation during storage [132]

1.7. References

Figures 2,3,4,6 were created with BioRender.com.

[1] Meyer, M.R. and H.H. Maurer, Toxicokinetics and Toxicogenetics, in Handbook of Forensic Medicine. 2014, Wiley, NJ. p. 889-899.

[2] Salt, A.N. and S.K. Plontke, Principles of local drug delivery to the inner ear. Audiol. Neurotol., 2009. 14(6): p. 350-360.

[3] Chouinard, G., K. Lefko-Singh, and E. Teboul, Metabolism of anxiolytics and hypnotics: benzodiazepines, buspirone, zoplicone, and zolpidem. Cell. Mol. Neurobiol., 1999. 19: p. 533-552.

[4] Schmidt, S., D. Gonzalez, and H. Derendorf, Significance of protein binding in pharmacokinetics and pharmacodynamics. J. Pharm. Sci., 2010. 99(3): p. 1107-1122.

[5] Olson, R.E. and D.D. Christ, Plasma protein binding of drugs, in Annual reports in medicinal chemistry. 1996, Elsevier. p. 327-336.

[6] Müller, W.E. and U. Wollert, Human serum albumin as a ‘silent receptor’for drugs and endogenous substances. J. Pharmacol., 1979. 19(2): p. 59-67.

[7] Scheife, R.T., Protein binding: what does it mean? Ann. Pharmacother., 1989. 23(7-8): p. S27-S31.

[8] Brandes, R., F. Lang, and R.F. Schmidt, Physiologie des Menschen: mit Pathophysiologie. 32 ed. 2019: Springer Berlin, Heidelberg

[9] E., M.N., WHO Recommendations for the production, control, and regulation of human plasma for fractionation. 2011.

[10] Howard, M.L., J.J. Hill, G.R. Galluppi, and M.A. McLean, Plasma protein binding in drug discovery and development. Comb. Chem. High Throughput Screen., 2010. 13(2): p. 170-187.

[11] McElnay, J. and P. D’arcy, Protein binding displacement interactions and their clinical importance. Drugs, 1983. 25: p. 495-513.

[12] DeVane, C.L., Clinical significance of drug binding, protein binding, and binding displacement drug interactions. Psychophrmacol. Bull., 2002. 36(3): p. 5-21.

[13] Sun, J. and M.W. Chang, Initialization of warfarin dosages using computer modeling. Arch. Phys. Med. Rehabil., 1995. 76(5): p. 453-456.

[14] Fanali, G., A. Di Masi, V. Trezza, M. Marino, M. Fasano, and P. Ascenzi, Human serum albumin: from bench to bedside. Mol. Asp. Med., 2012. 33(3): p. 209-290.

[15] Spinella, R., R. Sawhney, and R. Jalan, Albumin in chronic liver disease: structure, functions and therapeutic implications. Hepatol. Int., 2016. 10: p. 124-132.

[16] Doweiko, J.P. and D.J. Nompleggi, The role of albumin in human physiology and pathophysiology, Part III: Albumin and disease states. J. Parenter. Enteral Nutr., 1991. 15(4): p. 476-483.

[17] Sudlow, G., D. Birkett, and D. Wade, The characterization of two specific drug binding sites on human serum albumin. Mol. Pharmacol., 1975. 11(6): p. 824-832.

[18] Sudlow, G., D. Birkett, and D. Wade, Further characterization of specific drug binding sites on human serum albumin. Mol. Pharmacol., 1976. 12(6): p. 1052-1061.

[19] Yamasaki, K., V.T.G. Chuang, T. Maruyama, and M. Otagiri, Albumin–drug interaction and its clinical implication. Biochim. Biophys. Acta - Gen., 2013. 1830(12): p. 5435-5443.

[20] Fournier, T., N. Medjoubi-N, and D. Porquet, Alpha-1-acid glycoprotein. Biochim. Biophys. Acta., 2000. 1482(1-2): p. 157-171.

[21] Hochepied, T., F.G. Berger, H. Baumann, and C. Libert, α1-Acid glycoprotein: an acute phase protein with inflammatory and immunomodulating properties. Cytokine. Growth. Factor. Rev., 2003. 14(1): p. 25-34.

[22] Berezhkovskiy, L.M., On the calculation of the concentration dependence of drug binding to plasma proteins with multiple binding sites of different affinities: determination of the possible variation of the unbound drug fraction and calculation of the number of binding sites of the protein. J. Pharm. Sci., 2007. 96(2): p. 249-257.

[23] Schönfeld, D.L., R.B. Ravelli, U. Mueller, and A. Skerra, The 1.8-Å crystal structure of α1-acid glycoprotein (Orosomucoid) solved by UV RIP reveals the broad drug-binding activity of this human plasma lipocalin. J. Mol. Biol., 2008. 384(2): p. 393-405.

[24] Kurz, H., H. Trunk, and B. Weitz, Evaluation of methods to determine protein-binding of drugs. Equilibrium dialysis, ultrafiltration, ultracentrifugation, gel filtration. Arzneimittel-forschung, 1977. 27(7): p. 1373-1380.

[25] Barre, J., J. Chamouard, G. Houin, and J. Tillement, Equilibrium dialysis, ultrafiltration, and ultracentrifugation compared for determining the plasma-protein-binding characteristics of valproic acid. Clin. Chem., 1985. 31(1): p. 60-64.

[26] Sebille, B., Methods of drug protein binding determinations. Fundam. Clin. Pharmacol., 1990. 4(S2): p. 151s-161s.

[27] Whitlam, J.B. and K.F. Brown, Ultrafiltration in serum protein binding determinations. J. Pharm. Sci., 1981. 70(2): p. 146-150.

[28] Chen, P., I. Mills, and F. Bartter, Ultrafiltration studies of steroid-protein binding. J. Endocrinol., 1961. 23(2): p. 129-137.

[29] Leow, K.P., A.W. Wright, T. Cramond, and M.T. Smith, Determination of the serum protein binding of oxycodone and morphine using ultrafiltration. Ther. Drug. Monit., 1993. 15(5): p. 440-447.

[30] Dorn, C., A. Kratzer, U. Liebchen, M. Schleibinger, A. Murschhauser, J. Schlossmann, F. Kees, P. Simon, and M.G. Kees, Impact of experimental variables on the protein binding of tigecycline in human plasma as determined by ultrafiltration. J. Pharm. Sci., 2018. 107(2): p. 739-744.

[31] Tang, Y., H. Zhu, Y. Zhang, and C. Huang, Determination of human plasma protein binding of baicalin by ultrafiltration and high-performance liquid chromatography. Biomed. Chromatogr., 2006. 20(10): p. 1116-1119.

[32] Zhirkov, Y.A. and V. Piotrovskii, On the usefulness of ultrafiltration in drug-protein binding studies. J. Pharm. Pharmacol., 1984. 36(12): p. 844-845.

[33] Bennett, J.V. and W.M. Kirby, A rapid, modified ultrafiltration method for determining serum protein binding and its application to new penicillins. J. Lab. Clin. Med., 1965. 66(5): p. 721-732.

[34] Ackerman, B.H., E.H. Taylor, K.M. Olsen, W. Abdel-Malak, and A.A. Pappas, Vancomycin serum protein binding determination by ultrafiltration. Drug Intell. Clin. Pharm., 1988. 22(4): p. 300-303.

[35] Wijkström, A. and D. Westerlund, Plasma protein binding of sulphadiazine, sulphamethoxazole and trimethoprim determined by ultrafiltration. J Pharm Biomed Anal, 1983. 1(3): p. 293-299.

[36] Carr, R.A., F.M. Pasutto, R.Z. Lewanczuk, and R.T. Foster, Protein binding of sotalol enantiomers in young and elderly human and rat serum using ultrafiltration. Biopharm. Drug. Dispos., 1995. 16(8): p. 705-712.

[37] Matsushuta, Y. and M. Ikuo, Measurement of protein binding by ultracentrifugation. Chem. Pharm. Bull., 1985. 33(7): p. 2948-2955.

[38] Srikanth, C.H., T. Chaira, S. Sampathi, V. Sreekumar, and R.B. Bambal, Correlation of in vitro and in vivo plasma protein binding using ultracentrifugation and UPLC-tandem mass spectrometry. Anlst., 2013. 138(20): p. 6106-6116.

[39] Nakai, D., K. Kumamoto, C. Sakikawa, T. Kosaka, and T. Tokui, Evaluation of the protein binding ratio of drugs by a micro-scale ultracentrifugation method. J. Pharm. Sci., 2004. 93(4): p. 847-854.

[40] Smart, G.A. and S.S. Brown, Preparative ultracentrifugation of small samples of plasma and the protein binding of methaqualone. Anal. Biochem., 1970. 35(2): p. 518-523.

[41] Volpp, M. and U. Holzgrabe, Determination of plasma protein binding for sympathomimetic drugs by means of ultrafiltration. Eur. J. Phar. Sci., 2019. 127: p. 175-184.

[42] Wang, X., C. Li, C. Du, J.-l. Gao, K.-X. Zhao, R. Shi, and Y. Jiang, Plasma protein binding monitoring of therapeutic drugs in patients using single set of hollow fiber centrifugal ultrafiltration. Bioanalysis, 2017. 9(7): p. 579-592.

[43] Mullokandov, E., J. Ahn, A. Szalkiewicz, and M. Babayeva, Protein binding drug-drug interaction between warfarin and tizoxanide in human plasma. Austin J. Pharmacol. Ther., 2014: p. 1-3.

[44] Miller, P., J. Wheeldon, and J. Brocklebank, The separation of unbound prednisolone in plasma by centrifugal ultrafiltration. J. Pharm. Pharmacol., 1987. 39(11): p. 939-941.

[45] Gu, X., S. Yu, Q. Peng, M. Ma, Y. Hu, and B. Zhou, Determination of unbound valproic acid in plasma using centrifugal ultrafiltration and gas chromatography: Application in TDM. Anal. Biochem., 2020. 588: p. 113475.

[46] Qian, Z.M., S.J. Qin, L. Yi, H.J. Li, P. Li, and X.D. Wen, Binding study of Flos Lonicerae Japonicae with bovine serum albumin using centrifugal ultrafiltration and liquid chromatography. Biomed. Chromatogr., 2008. 22(2): p. 202-206.

[47] Bowers, W.F., S. Fulton, and J. Thompson, Ultrafiltration vs equilibrium dialysis for determination of free fraction. Clin. Pharmacokinet., 1984. 9(Suppl 1): p. 49-60.

[48] David, B.M., R. Tjokrosetio, and K.F. Ilett, Plasma protein binding of disopyramide by equilibrium dialysis and ultrafiltration. Ther. Drug. Monit., 1983. 5(1): p. 81-86.

[49] Fabresse, N., I. Uteem, E. Lamy, Z. Massy, I.A. Larabi, and J.-C. Alvarez, Quantification of free and protein bound uremic toxins in human serum by LC-MS/MS: comparison of rapid equilibrium dialysis and ultrafiltration. Clin. Chim. Acta., 2020. 507: p. 228-235.

[50] Oellerich, M. and H. Müller-Vahl, The EMIT® FreeLevel™ Ultrafiltration Technique Compared with Equilibrium Dialysis and Ultracentrifugation to Determine Protein Binding of Phenytoin. Clin. Pharmacokinet., 1984. 9(Suppl 1): p. 61-70.

[51] Surks, M.I., K.H. Hupart, C. Pan, and L.E. Shapiro, Normal free thyroxine in critical nonthyroidal illnesses measured by ultrafiltration of undiluted serum and equilibrium dialysis. J. Clin. Endocrinol. Metab., 1988. 67(5): p. 1031-1039.

[52] Christensen, J.H., F. Andreasen, and E.B. Jensen, The binding of thiopental to serum proteins determined by ultrafiltration and equilibrium dialysis. Acta Pharmcol. Toxicol., 1980. 47(1): p. 24-32.

[53] Brors, O., G. Sager, D. Sandnes, and S. Jacobsen, Binding of theophylline in human serum determined by ultrafiltration and equilibrium dialysis. Br. J. Clin. Pharmacol., 1983. 15(4): p. 393-397.

[54] Eriksson, M.A., J. Gabrielsson, and L.B. Nilsson, Studies of drug binding to plasma proteins using a variant of equilibrium dialysis. J Pharm Biomed Anal, 2005. 38(3): p. 381-389.

[55] Wan, H. and M. Rehngren, High-throughput screening of protein binding by equilibrium dialysis combined with liquid chromatography and mass spectrometry. J. Chromatogr. A, 2006. 1102(1-2): p. 125-134.

[56] Girard, I. and S. Ferry, Protein binding of methohexital. Study of parameters and modulating factors using the equilibrium dialysis technique. J Pharm Biomed Anal, 1996. 14(5): p. 583-591.

[57] Banker, M.J., T.H. Clark, and J.A. Williams, Development and validation of a 96-well equilibrium dialysis apparatus for measuring plasma protein binding. J. Pharm. Sci., 2003. 92(5): p. 967-974.

[58] Fielding, L., NMR methods for the determination of protein–ligand dissociation constants. Prog Nucl Magn Reson Spectrosc., 2007. 51(4): p. 219-242.

[59] Teilum, K., M.B.A. Kunze, S. Erlendsson, and B.B. Kragelund, (S) Pinning down protein interactions by NMR. Protein Sci., 2017. 26(3): p. 436-451.

[60] Krishnan, V., Ligand screening by saturation-transfer difference (STD) NMR spectroscopy. Curr. Anal. Chem., 2005. 1(3): p. 307-320.

[61] Mayer, M. and B. Meyer, Characterization of ligand binding by saturation transfer difference NMR spectroscopy. Angew. Chem. Int. Ed., 1999. 38(12): p. 1784-1788.

[62] Viegas, A., J. Manso, F.L. Nobrega, and E.J. Cabrita, Saturation-transfer difference (STD) NMR: a simple and fast method for ligand screening and characterization of protein binding. J. Chem. Educ., 2011. 88(7): p. 990-994.

[63] Walpole, S., S. Monaco, R. Nepravishta, and J. Angulo, STD NMR as a technique for ligand screening and structural studies, in Methods Enzymol. 2019, Elsevier. p. 423-451.

[64] Claridge, T.D., High-resolution NMR techniques in organic chemistry. Vol. 27. 2016: Elsevier

[65] Zartler, E.R., J. Yan, H. Mo, A.D. Kline, and M.J. Shapiro, 1D NMR methods in ligand-receptor interactions. Curr. Top. Med. Chem., 2003. 3(1): p. 25-37.

[66] Furukawa, A., T. Konuma, S. Yanaka, and K. Sugase, Quantitative analysis of protein–ligand interactions by NMR. Prog Nucl Magn Reson Spectrosc., 2016. 96: p. 47-57.

[67] Dalvit, C., G. Fogliatto, A. Stewart, M. Veronesi, and B. Stockman, WaterLOGSY as a method for primary NMR screening: practical aspects and range of applicability. J. Biomol. NMR, 2001. 21: p. 349-359.

[68] Ermakova, E.A., A.G. Danilova, and B.I. Khairutdinov, Interaction of ceftriaxone and rutin with human serum albumin. WaterLOGSY-NMR and molecular docking study. J. Mol. Struct., 2020. 1203: p. 127444.

[69] Huang, R. and I.K. Leung, Protein–small molecule interactions by WaterLOGSY. Methods Enzymol., 2019. 615: p. 477-500.

[70] Raingeval, C., O. Cala, B. Brion, M. Le Borgne, R.E. Hubbard, and I. Krimm, 1D NMR WaterLOGSY as an efficient method for fragment-based lead discovery. J. Enzyme Inhib. Med. Chem., 2019. 34(1): p. 1218-1225.

[71] Goldflam, M., T. Tarragó, M. Gairí, and E. Giralt, NMR Studies of Protein-Ligand Interactions, in Protein NMR Techniques. 2012, Humana Totowa, NJ. p. 233-259.

[72] Maurer, T., Protein-Ligand Interactions: Methods and Applications, in Methods in Molecular Biology. 2005, Humana New York, NY. p. 197-213.

[73] Ludwig, C. and U.L. Guenther, Ligand based NMR methods for drug discovery. Front Biosci, 2009. 14(4565-74): p. 24.

[74] Shortridge, M.D., D.S. Hage, G.S. Harbison, and R. Powers, Estimating protein−ligand binding affinity using high-throughput screening by NMR. J. Comb. Chem., 2008. 10(6): p. 948-958.

[75] Ali, M.S. and H.A. Al-Lohedan, Interaction of human serum albumin with sulfadiazine. J. Mol. Liq., 2014. 197: p. 124-130.

[76] Ding, F., G. Zhao, S. Chen, F. Liu, Y. Sun, and L. Zhang, Chloramphenicol binding to human serum albumin: determination of binding constants and binding sites by steady-state fluorescence. J. Mol. Struct., 2009. 929(1-3): p. 159-166.

[77] Möller, M. and A. Denicola, Study of protein-ligand binding by fluorescence. Biochem. Mol. Biol. Educ., 2002. 30(5): p. 309-312.

[78] Naik, P.N., S.T. Nandibewoor, and S.A. Chimatadar, Non-covalent binding analysis of sulfamethoxazole to human serum albumin: Fluorescence spectroscopy, UV–vis, FT-IR, voltammetric and molecular modeling. J. Pharm. Anal., 2015. 5(3): p. 143-152.

[79] Steiner, R., J. Roth, and J. Robbins, the binding of thyroxine by serum albumin as measured by fluorescence quenching. J. Biol. Chem., 1966. 241(3): p. 560-567.

[80] Wang, C., Q.-H. Wu, Z. Wang, and J. Zhao, Study of the interaction of carbamazepine with bovine serum albumin by fluorescence quenching method. Anal. Sci., 2006. 22(3): p. 435-438.

[81] Wani, T.A., A.H. Bakheit, M. Abounassif, and S. Zargar, Study of interactions of an anticancer drug neratinib with bovine serum albumin: spectroscopic and molecular docking approach. Front. Chem., 2018. 6: p. 47.

[82] Zhu, S. and Y. Liu, Spectroscopic analyses on interaction of Naphazoline hydrochloride with bovine serum albumin. Spectrochim. Acta A Mol. Biomol. Spectrosc., 2012. 98: p. 142-147.

[83] Hu, Y.-J., Y. Ou-Yang, C.-M. Dai, Y. Liu, and X.-H. Xiao, Binding of berberine to bovine serum albumin: spectroscopic approach. Mol. Biol. Rep., 2010. 37: p. 3827-3832.

[84] Caldwell, G.W. and Z. Yan, Isothermal titration calorimetry characterization of drug-binding energetics to blood proteins, in Optimization in Drug Discovery: in Vitro Methods. 2004, Humana Totowa, NJ. p. 123-149.

[85] Damian, L., Isothermal titration calorimetry for studyin protein-ligand interactions, in Protein-Ligand Interactions: Methods and Applications. 2013, Humana New York, NY. p. X, 530.

[86] Lewis, E.A. and K.P. Murphy, Isothermal titration calorimetry. Protein-Ligand Interactions: Methods and Applications, 2005: p. 1-15.

[87] Srivastava, V.K. and R. Yadav, Isothermal titration calorimetry, in Data processing handbook for complex biological data sources. 2019, Elsevier. p. 125-137.

[88] Velázquez-Campoy, A., H. Ohtaka, A. Nezami, S. Muzammil, and E. Freire, Isothermal titration calorimetry. Curr Protoc Cell Biol, 2004. 23(1): p. 17.8. 1-17.8. 24.

[89] Anguizola, J., C. Bi, M. Koke, A. Jackson, and D.S. Hage, On-column entrapment of alpha 1-acid glycoprotein for studies of drug-protein binding by high-performance affinity chromatography. Anal. Bioanal. Chem., 2016. 408: p. 5745-5756.

[90] Hage, D.S., High-performance affinity chromatography: a powerful tool for studying serum protein binding. J. Chromatogr. B, 2002. 768(1): p. 3-30.

[91] Hage, D.S., A. Jackson, M.R. Sobansky, J.E. Schiel, M.J. Yoo, and K. Joseph, Characterization of drug–protein interactions in blood using high-performance affinity chromatography. J. Sep. Sci., 2009. 32(5-6): p. 835-853.

[92] Hage, D.S., T.A. Noctor, and I.W. Wainer, Characterization of the protein binding of chiral drugs by high-performance affinity chromatography interactions of R-and S-ibuprofen with human serum albumin. J. Chromatogr. A, 1995. 693(1): p. 23-32.

[93] Kurlbaum, M. and P. Högger, Plasma protein binding of polyphenols from maritime pine bark extract (USP). J Pharm Biomed Anal, 2011. 54(1): p. 127-132.

[94] Li, Z., S.R. Beeram, C. Bi, D. Suresh, X. Zheng, and D.S. Hage, High-performance affinity chromatography: applications in drug–protein binding studies and personalized medicine. Adv. Protein Chem. Struct. Biol., 2016. 102: p. 1-39.

[95] Mallik, R., M.J. Yoo, C.J. Briscoe, and D.S. Hage, Analysis of drug–protein binding by ultrafast affinity chromatography using immobilized human serum albumin. J. Chromatogr. A, 2010. 1217(17): p. 2796-2803.

[96] Singh, S.S. and J. Mehta, Measurement of drug–protein binding by immobilized human serum albumin-HPLC and comparison with ultrafiltration. J. Chromatogr. B, 2006. 834(1-2): p. 108-116.

[97] Busch, M., L. Carels, H. Boelens, J. Kraak, and H. Poppe, Comparison of five methods for the study of drug–protein binding in affinity capillary electrophoresis. J. Chromatogr. A, 1997. 777(2): p. 311-328.

[98] Chu, Y.H., L.Z. Avila, H.A. Biebuyck, and G.M. Whitesides, Use of affinity capillary electrophoresis to measure binding constants of ligands to proteins. J. Med. Chem., 1992. 35(15): p. 2915-2917.

[99] Zhang, B., Y.X. Li, H.N. Gao, J. Bian, and J.J. Bao, Rapid determination of protein binding constant by a pressure-mediated affinity capillary electrophoresis method. Electrophoresis, 2011. 32(24): p. 3589-3596.

[100] Chu, Y.-H., W.J. Lees, A. Stassinopoulos, and C.T. Walsh, using affinity capillary electrophoresis to determine binding stoichiometries of protein-ligand interactions. Biochemistry, 1994. 33(35): p. 10616-10621.

[101] Albishri, H.M., S.E. Deeb, N. AlGarabli, R. AlAstal, H.A. Alhazmi, M. Nachbar, D.A. El-Hady, and H. Wätzig, Recent advances in affinity capillary electrophoresis for binding studies. Bioanalysis, 2014. 6(24): p. 3369-3392.

[102] Busch, M., J. Kraak, and H. Poppe, Principles and limitations of methods available for the determination of binding constants with affinity capillary electrophoresis. J. Chromatogr. A, 1997. 777(2): p. 329-353.

[103] Ridings, J.E., The thalidomide disaster, lessons from the past, in Teratogenicity Testing: Methods and Protocols. 2013, Humana New York, NY. p. 575-586.

[104] Hellwich, K.-H. and K.-H. Hellwich, Eutomer. Stereochemie—Grundbegriffe, 2002: p. 40-41.

[105] Teo, S.K., W.A. Colburn, W.G. Tracewell, K.A. Kook, D.I. Stirling, M.S. Jaworsky, M.A. Scheffler, S.D. Thomas, and O.L. Laskin, Clinical pharmacokinetics of thalidomide. Clin. Pharmacokinet., 2004. 43: p. 311-327.

[106] Chuang, V.T.G. and M. Otagiri, Stereoselective binding of human serum albumin. Chirality, 2006. 18(3): p. 159-166.

[107] Kauffman, R.E., M.W. Lieh-Lai, H.G. Uy, and M. Aravind, Enantiomer-selective pharmacokinetics and metabolism of ketorolac in children. Clin. Pharmacol. Ther., 1999. 65(4): p. 382-388.

[108] Engelhardt, H., W. Beck, J. Kohr, and T. Schmitt, Kapillarelektrophorese: Methoden und Möglichkeiten. 1994, Friedr. Viewg& Sohn Verlagsgesellschaft mbH. p. 3-33.

[109] Wren, S., The separation of enantiomers by capillary electrophoresis. Vol. 6. 2013: Springer Science & Business Media

[110] Wätzig, H., M. Degenhardt, and A. Kunkel, Strategies for capillary electrophoresis: Method development and validation for pharmaceutical and biological applications. Electrophoresis, 1998. 19(16-17): p. 2695-2752.

[111] Kuhn, R., Enantiomeric separation by capillary electrophoresis using a crown ether as chiral selector. Electrophoresis, 1999. 20(13): p. 2605-2613.

[112] Bernardo-Bermejo, S., E. Sánchez-López, M. Castro-Puyana, and M.L. Marina, Chiral capillary electrophoresis. Trends in Analytical Chemistry, 2020. 124: p. 115807.

[113] Fanali, S. and B. Chankvetadze, Some thoughts about enantioseparations in capillary electrophoresis. Electrophoresis, 2019. 40(18-19): p. 2420-2437.

[114] Chankvetadze, B. and G.K. Scriba, Cyclodextrins as chiral selectors in capillary electrophoresis: Recent trends in mechanistic studies. Trends Analyt. Chem., 2023: p. 116987.

[115] Schmitt, T. and H. Engelhardt, Charged and uncharged cyclodextrins as chiral selectors in capillary electrophoresis. Chromatographia, 1993. 37: p. 475-481.

[116] Fahr, A. and R. Voigt, Voigt Pharmazeutische Technologie. 2021, Deutscher Apotheker Verlag. p. 3-5.

[117] Mannhold, R., H. Buschmann, and J. Holenz, Innovative Dosage Forms: Design and Development at Early Stage. Vol. 76. 2019: John Wiley & Sons

[118] Cha, J., T. Gilmor, P. Lane, and J.S. Ranweiler, Stability studies, in Separation Science and Technology. 2011, Elsevier. p. 459-505.

[119] Irshad, K., M.S.H. Akash, K. Rehman, and I. Imran, Principles of Pharmaceutical Analysis in Drug Stability and Chemical Kinetics. Drug Stability and Chemical Kinetics, 2020: p. 1-18.

[120] Bharate, S.S., S.B. Bharate, and A.N. Bajaj, Interactions and incompatibilities of pharmaceutical excipients with active pharmaceutical ingredients: a comprehensive review. J. Excip. Food Chem., 2016. 1(3).

[121] Grangeia, H.B., C. Silva, S.P. Simões, and M.S. Reis, Quality by design in pharmaceutical manufacturing: A systematic review of current status, challenges and future perspectives. Eur. J. Pharm. Biopharm., 2020. 147: p. 19-37.

[122] Patil, A.S. and A.M. Pethe, Quality by Design (QbD): A new concept for development of quality pharmaceuticals. International journal of pharmaceutical quality assurance, 2013. 4(2): p. 13-19.

[123] Pramod, K., M.A. Tahir, N.A. Charoo, S.H. Ansari, and J. Ali, Pharmaceutical product development: A quality by design approach. International journal of pharmaceutical investigation, 2016. 6(3): p. 129.

[124] James, K.C., The hydrolysis of acetylsalicylic acid from aqueous suspension. J. Pharm. Pharmacol., 1958. 10(1): p. 363-369.

[125] Vries, H.d. and G.M.B.v. Henegouwen, Photodegradation of nifedipine under in vivo-related circumstances. Photochemistry and photobiology, 1995. 62(6): p. 959-963.

[126] Severin, G., Spontaneous racemization of chlorthalidone: Kinetics and activation parameters. Chirality, 1992. 4(4): p. 222-226.

[127] Hussar, D.A., P.J. Niebergall, E.T. Sugita, and J.T. Doluisio, Aspects of the epimerization of certain tetracycline derivatives. J. Pharm. Pharmacol., 1968. 20(7): p. 539-546.

[128] Aguiar, A.J., J. Krc Jr, A.W. Kinkel, and J.C. Samyn, Effect of polymorphism on the absorption of chloramphenicol from chloramphenicol palmitate. J. Pharm. Sci., 1967. 56(7): p. 847-853.

[129] Manning, M.C., D.K. Chou, B.M. Murphy, R.W. Payne, and D.S. Katayama, Stability of protein pharmaceuticals: an update. Pharm. Res., 2010. 27: p. 544-575.

[130] Dao, H., P. Lakhani, A. Police, V. Kallakunta, S.S. Ajjarapu, K.-W. Wu, P. Ponkshe, M.A. Repka, and S. Narasimha Murthy, Microbial stability of pharmaceutical and cosmetic products. AAPS PharmSciTech, 2018. 19: p. 60-78.

[131] Kurmi, M., A. Sahu, S.K. Tiwari, and S. Singh, Stability behaviour of antiretroviral drugs and their combinations. 6: evidence of formation of potentially toxic degradation products of zidovudine under hydrolytic and photolytic conditions. RSC Adv., 2017. 7(30): p. 18803-18814.

[132] Chi, E.Y., S. Krishnan, T.W. Randolph, and J.F. Carpenter, Physical stability of proteins in aqueous solution: mechanism and driving forces in nonnative protein aggregation. Pharm. Res., 2003. 20: p. 1325-1336.

2. AIM OF THE THESIS

Many drugs have been used successfully in therapy for several decades. Although great empirical knowledge has been gained, often basic data, such as the extent of protein binding is not known.

Today, the determination of the extent of plasma protein binding is standard in drug approval, but it was not in the past. Many drugs are available as enantiomers and racemates. Since the thalidomide scandal, people have been aware of the influence and consequences stereoselective processes can have in the organism.

The drugs ephedrine, pseudoephedrine, and ketamine are commercially available as pure enantiomers. A previously published study indicated stereoselective protein binding of ephedrine and pseudoephedrine in human serum. Whether stereoselective binding to the 2nd most important binding plasma protein - AGP - is present should be investigated here. In addition, two ephedra derivatives, methylephedrine and norephedrine, should be analyzed as well and the influence of the different basic properties and substitutions of the amine should be studied. The extent of plasma protein binding of racemic ketamine has been studied previously. However, only binding to AGP and not to albumin was investigated for stereoselectivity. Since albumin is the major binding plasma protein, the possible stereoselective binding of racemic and enantiomerically pure ketamine to albumin is of interest. All drugs should be analyzed by ultrafiltration followed by cyclodextrin modified CE and further characterized using NMR ligand screening methods such as STD-, waterLOGSY, and CPMG-NMR. For the separation of the ketamine enantiomers, a suitable “chiral” CE method should be developed and validated using statistical experimental design.

Just like plasma protein binding, stability studies are essential in the context of drug approval. New technologies make it possible to better understand stability-related degradation pathways, ensure the quality of the drug, and thus protect patients. In collaboration with a pharmaceutical company, a stability problem with ketamine was to be investigated. Aqueous solutions of the API became yellow under influence of heat. This discoloration could not be attributed to any previously known impurity of ketamine. High-resolution mass spectrometry (HR-MS) should be used to establish an impurity profile and provide a structural elucidation of the impurity responsible for the yellow discoloration.

3. RESULTS

3.1. Characterization of binding properties of ephedrine derivatives to human alpha-1-acid glycoprotein

Sebastian Schmidt, Markus Zehe, Ulrike Holzgrabe

Reprinted with permission from European Journal of Pharmaceutical Sciences 181 (2023) 106333

https://doi.org/10.1016/j.ejps.2022.106333

Abstract

Most drugs, especially those with acidic or neutral moieties, are bound to the plasma protein albumin, whereas basic drugs are preferentially bound to human alpha-1-acid glycoprotein (AGP). The protein binding of the long-established drugs ephedrine and pseudoephedrine, which are used in the treatment of hypotension and colds, has so far only been studied with albumin. Since in a previous study a stereoselective binding of ephedrine and pseudoephedrine to serum but not to albumin was observed, the aim of this study was to check whether the enantioselective binding behavior of ephedrine and pseudoephedrine, in addition to the derivatives methylephedrine and norephedrine, is due to AGP and to investigate the influence of their different substituents and steric arrangement. Discontinuous ultrafiltration was used for the determination of protein binding. Characterization of ligand-protein interactions of the drugs were obtained by saturation transfer difference nuclear magnetic resonance spectroscopy. Docking experiments were performed to analyze possible ligand-protein interactions. The more basic the ephedrine derivative is, the higher is the affinity to AGP. There was no significant difference in the binding properties between the individual enantiomers and the diastereomers of ephedrine and pseudoephedrine.

Graphical Abstract

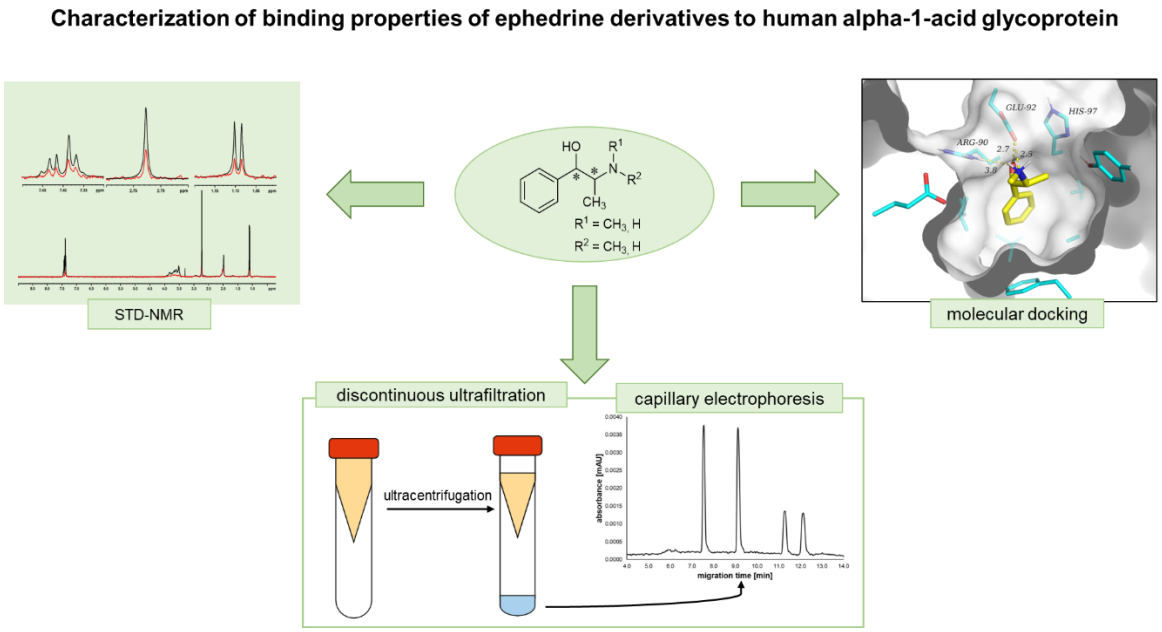

1. Introduction

Many different factors influence the drug therapy, among them bioavailability, metabolism, and solubility. Above all, binding to proteins such as albumin, has huge influence on the success of the respective drug therapy. If a drug is strongly bound, the effective dosage is substantially reduced and hence, the drug cannot develop its full effect. Albumin is the protein with the largest proportion among all plasma proteins and performs the most important functions, such as transport of endogenous and exogenous substances through the body. It binds mainly acidic and neutral substances at two binding sites (Sudlow et al., 1975). Diseases can increase or decrease protein concentration, which affects the extent of protein binding (Tillement et al., 1978). Besides albumin, there are other plasma proteins which only make up a small proportion of the total quantity such as lipoproteins or alpha-1-acid glycoprotein (AGP) also known as orosomucoid, with AGP being only 3% of the plasma proteins. However, it is the second most important transport protein for drugs besides albumin. AGP is a highly glycosylated acute phase protein with a molecular mass of 42 kDa and widely used as an inflammation marker in laboratory diagnostics. Its carbohydrate content is very high at 45% and responsible for the immunomodulatory activities of the protein (Fournier et al., 2000). There are two variants of AGP, variant A and F1*S, which occur in a 1:2 to 1:3 ratio in humans (Yuasa et al., 1993). AGP transports mainly basic substances but lipophilic ones as well. This is significant as most drugs have basic structural elements (Charifson and Walters, 2014). The binding behavior of drugs to AGP was often described as binding to a single dominant high-affinity binding site with several low-affinity binding sites or two main binding sites with the same affinity and these

two binding sites differ primarily in their affinity for basic and acidic drugs (Berezhkovskiy, 2007). In 2008, Schönfeld et al. characterized the non-glycosylated crystal structure of AGP with one main binding site, which differs depending on the variant (Schönfeld et al., 2008). In a review by Israili and Dayton the binding of many different drugs to AGP were evaluated (Israili and Dayton, 2001). The basic drugs ephedrine (E) and pseudoephedrine (PE), which are used to treat hypotension and colds, have not been characterized. Nevertheless, there have been studies on protein binding of E and PE with albumin (Guo et al., 2003; Huang et al., 2011; Till and Benet, 1979; Yang and Hage, 1994).

Volpp and Holzgrabe showed that the binding of E and PE is increased in human serum compared to the isolated albumin and indicating that these drugs may bind to another plasma protein (Volpp and Holzgrabe, 2019). In addition, differences in protein binding of the individual enantiomers and diastereomers were found in human serum, which suggest a stereoselectivity of the binding process. Due to the basic structure of E and PE, binding to AGP seems obvious, which is why binding experiments with E and PE as well as the derivatives norephedrine (NE) and methylephedrine (ME) were performed. For the determination of the extent of the protein binding of ephedrine derivatives to AGP discontinuous ultrafiltration (DUF) was used and for structural studies saturation transfer difference-NMR (STD-NMR) was chosen. To the best of our knowledge, STD-NMR has only been used by Becker and Cruz (Becker and Larive, 2008; Cruz and Larive, 2012) to investigate protein binding of drugs to AGP due to the challenging nature of a polar binding site and the strong glycosylation. One of the drugs examined was the β-receptor antagonist propranolol, which has some structural similarity to the ephedrine derivatives. Stereoselective differences in binding behavior were also found for both propranolol enantiomers, which is why enantioselective binding seems possible for the ephedrine derivatives and their enantiomers. Overall, the aim of this study was to investigate the binding properties of different ephedrine derivatives and their respective enantiomers (cf. Fig. 1) to AGP and to study the influence of structural differences and stereoselective binding.

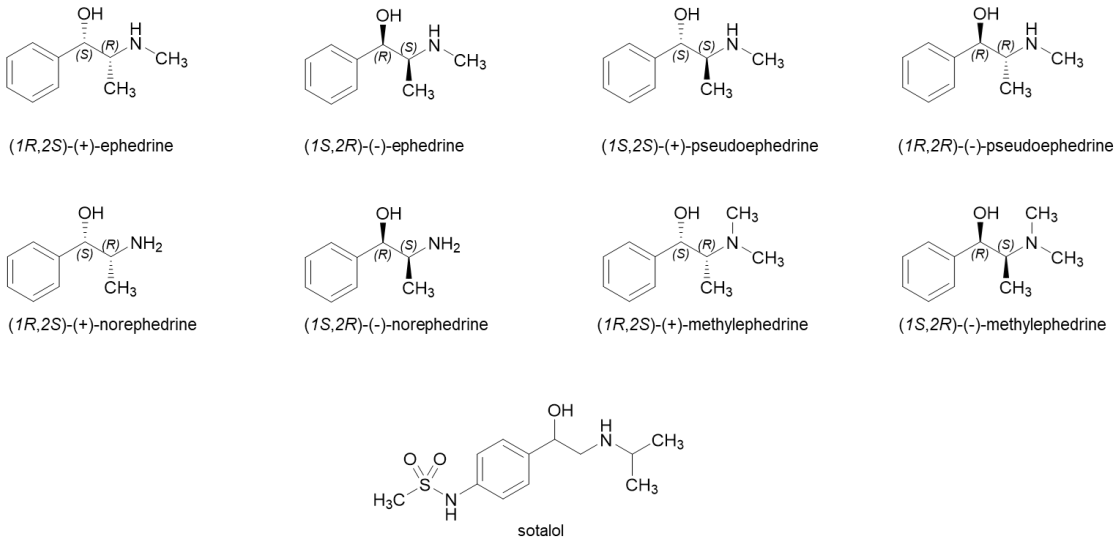

Fig. 1. Structural formulas of studied drugs

2. Materials and methods

2.1. Chemicals

(+)-Ephedrine hemihydrate, (-)-pseudoephedrine, (+)-pseudoephedrine, (+)-norephedrine, (-)-norephedrine, sotalol hydrochloride and α_1-acid Glycoprotein from human plasma were purchased from Sigma Aldrich (Basel, Switzerland), while (-)-ephedrine from Caelo (Hilden, Germany). (+)-Methylephedrine and (-)-methylephedrine were obtained from Fluka (Buchs, Switzerland). The buffer salts sodium dihydrogenphosphate (anhydrous), disodium hydrogenphosphate, tripotassium phosphate, sodium azide and sodium chloride were purchased from Sigma Aldrich (Basel, Switzerland), phosphoric acid 85% and sodium hydroxide from VWR Chemicals (Darmstadt, Germany), hepktakis-(2,3-di-O-acetyl-6-sulfo-)-β-cyclodextrin (HDAS-β-CD) from Regis Technologies (Morton Grove, Texas, US), 0.1 M hydrochloric acid solution from Bern Kraft (Duisburg, Germany) and deuterated water from Deutero GmbH (Kastellaun, Germany), while Millipore water was obtained from an in-house water purification system from Merck Millipore (Darmstadt, Germany).

2.2. Instruments

pH measurements were performed with a pH meter from Metrohm (Filderstadt, Germany). The samples were centrifuged with a centrifuge 5702 and incubated in a thermomixer, both from Eppendorf (Hamburg, Germany). The capillary electrophoresis (CE) system used was a P/ACE MDQ system from Beckman Coulter (Brea, California, US) with a photodiode array detector.

2.3. Discontinuous ultrafiltration

As incubation medium a 30 mM sodium dihydrogen/disodium hydrogen phosphate buffer, with 100 mM sodium chloride and a pH of 7.40 was used. The pH was adjusted with 0.1 M sodium hydroxide solution. The ionic strength and pH of the buffer correspond to the physiological conditions of the blood (Oehlmann, 1996). 180 µM AGP, 360 µM racemic mixture of each drug derivative and 225 µM sotalol stock solution were prepared by dissolving the required amount in incubation buffer. Five drug-protein ratios were incubated and covered the range from 0.8 to 1.5. The protein concentration was held constant at 80 µM while the determined drug concentration differed in the range from 50-120 µM. Drug and protein stock solutions were mixed with the respective amount of incubation buffer in 1.5 ml Eppendorf tubes and incubated at 37 °C for 30 min. After equilibration was reached the internal standard sotalol was added in a final concentration of 50 µM. The solution was transferred directly into the Amicon® Ultra 0.5 ml ultracentrifugation unit with a molecular cutoff of 3 kDa (Merck, Darmstadt, Germany) and centrifuged for 5 min at 4400 rpm. After centrifugation, the solution was filled into vials and assessed by means of CE. This was performed in triplicate per drug-protein ratio.

2.4. Capillary electrophoresis

A fused silica capillary from BGB Analytik Vertrieb (Rheinfelden, Germany) with an internal diameter of 50 µM, a total length of 52 cm and an effective length of 40 cm was chosen for the separation. The background electrolyte (BGE) consisted of a 100 mM sodium dihydrogenphosphate/phosphoric acid (85%, w/w) buffer, adjusted to a pH of 3.0 with 1.0 M sodium hydroxide solution, and 3 mM HDAS-β-CD. Samples were injected at a pressure of 10.0 psi for 5.0 s and separated at room temperature in the cationic injection mode, using a constant voltage of 20.0 kV for 20.0 min. The capillary was conditioned first with 1.0 M sodium hydroxide solution, second with 2.0 M hydrochloric acid and third with Millipore® water at a pressure of 30.0 psi, each for 10.0 min. Subsequently, the capillary was rinsed with BGE for 2 min and a voltage of 20.0 kV for 20 min was applied. Before each sample injection, the capillary was rinsed 2.0 min with 0.1 M hydrochloric acid, 2.0 min Millipore® water and 5.0 min with BGE at a pressure of 20.0 psi. Analytes were detected at a wavelength of 194 nm. Data evaluation was performed with 32 Karat Software 8.0 from Sciex (Darmstadt, Germany).

2.5. Saturation Transfer Difference NMR

The measurements were carried out on a Bruker III Avance spectrometer operating at 400.13 MHz equipped with a PABBI inverse probe (Karlsruhe, Germany). The pulse frequency stddiffesgp.3 was used, coupled with an excitation sculpting pulse frequency for

water signal suppression at 4.703 ppm. The scan count was 8 scans with 16 dummy scans and a loop counter of 64. The spectral width was set to 15.98 ppm and the transmitter offset to 4.70 ppm. The measurement temperature was 300 K. The solvent used was a deuterated 30 mM phosphate buffer containing 25 mM sodium chloride. For preparation, tripotassium phosphate was weighed, dissolved in deuterium oxide, and adjusted to a pD of 7.4 with deuterated hydrochloric acid. For stability to microbial attack 0.02 % sodium azide was added. 2.0 mM from each enantiomer and 40 µM protein stock solutions were prepared by dissolving the required amounts in the buffer. The ligand-protein solutions were prepared by mixing the stock solutions with the respective amount of buffer to obtain a ligand-protein ratio of 20:1. Protein concentration was held constant at 15 µM. Each sample was measured at four different saturation times from 1 to 4 s with a constant relaxation delay of 4 s. Data were integrated and evaluated with TopSpin 4.0.9 from Bruker (Karlsruhe, Germany).

2.6. Molecular Docking

Docking studies with AutoDock (Morris et al., 1998) were executed on the crystal structure of the human AGP A variant in complex with amitriptyline (PDB code 3APV, chain A (Nishi et al., 2011)). Using MOE (Molecular Operating Environment; Chemical Computing Group ULC, Montreal, QC, Canada) ligand atoms as well as waters and other small molecules were extracted, terminal residues were kept in the charged form. Polar hydrogens were added with the program PROTONATE of the AMBER software package (Case et al., 2005; Case et al., 2008). Kollmann charges and solvation parameters were assigned to generate the PDBQS-files required for the calculation of the docking grids by AutoGrid (60 x 60 x 60 grid points, spacing 0.375 Å; centered on binding site placing the grid center near atom OE2 of Glu-92). Ligand building, addition of protons and energy minimization (gradient: 0.001 kcal/mol/Å; MMFF94 forcefield) were performed with MOE. The docking was carried out using the Lamarckian Genetic Algorithm (10 x 10^6 energy evaluations, population size of 350 individuals, max. 50.000 generations, 300 iterations in Solis and Wets local search, 50 GA runs) which resulted in a very accurate reproduction of the experimentally observed binding mode of amitriptyline (98% top poses with RMS-deviations below 2 Å).

3. Results and discussion

3.1. Discontinuous ultrafiltration and capillary electrophoresis analysis

The procedure of DUF is characterized by mixing drug and protein solution. After incubation, the formed drug-protein complex is centrifuged off while the free drug remains in the centrifugate. The free drug concentration was determined by means of CE. HDAS-β-CD was chosen as the chiral selector because good separations of ephedrine derivatives and their enantiomers have already been shown in the past (Wedig et al., 2002). In addition, a good separation of the sotalol enantiomers had to be achieved because only the racemic sotalol is commercially available. Sotalol hydrochloride was used as internal standard because it is reported not to bind to APG (Belpaire et al., 1982; Israili and Dayton, 2001). To avoid possible binding of sotalol to AGP, the internal standard was added just before centrifugation. As can be seen in Fig. 2 a separation of all ephedrine derivatives as well as the sotalol enantiomers was accomplished within 15 min.

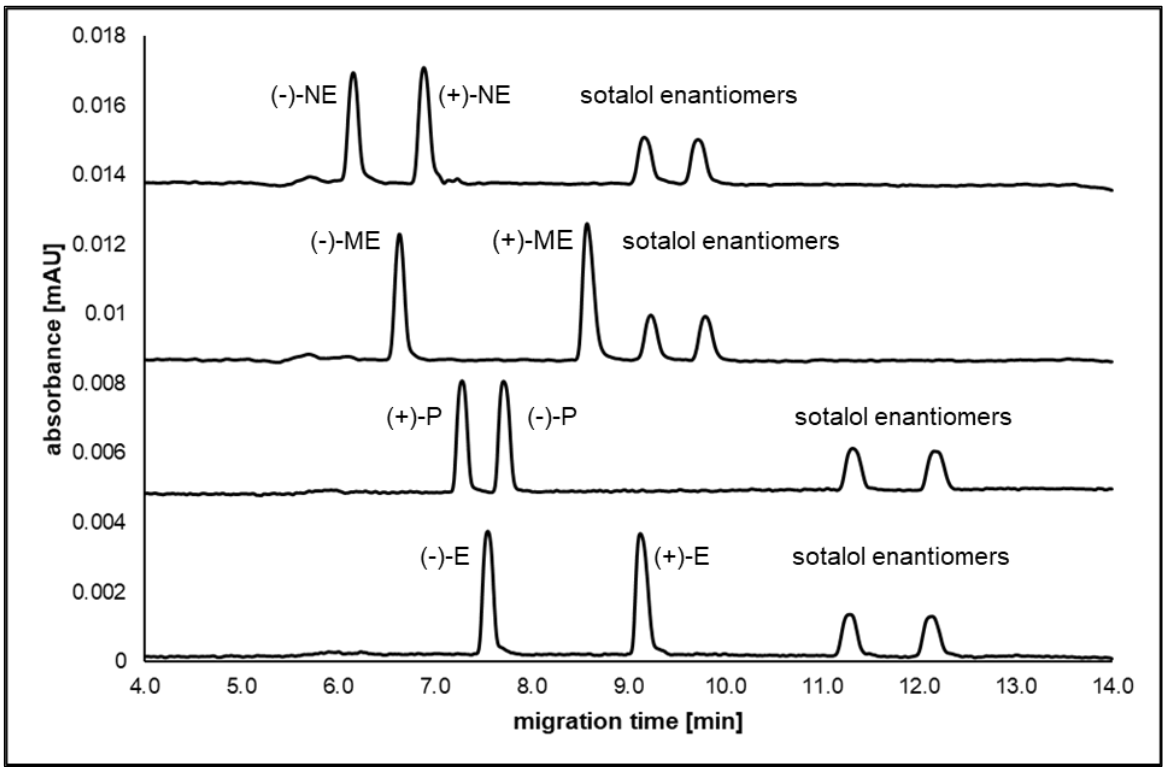

Fig. 2. Electropherogramm of the drugs used at a concentration of 100 µM and 50 µM internal standard; method parameters: 20.0 kV, 100 mM sodium dihyrogenphosphate/phosphoric acid buffer pH value 3.0, 3 mM HDAS-β-CD, total capillary length 52 cm, effective capillary length 40 cm

The greater the excess of the drug concentration the more the binding sites of the protein are occupied. The binding of a ligand to a protein is based on an equilibrium reaction following.

$$\text{Eq. (1)} \qquad \text{ligand} + \text{protein} \rightleftharpoons \text{ligand} - \text{protein complex}$$

This reaction can be described by the affinity constant $K_{aff.}$, which is the applied law of mass action to Eq. (1) (Du et al., 2016). To characterize the affinity constant K_{aff} and the binding behavior, several different drug-protein ratios must be incubated, and the free drug concentration measured. Either the protein concentration or the drug concentration is kept constant. In healthy humans, the plasma concentration of AGP is between 10-20 µM (Bteich, 2019). Since the drug excess would have been too large and no significant change in free concentration would have been detected it was not possible to use a physiological concentration of AGP in the DUF experiments. Therefore, a AGP concentration of 80 µM was chosen. Lowering the drug concentration was no option, as drug concentrations would have fallen below the limit of quantification (LOQ). The LOQ of the drugs used can be found in Table S1. LC-MS is also used in combination with ultrafiltration (Fabresse et al., 2020), as the better sensitivity allows work in physiological conditions. However, CE was chosen because of its advantages in the separation of enantiomers, as the stereoselectivity of protein binding was to be investigated. In this study an approach was chosen to work in a drug-protein ratio of 0.8-1.5 resulting in a constant protein concentration of 80 µM. The fraction bound to the protein (f_{bound}) is calculated according to Eq. (2) and Eq. (3) by subtracting the concentration of unbound drug (c_{free}) determined by CE in the sample from the total concentration of drug (c_{total}) used considering the concentration of the internal standard and dividing the resulting bound concentration (c_{bound}) of drug by c_{total}.

$$\text{Eq. (2)} \qquad c_{bound} = c_{total} - c_{free}$$

$$\text{Eq. (3)} \qquad f_{bound} = \frac{c_{bound}}{c_{total}}$$

K_{aff} can be determined using graphical approaches, e.g. the Klotz or Scatchard plot (Klotz and Hunston, 1971; Scatchard, 1949). The amount of drug which is bound per mole of protein can be expressed by r which corresponds to the quotient of the bound drug concentration to the total protein concentration ($c_{protein}$).

$$\text{Eq. (4)} \qquad r = \frac{c_{bound}}{c_{protein}}$$

The Klotz plot makes use of the relationship between r and the free drug concentration as a double-reciprocal approach. If there is only one binding site, a linear graph is gained; if there are several binding sites, a curve is obtained whose evaluation is much more complex. Fig. 3 shows the linear Klotz plot of (-)-ephedrine as an example indicating the presence of one main binding site.

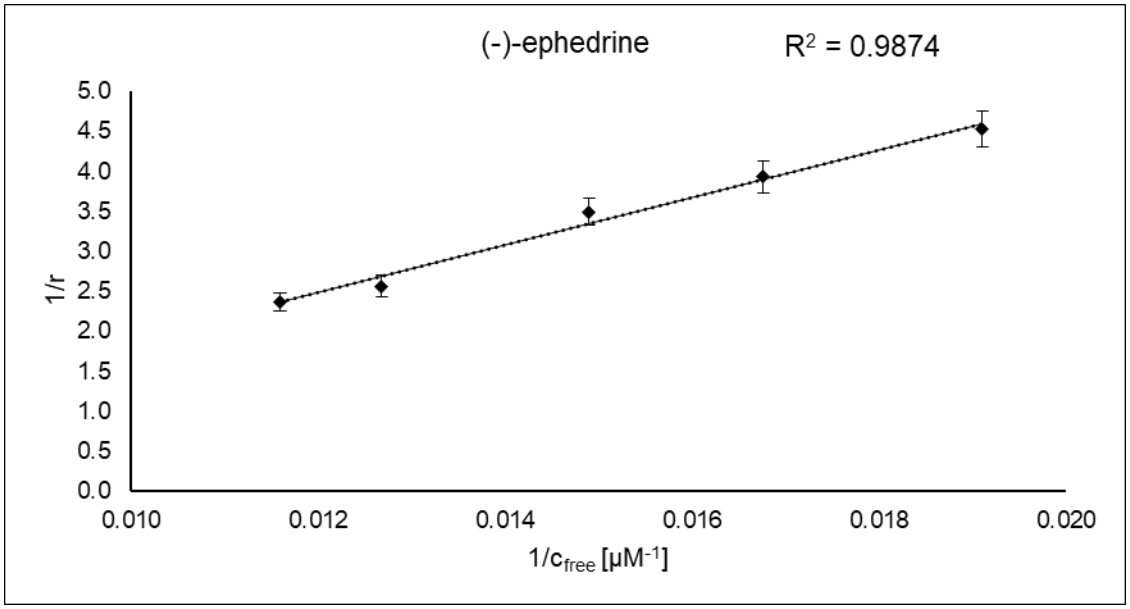

Fig. 3. Klotz plot of (-)-ephedrine; reciprocal application of r against c_{free} with r equal to the quotient of c_{bound} by $c_{protein}$, error bars indicate the relative standard deviation

K_{aff} is the quotient of the intercept with the slope of the determined regression line while n, number of binding sites, is the reciprocal value of the intercept (Klotz and Hunston, 1971). The enantiomers of E, PE, and ME all showed a linearized Klotz Plot, while both NE enantiomers could not be graphically analyzed. The diastereomers E and PE including their respective enantiomers showed no significant difference in their binding behavior. ME showed low protein binding with the dextrorotatory enantiomer showing even lower binding compared to E and PE. Hardly any binding was found for both NE enantiomers. As was mentioned earlier, one main binding site is present when a linearized Klotz plot is obtained. For all derivatives except NE this is the case. An overview of the obtained plots is given in Fig. S1. To confirm the result, K_{aff} for each ligand-protein ratio and the resulting total K_{aff} as average of each individual K_{aff} was calculated by Eq. (5) with the generated data and transformed into the pK_{aff}, which is the negative decimal logarithm of K_{aff}, for better usability. In the presence of only one main binding site and selective binding, pK_{aff} must be constant over the different ratios (Volpp and Holzgrabe, 2019).

$$\text{Eq. (5)} \qquad K_{aff} = \frac{f_{bound}}{1 - f_{bound}} \times \frac{1}{c_{protein}}$$

Fig. S2 shows this was the case for the enantiomers of E, PE, and ME, while the enantiomers of NE showed a larger scatter.

The results obtained with both methods are compared in Table 1. The ultrafiltration units were tested for non-specific binding of the drugs. No significant adsorption on the ultrafiltration device was observed. The minimal deviations were considered in the results presented. The values of the pK_{aff} differ significantly but are of the same order of

magnitude. Both approaches support the notion, that there is only one main binding site. The protein binding of all tested drugs was less than 30%, which is why it can be assumed that the binding of AGP is not clinically relevant.

Table 1 Comparison of pK_{aff} calculated according to Eq. (5) as the average value of the respective enantiomer, dissociation constant K_D as reciprocal value of K_{aff}, the determined protein binding by means of DUF and its graphical evaluation by means of Klotz plot with n being equal to the number of binding sites

				Klotz plot	
	pK_{aff}	K_D	% bound	pK_{aff}	n
(+)-E	3.62 ± 0.02	240 µM	25.0 ± 0.9	3.29	1.82
(-)-E	3.65 ± 0.03	221 µM	26.5 ± 1.6	3.56	0.91
(+)-PE	3.71 ± 0.03	176 µM	29.1 ± 1.4	3.46	1.45
(-)-PE	3.68 ± 0.04	209 µM	27.6 ± 2.0	3.79	0.46
(+)-ME	3.34 ± 0.03	429 µM	14.9 ± 1.0	3.63	0.68
(-)-ME	3.42 ± 0.03	383 µM	17.3 ± 0.9	3.43	1.16
(+)-NE	2.96 ± 0.14	956 µM	6.8 ± 1.9	graphical evaluation	
(-)-NE	3.02 ± 0.11	1087 µM	7.7 ± 1.7	was not possible	

3.2. Saturation Transfer Difference-NMR

STD-NMR is a well-established method in screening for possible binding of small molecules to respective targets, e.g. proteins (Krishnan, 2005). The principle of STD-NMR is based on the nuclear overhauser effect. When a drug binds to a protein, a proton of the protein can interact with a proton of the ligand and transfer energy in form of saturation. Saturating the protein´s protons with the aid of a specific pulse, this saturation is transferred to the proton of the ligand in case of binding. A completely saturated proton does not show a signal in the spectrum any longer. Since the saturation is not completely transferred to the proton of the ligand, an attenuated signal is obtained. By subtracting an on-resonance-spectrum (with saturation pulse) with an off-resonance-spectrum (without saturation pulse) a difference spectrum is obtained. Different signals indicate ligand protons that are in proximity to protons of the protein and thus were saturated by saturation. For each protein, the appropriate saturation pulse must be found, depending on the chemical structure. Ideally, the saturation pulse should not interfere with the signals of the ligand. Three different saturation pulses were applied with 6.22 ppm, 1.97 ppm

and -1.00 ppm. Only the saturation pulse at -1.00 ppm did not interfere, so it was chosen as the saturation pulse for the STD measurements. The corresponding NMR spectra are shown in Fig. S3. The drug excess should be as high as possible, but at least equal to 0.5 to 2 times of the dissociation constant K_D to ensure adequate saturation (Mayer, 2001). K_D values were calculated as reciprocal values from the previously determined K_{aff} values from the DUF measurements and are shown in Table 1. Fig. 4 shows the ^{1}H spectra of (-)-E and AGP. The C**H**-N signal at 3.50 ppm of the ephedrine derivatives overlapped with the signals from AGP and was therefore not suitable for evaluation. The H_{benzyl} signal at 5.00 ppm was cancelled out by the water suppression and could thus not be detected. The aromatic protons are overlapping, thus individual analysis was not possible. The exchangeable protons of the hydroxyl group and the amine group were not seen due to a deuterium exchange by the buffer used. An overlay between an off-resonance-spectrum (black) and an on-resonance-spectrum (red) of a mixture of (+)-E with AGP is displayed in Fig. 5.

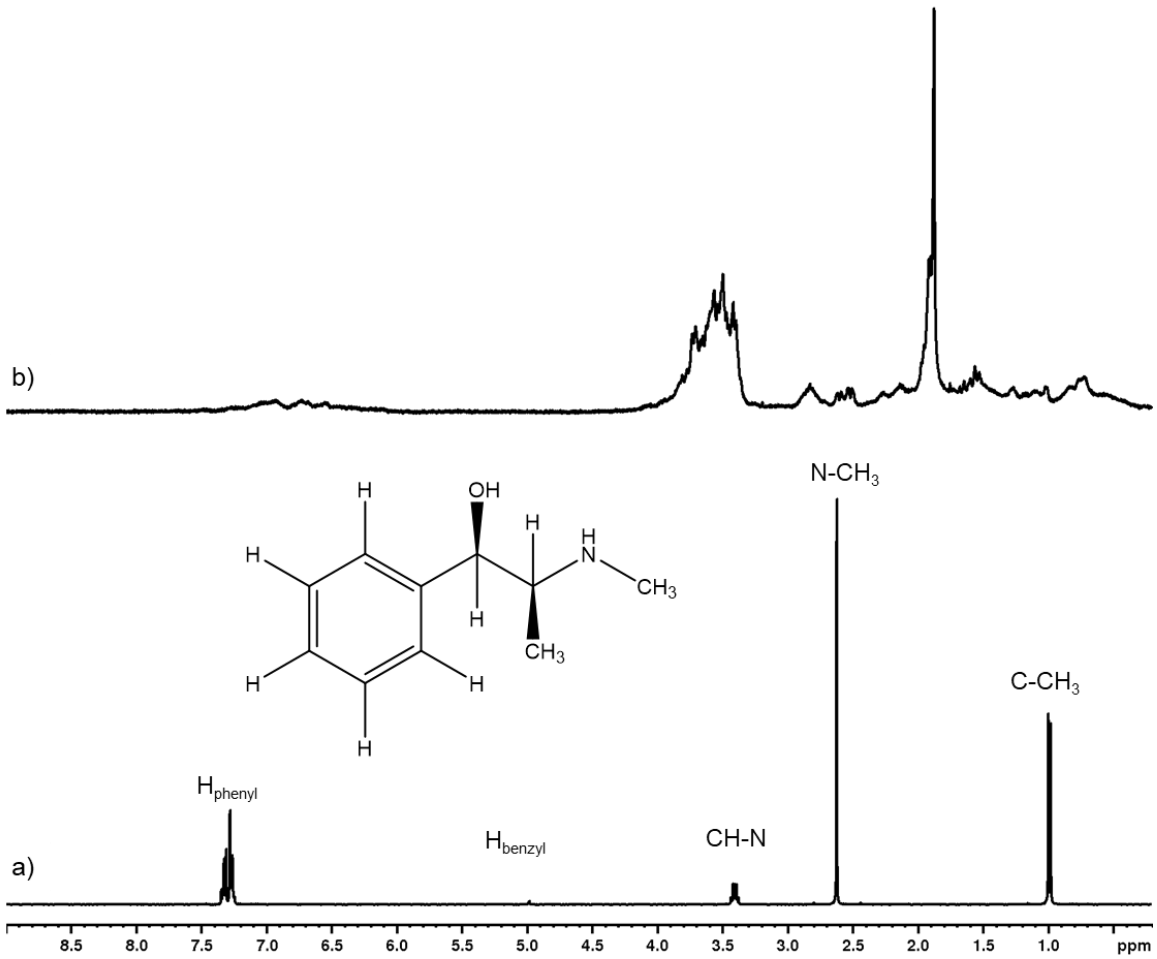

Fig. 4. NMR spectra overlay a) ^{1}H-spectrum of AGP b) ^{1}H-Spectrum of (-)-ephedrine; both spectra were recorded with water signal suppression

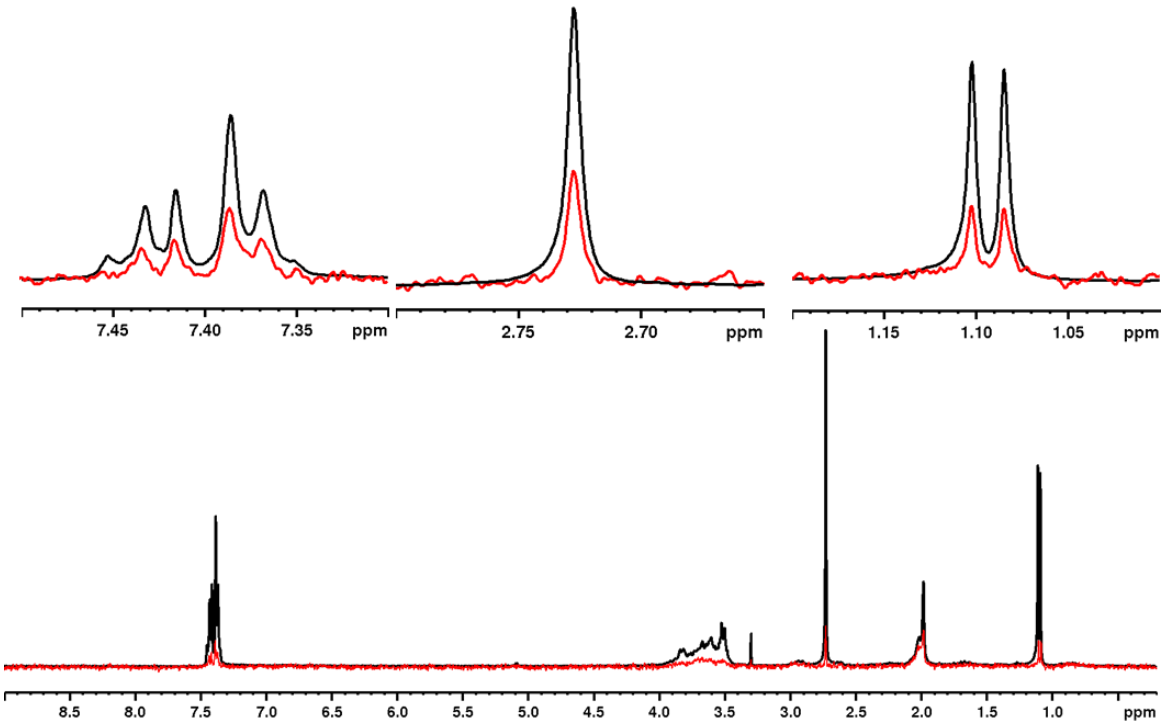

Fig. 5. Overlay of the off-resonance spectra (black) and the on-resonance spectra (red) of (-)-ephedrine with a saturation pulse of -1 ppm

The STD factor is calculated according to Eq. (6) with the integrals of each individual proton.

$$\text{Eq. (6)} \qquad \text{STD factor} = \frac{\text{integral}_{\text{off-resonance}} - \text{integral}_{\text{on-resonance}}}{\text{integral}_{\text{off-resonance}}} * 100$$

For epitope mapping, all STD factors are normalized to the strongest one (Viegas et al., 2011). The STD factor intensity depends on the saturation time, rebinding processes, drug and protein concentration and binding kinetics, respectively (Walpole et al., 2019). With longer saturation times, more intensive signals are obtained. The measurements were performed at saturation times of 1, 2, 3 and 4 seconds. Plotting STD-factor against the saturation time, revealed an adsorption isotherm, which can be described by Eq. (7). STD-factor(t_{sat}) is the factor at a certain saturation time, k_{sat} the saturation rate constant, t_{sat} the saturation time and STD-factor max the maximum STD-factor intensity.

$$\text{Eq. (7)} \qquad \text{STD} - \text{factor}\,(t_{sat}) = \text{STD} - \text{factor}_{max} \times (1 - e^{-k_{sat} \times t_{sat}})$$

To account for ligand and protein concentration (c_{ligand} respectively $c_{protein}$), the STD-amplification factor (STD-AF) is used instead of the STD factor. It is calculated according to Eq. (8).

$$\text{Eq. (8)} \qquad \text{STD} - \text{AF} = \text{STD} - \text{factor} \times \frac{c_{\text{ligand}}}{c_{\text{protein}}}$$

As can be seen in Fig. 6, at a saturation time starting from 3 s, almost complete saturation is reached for protons H_{phenyl}, N-C**H**$_3$, and C-C**H**$_3$. In the rising part of the adsorption isotherm, the STD-factor is still relatively independent of the saturation time. Therefore, a saturation time of 2 s was chosen for epitope mapping.

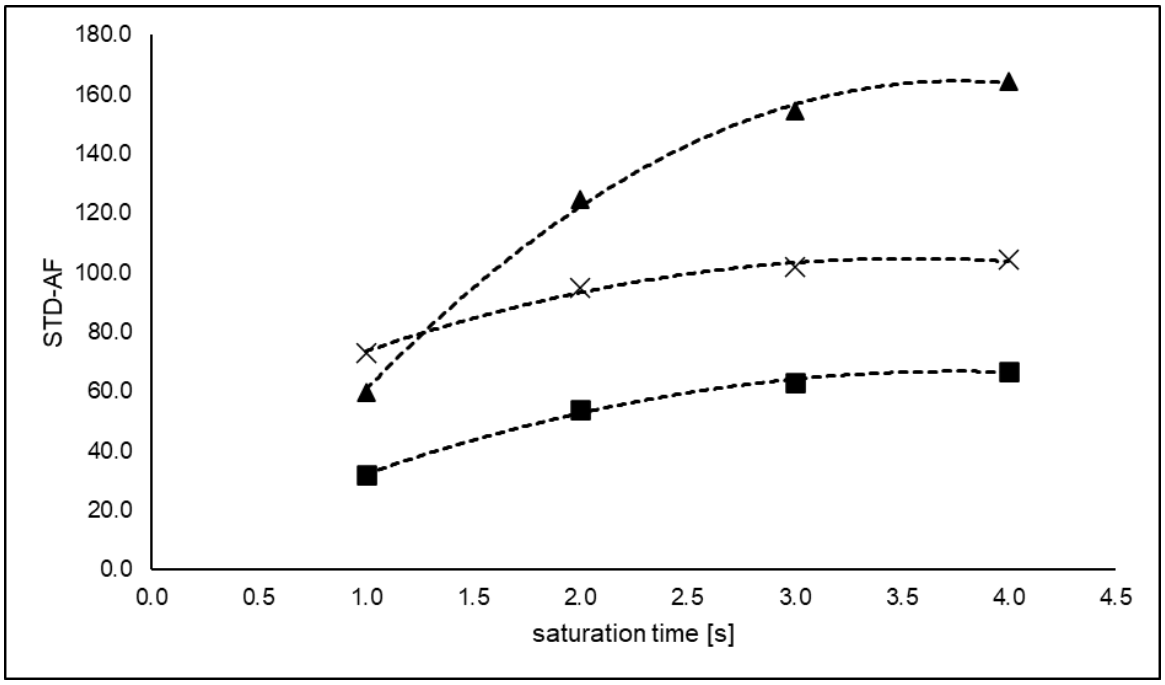

Fig. 6. Adsorption isotherm of the protons of (-)-E, application of the STD-amplification factor = STD-AF at the saturation times 1, 2, 3 and 4 s with STD AF being the obtained STD-factor multiplicated with the ligand excess, ▲= H_{phenyl}, ■ = C-C**H**$_3$, X = N-C**H**$_3$

In contrast to the DUF it was possible to use a physiological concentration of 15 µM AGP. Becker et al. showed that the influence of nonspecific interactions by increasing the ligand excess does not discriminate between the individual enantiomers (Becker and Larive, 2008). The higher the ligand excess, the more the STD factors of some protons of the individual enantiomers converged. To investigate this effect, different ligand excesses between 10:1 to 40:1 were tested. The results are shown in Table S2. No influence of the ligand concentration on the STD factor could be detected. A drug concentration of 300 µM representing an excess of 20:1 showed good results with all investigated drugs and was therefore used. Results are summarized in Table 2. In all ephedrine derivatives, the aromatic protons H_{phenyl} and C-CH_3 from the sidechain are the most affected ones. The alkyl substituents attached to the amine show weaker effects. In E and ME, the substituent of the dextrorotatory enantiomer showed a more intensive STD-factor while in PE there is no significant difference between the enantiomers.

Table 2 STD epitope maps for the used ephedrine derivatives at a concentration of 300 µM per ligand and a AGP concentration of 15 µM (values are expressed as a percentage in comparison to the most intense normalized STD-factor signal), n/a = not applicable

	E		**PE**		**ME**		**NE**	
	(+)	(-)	(+)	(-)	(+)	(-)	(+)	(-)
H_{phenyl}	93.6%	100.0%	100.0%	100.0%	100.0%	93.7%	100.0%	93.8%
C-CH_3	100.0%	79.5%	85.2%	84.1%	96.8%	100.0%	86.1%	100.0%
N-CH_3	79.2%	40.0%	60.8%	58.8%	72.9%	52.8%	n.a.	n.a.

3.3. Molecular Docking

Kaliszan et al. showed a proposal for the main binding site of AGP (Kaliszan et al., 1995). According to their findings, the high affinity binding pocket for basic substances is funnel shaped, with a negatively charged anionic region at the inner end and lipophilic regions at the edge and outer end. At the anionic area, mainly the positively charged basic nitrogen interacts, while at the lipophilic regions, mainly aliphatic and aromatic hydrocarbon interactions take place. The funnel shaped pocket is also a steric restriction and thus enantiomers can bind differently. In 2008, Schönfeld et al. succeeded in characterizing the crystal structure of the non-glycosylated protein. Variant F1*S has a third domain in the binding pocket compared to variant A and thus a larger opening which facilitates the entry of ligands and is a steric restriction. However, both variants have the anionic region postulated by Kaliszan. Previous experiments (Nishi et al., 2011) showed that variant A is mainly responsible for binding basic substances, which is why the docking experiments were carried out with this variant. The results of E and PE can be seen in Fig. 7, the results of ME and NE can be found in Fig. S4. Despite structural differences, the same interactions were found on all docked ligands. The phenyl ring shows van der Waal and π-π interactions in the hydrophobic pocket. The amine function forms a salt bridge to Glu92 and a cation interaction to His97. The hydroxyl group is stuck between Arg90 and Glu92 and forms hydrogen bonds to both sidechains. The respective enantiomers are present in the binding pocket in a different orientation (cf. Fig. 7) but show the same interactions. Based on the docking results, there is no difference in the binding process between the enantiomers of each ligand.

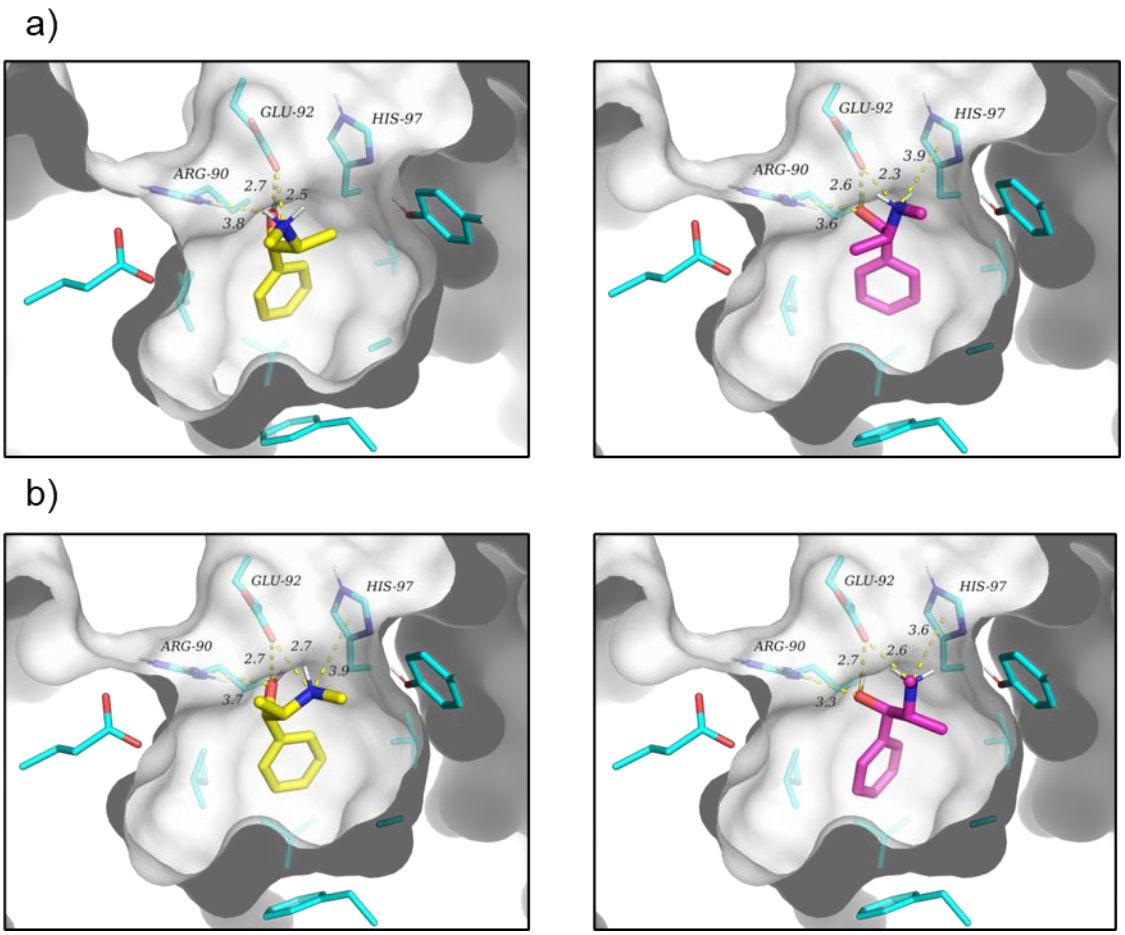

Fig. 7- docking results of a) ephedrine and b) pseudoephedrine with variant A of AGP; yellow = (+) enantiomer; pink = (-)-enantiomer

Nevertheless, stereochemistry and molecule size can have an influence on binding. As already mentioned, the opening of the binding pocket has steric restrictions, which is why some drugs can penetrate more easily than others. In addition, a substituent on the basic nitrogen increases the size of the molecule and thus makes penetration into the binding pocket more difficult. However, the tested ligands measured showed no significant differences between their enantiomers and penetrated the binding pocket without restriction.

The influence of a substituent of the basic nitrogen is less decisive for the molecular size than for the degree of protonation and the solvation of the amine, which has a significantly influence on the binding. Negatively charged and uncharged xenobiotics bind primarily to albumin, while positively charged drugs bind preferred to AGP. Therefore, binding to AGP should be significantly favored by increased protonation. All investigated ephedrine derivatives are weak bases (cf. Table 3 for exact pK_a values and ratio of charged to uncharged species at physiological pH value).

Table 3 pK_a values of the measured drug substances (Dong et al., 2015; Shalaeva et al., 2008) and ratio of charged to uncharged species at pH 7.40

drug	pK_a	ratio of charged to uncharged species at pH 7.40
pseudoephedrine	9.74	218:1
ephedrine	9.64	173:1
methylephedrine	9.40	100:1
norephedrine	9.12	52:1

The basicity of the drug substances decreases in the following order, considering their respective substitution: PE > E > ME > NE. NE and ME are least charged at physiological pH of 7.40 and thus should have a lowered protein binding to AGP in comparison to E and P. The pK_a value difference between the diastereomers E and PE is 0.1 and thus they differ only slightly in their protonation and solvation. Still PE is more charged than E at physiological pH. Comparing the results of the DUF with basicity of the drugs shows the same pattern. While PE and E show similar protein binding with PE being the stronger bound ligand, the protein binding decreases with declining basicity. ME thus has a lower binding than PE and E, and NE the lowest. An alkyl substituent of the basic nitrogen thus only influences the protein binding not via its change in molecular size but via the change in basicity.

4. Conclusions

The binding behavior of various ephedrine derivatives to AGP was successfully determined by means of DUF and STD-NMR and supported by docking experiments. The decrease in protein binding correlates with the decrease in protonation at physiological pH value. The more basic the ligand is, its affinity is higher to AGP. The docking experiments showed three main interactions, van der Waals and π-π-interactions of the phenyl ring, a cation interaction of the amine and hydrogen bonding of the hydroxy group. The DUF, STD-NMR and docking experiments showed no significant differences in the binding behavior between the respective enantiomers. The binding of the ephedrine derivatives to AGP is therefore not enantioselective.

Funding

This publication was supported by the Open Access Publication Fund of the University of Wuerzburg.

Conflict of interests:

None of the authors of this paper does have a financial or personal relationship with other people or organizations that could inappropriately influence or bias the content of the paper.

Acknowledgements:

Many thanks to Dr. Curd Schollmayer for his help in the discussions and the implementations of the STD-NMR measurements and Prof. Dr. Christoph Sotriffer for his help regarding the docking experiments.

SUPPLEMENTARY MATERIAL

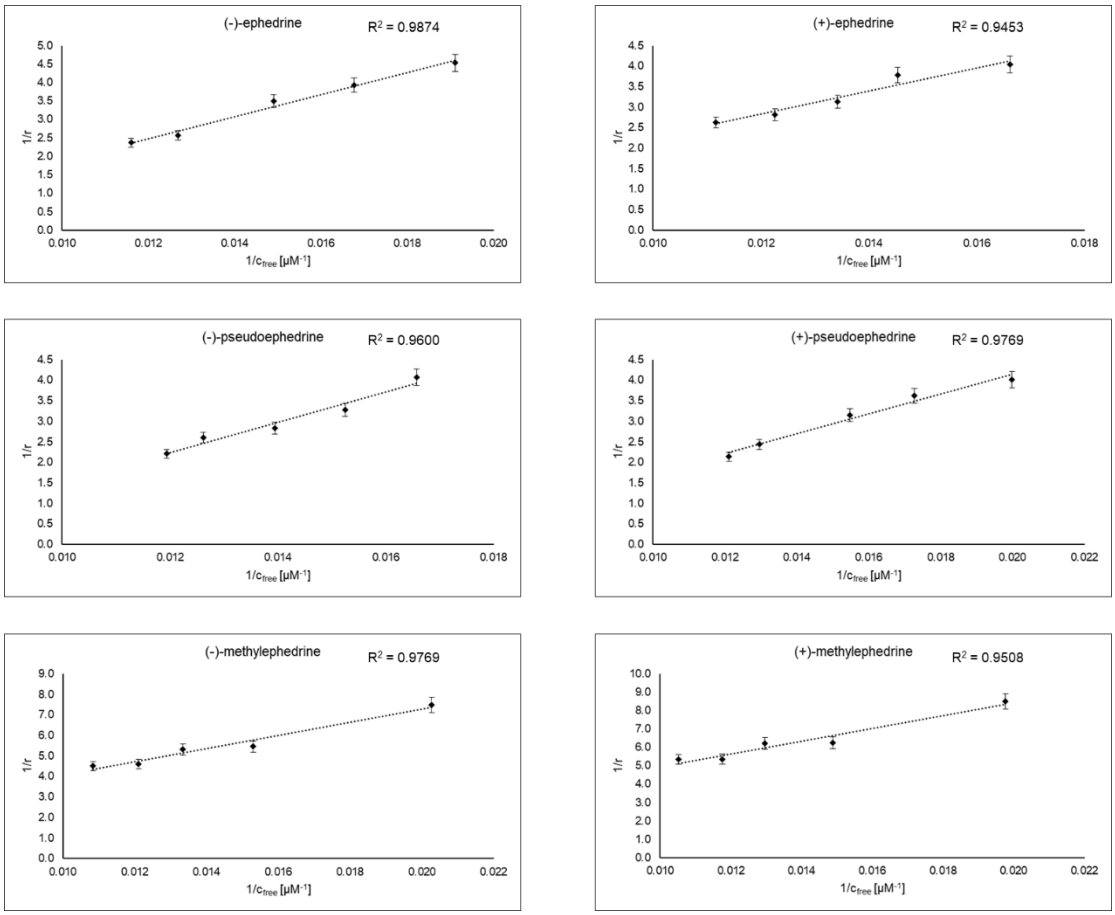

Fig. S1 Klotz plots of the used ephedrine derivatives; reciprocal application of r against c_{free} with r equal to the quotient of c_{bound} by $c_{protein}$, error bars indicate the relative standard deviation

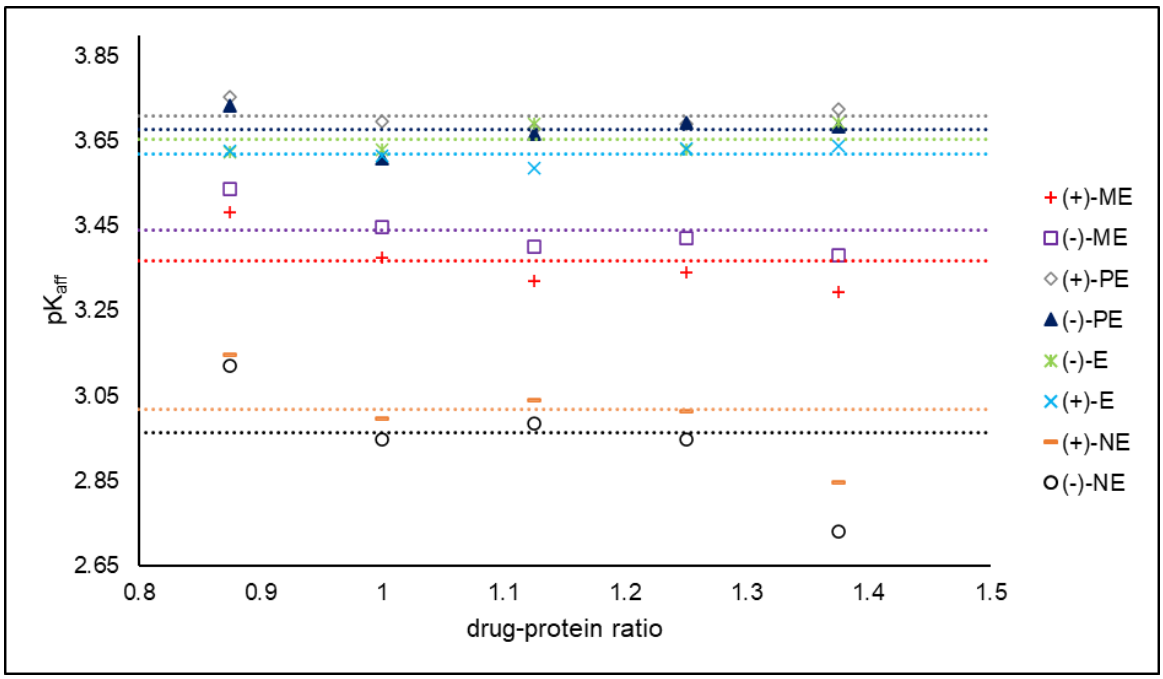

Fig. S2 Representation of pK_{aff} of the individual enantiomers over different drug-protein ratios; the dotted line indicates the respective mean value

Table S1 LOQ of the drugs used

drug	regression line	σ	R^2	LOQ
(+)-E	y = 22.712x – 27.534	21.27	1	9.4 µM
(-)-E	y = 25.319x – 35.978	34.98	0.9999	13.8 µM
(+)-PE	y = 21.361x + 16.136	47.72	0.9993	22.3 µM
(-)-PE	y = 21.215x + 6.9329	39.08	0.9997	18.4 µM
(+)-ME	y = 28.242x – 141.34	79.41	0.9985	29.4 µM
(-)-ME	y = 27.637x – 111.51	70.25	0.9966	27.7 µM
(+)-NE	y = 24.624x -45.174	62.74	0.9993	30.1 µM
(-)-NE	y = 24.116x – 41.267	73.34	0.9990	23.9 µM
sotalol enantiomer 1	y = 13.01x – 29.446	23.00	0.9989	17.7 µM
sotalol enantiomer 2	y = 13.096x + 9.6465	18.72	0.9996	14.3 µM

Table S2 Comparison of epitope mapping of the ephedrine derivatives and their enantiomers at different ligand concentrations and an AGP concentration of 15 µM (values are expressed as a percentage in comparison to the most intense normalized STD-factor)

enantiomer	ligand concentration	H_{phenyl}	$C\text{-}CH_3$	$N\text{-}CH_3$
(+)-NE	200 µM	100%	85.2%	-
	300 µM	100%	86.1%	-
	400 µM	100%	86.0%	-
	500 µM	100%	87.0%	-
	600 µM	100%	89.0%	-
(-)-NE	200 µM	91.3%	100%	-
	300 µM	93.8%	100%	-
	400 µM	94.2%	100%	-
	500 µM	93.9%	100%	-
	600 µM	91.3%	100%	-
(+)-E	200 µM	96.2%	64.8%	100%
	300 µM	93.6%	79.2%	100%
	400 µM	100%	73.4%	91.6%
	500 µM	100%	85.5%	94.7%
	600 µM	100%	81.6%	95.8%
(-)-E	200 µM	100%	79.3%	39.2%
	300 µM	100%	79.5%	40.0%
	400 µM	100%	80.8%	44.8%
	500 µM	100%	95.3%	35.6%
	600 µM	100%	88.2%	44.9%
(+)-PE	200 µM	100%	81.3%	59.1%
	300 µM	100%	85.2%	60.8%
	400 µM	100%	84.3%	62.4%
	500 µM	100%	82.2%	58.1%
	600 µM	100%	85.1%	60.1%
(-)-PE	200 µM	100%	83.1%	56.4%
	300 µM	100%	84.1%	58.8%
	400 µM	100%	82.4%	55.4%
	500 µM	100%	81.6%	60.2%
	600 µM	100%	80.9%	57.3%
(+)-ME	200 µM	100%	93.2%	70.0%
	300 µM	100%	96.8%	72.9%
	400 µM	100%	95.4%	73.6%
	500 µM	100%	94.6%	75.5%
	600 µM	100%	91.2%	72.3%
(-)-ME	200 µM	91.2%	100%	51.2%
	300 µM	93.7%	100%	52.8%
	400 µM	95.4%	100%	52.0%
	500 µM	96.3%	100%	54.3%
	600 µM	94.5%	100%	53.1%

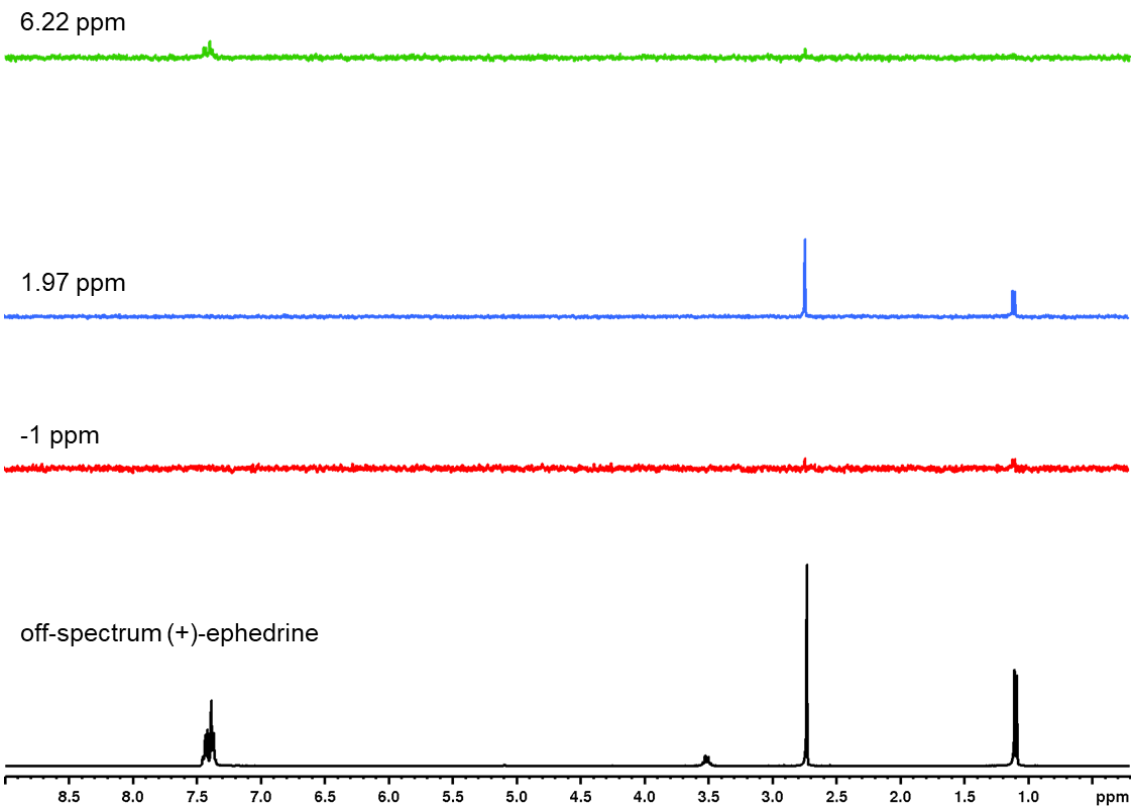

Fig. S3 On-resonance spectrum at the respective saturation pulses in comparison to the off-spectrum without saturation pulse of (+)-ephedrine all spectra were obtained with water signal suppression

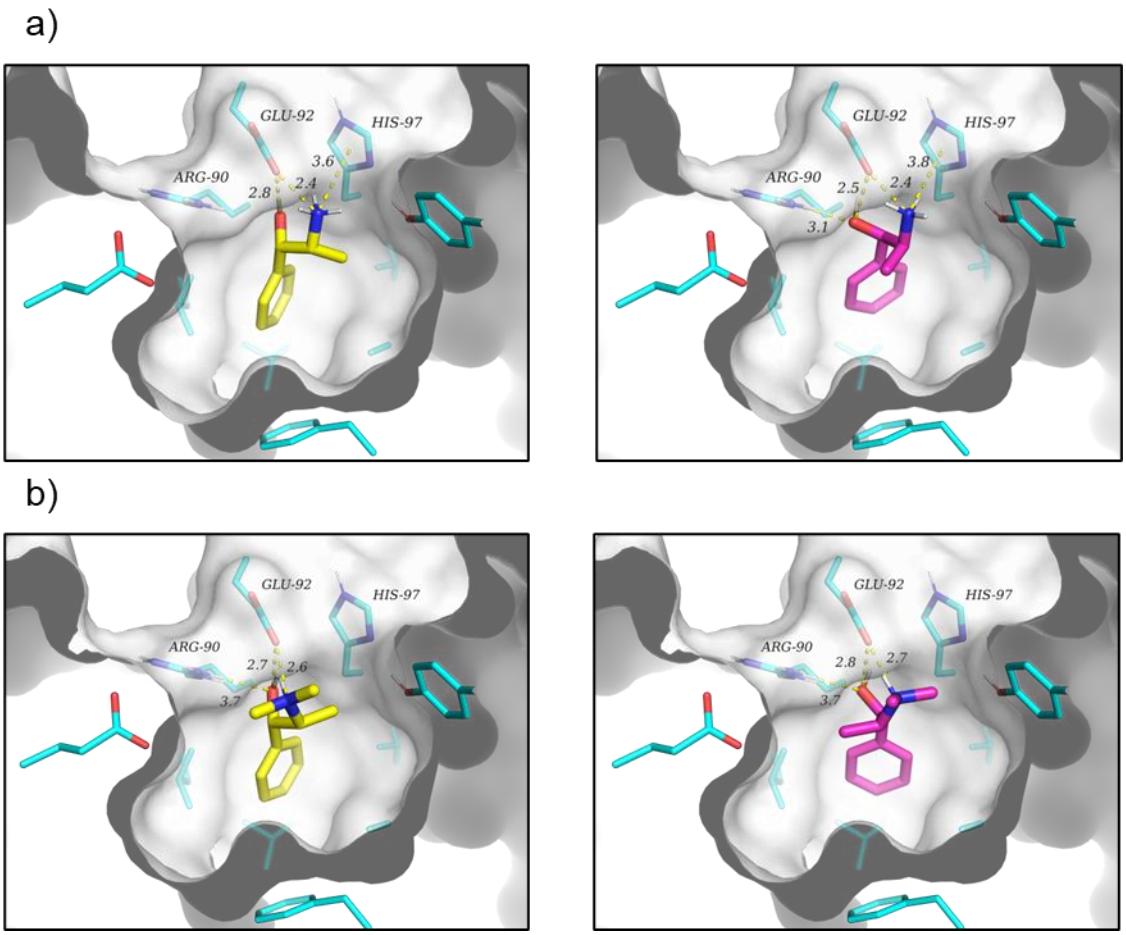

Fig. S3 Docking results of a) norephedrine and b) methylephedrine with varian A of AGP; yellow = (+)-enantiomer; pink = (-)-enantiomer

References:

Becker, B.A., Larive, C.K., 2008. Probing the binding of propranolol enantiomers to α1-acid glycoprotein with ligand-detected NMR experiments. J Phys Chem B 112, 13581-13587.https://doi.org/10.1021/jp8060366

Belpaire, F., Bogaert, M., Rosseneu, M., 1982. Binding of β-adrenoceptor blocking drugs to human serum albumin, to α 1-acid glycoprotein and to human serum. Eur J Clin Pharmacol 22, 253-256.https://doi.org/10.1007/BF00545224

Berezhkovskiy, L.M., 2007. On the calculation of the concentration dependence of drug binding to plasma proteins with multiple binding sites of different affinities: determination of the possible variation of the unbound drug fraction and calculation of the number of binding sites of the protein. J Pharm Sci 96, 249-257.https://doi.org/10.1002/jps.20777

Bteich, M., 2019. An overview of albumin and alpha-1-acid glycoprotein main characteristics: highlighting the roles of amino acids in binding kinetics and molecular interactions. Heliyon 5, e02879.https://doi.org/10.1016/j.heliyon.2019.e02879

Case, D.A., Cheatham III, T.E., Darden, T., Gohlke, H., Luo, R., Merz Jr, K.M., Onufriev, A., Simmerling, C., Wang, B., Woods, R.J., 2005. The Amber biomolecular simulation programs. J Comput Chem 26, 1668-1688

Case, D.A., Darden, T.A., Cheatham, T.E., Simmerling, C.L., Wang, J., Duke, R.E., Luo, R., Crowley, M., Walker, R.C., Zhang, W., 2008. Amber 10. University of California.

Charifson, P.S., Walters, W.P., 2014. Acidic and basic drugs in medicinal chemistry: a perspective. J Med Chem 57, 9701-9717.https://doi.org/10.1021/jm501000a

Cruz, J.R., Larive, C.K., 2012. Determination of the binding epitope of lidocaine with AGP: minimizing the effects of nonspecific binding in saturation transfer difference experiments. Anal Bioanal Chem 402, 337-347.https://doi.org/10.1007/s00216-011-5358-8

Dong, Y.-M., An, Q., Lu, N.-W., Li, N., 2015. Development micellar HPLC method for simultaneous determination of ephedrine, pseudoephedrine, and methylephedrine in Ephedra Herb and traditional Chinese medicinal preparations. Acta Chromatogr 27, 355-372.https://doi.org/10.1556/achrom.27.2015.2.11

Du, X., Li, Y., Xia, Y.-L., Ai, S.-M., Liang, J., Sang, P., Ji, X.-L., Liu, S.-Q., 2016. Insights into protein–ligand interactions: mechanisms, models, and methods. International Journal of Molecular Sciences 17, 144

Fabresse, N., Uteem, I., Lamy, E., Massy, Z., Larabi, I.A., Alvarez, J.-C., 2020. Quantification of free and protein bound uremic toxins in human serum by LC-MS/MS: comparison of rapid equilibrium dialysis and ultrafiltration. Clinica Chimica Acta 507, 228-235.https://doi.org/10.1016/j.cca.2020.04.032

Fournier, T., Medjoubi-N, N., Porquet, D., 2000. Alpha-1-acid glycoprotein. Biochim Biophys Acta 1482, 157-171.https://doi.org/10.1016/S0167-4838(00)00153-9

Guo, B., Xia, Z., Chen, G., Yin, Y., Xu, H., 2003. Study on the interaction of ephedrine, caffeine and acetaminophen with bovine serum albumin by capillary electrophoresis with partial filling technique. Chin J Chromatogr (Se Pu) 21, 367-370.http://dx.doi.org/10.3321/j.issn:1000-8713.2003.04.015

Huang, Q., Zhang, A.-p., Hao, J., Yang, J.-y., Mao, H.-s., 2011. Study on the interaction of ephedrine hydrochloride and pseudoephedrine hydrochloride with human serum albumin by spectroscopy. JAST, 04

Israili, Z., Dayton, P., 2001. Human alpha-1-glycoprotein and its interactions with drugs. Drug Metab Rev 33, 161-235.https://doi.org/10.1081/DMR-100104402

Kaliszan, R., Nasal, A., Turowski, M., 1995. Binding site for basic drugs on α1-acid glycoprotein as revealed by chemometric analysis of biochromatographic data. Biomed Chromatogr 9, 211-215.https://doi.org/10.1002/bmc.1130090504

Klotz, I.M., Hunston, D.L., 1971. Properties of graphical representations of multiple classes of binding sites. Biochemistry 10, 3065-3069

Krishnan, V., 2005. Ligand screening by saturation-transfer difference (STD) NMR spectroscopy. Curr Anal Chem 1, 307-320.https://doi.org/10.2174/157341105774573956

Mayer, M., 2001. STD-NMR-Spektroskopie: Eine neue Methode zur Identifizierung und Charakterisierung von Ligand-Rezeptor-Interaktionen. University of Hamburg.

Morris, G.M., Goodsell, D.S., Halliday, R.S., Huey, R., Hart, W.E., Belew, R.K., Olson, A.J., 1998. Automated docking using a Lamarckian genetic algorithm and an empirical binding free energy function. J Comput Chem 19, 1639-1662.https://doi.org/10.1002/(SICI)1096-987X(19981115)19:14%3C1639::AID-JCC10%3E3.0.CO;2-B

Nishi, K., Ono, T., Nakamura, T., Fukunaga, N., Izumi, M., Watanabe, H., Suenaga, A., Maruyama, T., Yamagata, Y., Curry, S., 2011. Structural insights into differences in drug-binding selectivity between two forms of human α1-acid glycoprotein genetic variants, the A and F1* S forms. J Biol Chem 286, 14427-14434.https://doi.org/10.1074/jbc.M110.208926

Oehlmann, M., 1996. Bestimmung der Blut-Eiweßbindung von Suramin und Analogen - Validierung eines rechnergesteuerten Verfahrens. University of Bonn.

Scatchard, G., 1949. The attractions of proteins for small molecules and ions. Ann N Y Acad Sci 51, 660-672.https://doi.org/10.1111/j.1749-6632.1949.tb27297.x

Schönfeld, D.L., Ravelli, R.B., Mueller, U., Skerra, A., 2008. The 1.8-Å crystal structure of α1-acid glycoprotein (Orosomucoid) solved by UV RIP reveals the broad drug-binding activity of this human plasma lipocalin. J Mol Biol 384, 393-405.https://doi.org/10.1016/j.jmb.2008.09.020

Shalaeva, M., Kenseth, J., Lombardo, F., Bastin, A., 2008. Measurement of dissociation constants (pKa values) of organic compounds by multiplexed capillary electrophoresis using aqueous and cosolvent buffers. J Pharm Sci 97, 2581-2606.https://doi.org/10.1002/jps.21287

Sudlow, G., Birkett, D., Wade, D., 1975. The characterization of two specific drug binding sites on human serum albumin. Mol Pharmacol 11, 824-832

Till, A.E., Benet, L.Z., 1979. Renal excretion of pseudoephedrine in the rat. JPET 211, 555-560

Tillement, J.-P., Lhoste, F., Giudicelli, J., 1978. Diseases and drug protein binding. Clin Pharmacokinet 3, 144-154.https://doi.org/10.2165/00003088-197803020-00004

Viegas, A., Manso, J., Nobrega, F.L., Cabrita, E.J., 2011. Saturation-transfer difference (STD) NMR: a simple and fast method for ligand screening and characterization of protein binding. J Chem Educ 88, 990-994.https://doi.org/10.1021/ed101169t

Volpp, M., Holzgrabe, U., 2019. Determination of plasma protein binding for sympathomimetic drugs by means of ultrafiltration. Eur J Phar. Sci 127, 175-184.https://doi.org/10.1016/j.ejps.2018.10.027

Walpole, S., Monaco, S., Nepravishta, R., Angulo, J., 2019. STD NMR as a technique for ligand screening and structural studies. Methods Enzymol 615, 423-451.https://doi.org/10.1016/bs.mie.2018.08.018

Wedig, M., Laug, S., Christians, T., Thunhorst, M., Holzgrabe, U., 2002. Do we know the mechanism of chiral recognition between cyclodextrins and analytes? J Pharm Biomed Anal 27, 531-540.https://doi.org/10.1016/S0731-7085(01)00579-9

Yang, J., Hage, D.S., 1994. Chiral separations in capillary electrophoresis using human serum albumin as a buffer additive. Anal Chem 66, 2719-2725

Yuasa, I., Weidinger, S., Umetsu, K., Suenaga, K., Ishimoto, G., Eap, B., Duche, J.C., Baumann, P., 1993. Orosomucoid system: 17 additional orosomucoid variants and proposal for a new nomenclature. Vox Sang 64, 47-55.https://doi.org/10.1111/j.1423-0410.1993.tb02514.x

3.2. Method Development, Optimization, and Validation of the Separation of Ketamine Enantiomers by Capillary Electrophoresis Using Design of Experiments

Sebastian Schmidt, Ulrike Holzgrabe

Reprinted with permission from Chromatographia (2023) 86, 87-95

https://doi.org/10.1007/s10337-022-04229-w

Abstract

Capillary electrophoresis was chosen as cost-effective and robust method to separate ketamine enantiomers. For the method development, first different native and modified cyclodextrins were tested. The most promising chiral selector was α-cyclodextrin. A design of experiments (DoE) was carried out, which started with the screening of relevant factors. Based on these results, the method was optimized according to the significant factors (buffer, respectively cyclodextrin concentration, pH value, voltage, temperature) of the screening based on the responses resolution and migration time of the later migrating enantiomer. The optimized conditions consisted of a background electrolyte with 275 mM TRIS, adjusted with 85% phosphoric acid to a pH of 2.50, and 5 mM α-cyclodextrin, at a temperature of 15 °C, an applied voltage of 30 kV and an injection pressure of 1.0 psi for 10 s. A fused-silica capillary with a total length of 70 cm and an effective length to the detector of 60 cm was used. The method was validated according to ICH guideline Q2 R(1). The limit of quantification was 3.51 µg/ml for *S*-ketamine and 3.98 µg/ml for *R*-ketamine. The method showed good linearity for racemic ketamine with R^2 of 0.9995 for *S*-ketamine and 0.9994 for *R*-ketamine. The lowest quantifiable content of *S*-ketamine found in *R*-ketamine was 0.45%.

1. Introduction

Ketamine has been used in drug therapy for over 50 years. Due to its antagonistic effect on the NMDA receptor, it is mainly applied in anesthesia [1]. Recently, research has also been conducted into other areas of application such as neuropathic pain and depression [2]. The dose-dependent effects are particularly interesting. Sub anesthetic doses lead to psychotic states such as hallucinations, floating sensations, and a lack of sense of time and space [3]. The effect of ketamine is not only limited to the NMDA receptor, but also acts on other receptors, which causes many physiological effects. Among them are

muscarinic, nicotinic, and opioid receptors, thus ketamine acts as a so-called dirty drug [4]. Because of its psychotic's effects, ketamine is abused as a party drug [5] and is therefore subject to strong legal restrictions on trade and therapy. Ketamine consists of two stereoisomers, which also differ in their effects. The *S*-enantiomer shows a higher potency than the *R*-enantiomer at the NDMA receptor and thus shows a higher anesthetic effect [6]. However, both the racemate and the enantiomerically pure *S*-ketamine are commercially available. To ensure the enantiomeric purity of *S*-ketamine, the European Pharmacopoeia makes use of HPLC with a chiral AGP column [7]. This column and chiral cellulose columns have already been used for the chiral separation of ketamine enantiomers by means of HPLC [8-10]. Unfortunately, chiral columns are very expensive. A cheaper alternative is chiral capillary electrophoresis (CE). With mainly cyclodextrins as chiral selectors [11], it is possible to easily separate the enantiomers from each other, as different diastereomeric complexes of the enantiomers are formed with the cyclodextrin. In the past, some methods have been published that use negatively charged sulphated cyclodextrins to separate the ketamine enantiomers [12-18]. However, as the degree of substitution of the cyclodextrin of different batches may differ [19], separations can be negatively affected, resulting in worse results. Single isomer cyclodextrins which do not have this disadvantage are to be preferred but are much more expensive due to the more complex production. Methods that have used native cyclodextrins such as α-cyclodextrin [20-22], β-cyclodextrin [23] and γ-cyclodextrin [24] have been published as well. The aim of this work was to develop a well reproducible and cheap method based on previous publications to improve the separation of the enantiomers of ketamine and to assess the enantiomeric purity of the respective enantiomer by means of CE. The focus was on achieving baseline separation with improved resolution using a native cyclodextrin and design of experiments (DoE) to statistically validate the method development.

2. Materials and methods

2.1. Chemicals

Sodium hydroxide platelets, phosphoric acid 85%, tris-(hydroxymethyl)-aminomethane (TRIS), β-cyclodextrin sulfated sodium, carboxymethyl-β-cyclodextrin sodium salt (CM-β-CD), 2-hydroxypropyl-β-cyclodextrin, β-cyclodextrin, methyl-β-cyclodextrin, heptakis-(2,3,6-tri-O-methyl)-β-cyclodextrin (TM-β-CD), racemic ketamine hydrochloride and *R*-ketamine hydrochloride were purchased from Sigma Aldrich (Darmstadt, Germany). α-cyclodextrin and γ-cyclodextrin were obtained from Wacker Chemie (München, Germany). Heptakis-(2,3-di-O-acetyl-6-sulfo-)-β-cyclodextrin (HDAS-β-CD) was bought from Regis Technologies (Morton Grove, Texas, US), 0,1 M sodium hydroxide solution

from VWR Chemicals (Darmstadt, Germany), hydrochloric acid 37% from Bernd Kraft (Duisburg, Germany) and neostigmine bromide from Roche (Grenzach, Germany). Deionized water was obtained from an in-house water purification system from Merck Millipore (Darmstadt, Germany).

2.2. Sample and buffer preparation

The background electrolyte (BGE) was prepared by weighing the appropriate amount of TRIS and adjusting it to the respective pH value with 85% phosphoric acid. The chiral selector was weighed in and dissolved in the BGE. For validation, stock solutions of 658.1 µg/ml racemic ketamine, 137.1 µg/ml *R*-ketamine and 274.2 µg/ml neostigmine bromide, as well as stock solutions of 1000 µg/ml *R*-ketamine, 187.5 µg/ml racemic ketamine and 750 µg/ml of neostigmine bromide in deionized water for the determination of the lowest amount of *S*-ketamine in *R*-ketamine. For the individual samples and the calibration points, the respective volumes of the stock solutions were transferred to a 5.0 mL flask and diluted with deionized water. For the determination of the lowest amount of *S*-ketamine the respective volumes of the stock solutions were mix up with deionized water to a total volume of 750 µl. Prior to use, BGE and sample solutions were filtered using a 0.45 µm PVDF filter (Carl Roth, Karlsruhe, Germany).

2.3. Instrumentation

pH measurements were performed with a pH meter from Metrohm (Filderstadt, Germany). The CE system used was a P/ACE MDQ system from Sciex (Darmstadt, Germany) with a photodiode array detector.

2.4. Electrophoretic conditions

A fused silica capillary from BGB Analytik Vertrieb (Rheinfelden, Germany) with an internal diameter of 50 µm, a total length of 70 cm and an effective length of 60 cm was chosen for the separation. Samples were injected at a pressure of 1.0 psi for 10.0 s. The capillary was conditioned first with 1.0 M sodium hydroxide solution, second with 2.0 M hydrochloric acid and third with deionized water at a pressure of 30.0 psi, each for 10.0 min. Subsequently, the capillary was rinsed with BGE for 2 min and a voltage of 20.0 kV for 20 min was applied. Before each sample injection, the capillary was rinsed 1.0 min with 0.1 M sodium hydroxide, 1.0 min deionized water and 2.0 min with BGE at a pressure of 20.0 psi. Analytes were detected at a wavelength of 194 nm.

2.5. Software

Data evaluation of the CE measurements was performed with 32 Karat Software 8.0 from Sciex (Darmstadt, Germany). The design of the experimental plans and the statistical evaluation were carried out with design expert 12.0 (Minneapolis, Minnesota, US).

3. Results and discussion

The aim was to develop a well reproducible and cheap method for the separation of ketamine enantiomers. Several methods are described in the literature, which used mainly a TRIS buffer or phosphate buffer with acidic pH value and a negatively charged sulfated cyclodextrin as chiral selector [13-15; 17; 18]. Inhomogeneously substituted cyclodextrins can have a negative influence on a separation, as already mentioned. To circumvent this problem and to avoid obtaining expensive single isomer cyclodextrins, special attention had to be paid to native cyclodextrins, where also already some methods were published [20-24]. Fillet et al. developed a procedure for the separation of enantiomers with neutral and charged cyclodextrins [25]. For basic drugs, like ketamine, a 100 mM phosphate buffer adjusted to pH 3.00 with triethanolamine is recommended. Starting concentrations of the chiral selectors are 5 mM for charged and 15 mM for neutral cyclodextrins. α-cyclodextrin, β-cyclodextrin, γ-cyclodextrin, methyl-β-cyclodextrin, TM-β-CD as neutral cyclodextrins were tested and sulfated β-cyclodextrin, CM-β-CD and HDAS-β-CD as charged cyclodextrins, respectively. For all charged cyclodextrins, no separation occurred either at positive voltage or negative voltage, even when the cyclodextrin concentration was increased up to 50 mM. α-cyclodextrin, β-cyclodextrin, and γ-cyclodextrin showed a separation but not yet a baseline separation, while TM-β-CD and methyl-β-CD showed no separation. Example electropherograms are shown in Fig. S1. When the concentration of the respective chiral selector was increased under positive voltage, the migration times increased as well but the resolution improved. The best results were found with α-cyclodextrin and γ-cyclodextrin. Further experiments were carried out with these two cyclodextrins. A TRIS phosphate buffer as well as a pure phosphate buffer with pH 3.0 were tried out as alternative background electrolyte. Only when the temperature was lowered, both enantiomers could be baseline separated from each other. Similar observation was reported by Amini et al. [20]. The combination of TRIS buffer with α-cyclodextrin and low temperature showed the best results with an improved resolution compared to previously published methods.

3.1. Screening

Based on the results of the preliminary investigations, the pH value of the separation buffer, the concentration of the TRIS buffer and α-cyclodextrin, temperature and voltage were selected as factors with which screening and further method optimization should be carried out. A screening experiment should provide as much information as possible with as few experiments as possible. A face-centered central composite (FCCC) design with six center points was used as the experimental design for the screening. A two-stage circumscribed central composite (CCC) design could not be performed because the CE system used could not cool the capillary below 15 °C, therefore there is a limitation to the factor level. The following parameters were chosen as the starting and center point: 200 mM TRIS buffer, adjusted to pH 3.0 with phosphoric acid, 50 mM α-cyclodextrin, 17.5 °C and a voltage of 27.5 kV. As analytical response the resolution based on Eq. (1) and the migration time of the later migrating enantiomer were chosen.

$$\text{Eq. (1)} \quad R_s = \frac{1{,}18 * (t_{mig\,2} - t_{mig\,1})}{(w_{0,5\,h\,1} + w_{0,5\,h\,2})}$$

The experimental plan with the respective factor levels and the obtained results can be found in Table 1. The running order was randomized. Regarding the buffer concentration, it could be seen, that an increase led to a prolongation of the migration time but also to a better resolution. A higher voltage led to significantly reduced migration times and at the same time also increased the resolution. Increasing the α-cyclodextrin concentration only increased the migration time and did not improve the resolution significantly. The selected factor level concentration of 60 mM already seems to be close at the optimum for chiral separation. The same effect can be seen with the change of the pH value, whereby a reduction in the pH value showed a minimal improvement in the resolution. Besides the buffer concentration, a change in temperature showed the greatest impact. Reducing the temperature produced better resolution, but also greatly slowed down migration times.

Table 1 Factor A = TRIS concentration [mM], Factor B = pH value, Factor C = temperature [°C], Factor D = voltage [kV], Factor E = α-cyclodextrin concentration [mM], Response 1 = resolution, Response 2 = migration time of the later migrating enantiomer [min]

Run	Factor A	Factor B	Factor C	Factor D	Factor E	Response 1	Response 2
1	150	2.5	20.0	30.0	60	1.51	22.6
2	250	3.5	20.0	25.0	40	1.62	28.5
3	250	3.5	15.0	30.0	40	2.05	27.4
4	200	3.0	17.5	27.5	50	1.75	27.5
5	150	2.5	15.0	25.0	60	1.73	32.7
6	150	3.5	20.0	30.0	40	1.70	25.5
7	150	3.5	15.0	25.0	40	1.42	17.2
8	200	3.0	17.5	27.5	50	1.75	26.9
9	150	2.5	20.0	25.0	40	1.47	23.5
10	250	3.5	20.0	30.0	60	1.71	25.2
11	250	3.5	15.0	25.0	60	1.96	38.2
12	200	3.0	17.5	27.5	50	1.72	26.2
13	150	3.5	20.0	25.0	60	1.43	25.2
14	150	3.5	15.0	30.0	60	1.67	24.1
15	250	2.5	20.0	25.0	60	1.69	31.4
16	250	2.5	15.0	30.0	60	2.03	30.0
17	250	2.5	20.0	30.0	40	1.69	21.5
18	200	3.0	17.5	27.5	50	1.70	25.4
19	250	2.5	15.0	25.0	40	1.99	32.4
20	150	2.5	15.0	30.0	40	1.69	21.0

An analysis of variance (ANOVA) was performed on the experimental data. Insignificant factors were removed one after another to the improve the quality of the model. If insignificant factors were involved in interactions which are significant, the factors were included in the model. The equations were recalculated after each factor elimination. Buffer concentration, temperature and voltage identified as significant factor with buffer concentration and temperature being the ones with the highest influence.

$$\text{Resolution} = 1.71 + 0.1325\ \text{A} - 0.0150\ \text{B} - 0.1075\ \text{C} + 0.0462\ \text{D} + 0.0063\ \text{E} - 0.0575\ \text{AC} + 0.0275\ \text{BC} + 0.0413\ \text{BD} - 0.0325\ \text{DE}$$

For the migration time, the statistical analysis is somewhat different. It is in the nature of the method used that all selected factors would have a significant influence. A higher buffer concentration slows down migration due to a higher ionic strength. A further slowdown is seen with an increased cyclodextrin concentration. A faster migration is obtained with a higher voltage and a higher temperature. An increase in pH value in the range of 2.5 to 8.0 is accompanied by a stronger EOF, which usually accelerates migration. Here, however, an increase showed a slight opposite effect. The greatest influence was shown by temperature and voltage.

$$\text{Migration time} = 27.79 + 1.52\ \text{A} + 0.9269\ \text{B} - 2.37\ \text{C} - 3.14\ \text{D} + 0.8636\ \text{E} + 1.01\ \text{AE} - 1.42\ \text{BE} + 1.41\ \text{D}$$

The coefficient of variation R^2 shows the fitting between experimental and modelled values. R^2adj. on the other hand, refers to the number of parameters used in the model. With $R^2 = 0.9702$ and R^2adj. = 0.9404 for the resolution and $R^2 = 0.9738$ and R^2adj. = 0.9505, respectively, for the migration time the data and the model showed a good fit, and the models can be used.

3.2. Method optimization

Buffer concentration, temperature and α-cyclodextrin concentration were selected as factors to be optimized. Since a high voltage resulted in both faster analysis times and better resolution, a maximum voltage of 30 kV was used for the method optimization. A lower pH value resulted in slightly better resolution. Therefore, a pH value of 2.5 was selected for the optimization. This has the additional side effect that the electroosmotic flow has little to no influence on the analysis. Since the used chiral selector is the most expensive component and the concentration of 60 mM in the screening experiments was already near the optimum, the concentration of the chiral selector was chosen as a factor to find out whether a lower concentration also led to a good analysis result besides the non-significantly influence on the separation to save costs. An FCCC design with six center points was selected for the method optimization. The following parameters were chosen as the starting and center point: 250 mM TRIS buffer, adjusted to pH 2.5 with phosphoric acid, 55 mM α-cyclodextrin, 16.0 °C. The voltage was held constant for all runs at 30 kV. The varied factor levels can be seen in Table 2.

Table 2 Factor A = TRIS concentration [mM], Factor B = temperature [°C], Factor C = α-cyclodextrin concentration [mM], Response 1 = resolution, Response 2 = migration time of the later migrating enantiomer [min]

Run	Factor A	Factor B	Factor C	Response 1	Response 2
1	225	15	50	1.76	26.5
2	225	16	55	1.71	25.9
3	250	16	55	1.82	27.1
4	275	16	55	1.88	27.9
5	275	15	60	1.92	30.6
6	275	17	60	1.82	28.3
7	250	16	55	1.82	27.1
8	250	16	55	1.79	27.1
9	250	16	55	1.81	27.1
10	250	16	55	1.83	27.1
11	275	17	50	1.84	26.4
12	250	16	50	1.84	26.4
13	250	16	55	1.80	27.2
14	225	15	60	1.79	28.4
15	225	17	50	1.70	24.5
16	225	17	60	1.69	26.3
17	250	16	60	1.82	28.2
18	250	15	55	1.81	28.6
19	275	15	50	1.96	29.0
20	250	17	55	1.77	26.3

An ANOVA was also performed for the method optimization. The modelling was analogous to the screening. To fit the model, the insignificant factors were excluded. The model for the resolution was based on a linear function and for the migration time on a quadratic function, respectively. The 3D surface plots of the factors and their response can be seen in Fig. 1.

$$\text{Resolution} = 1.809 + 0.77\ \text{A} - 0.042\ \text{B}$$

$$\text{migration time} = 27.0705 + 1.0577\ \text{A} - 1.1286\ \text{B} + 0.8967\ \text{C} - 0.083625\ \text{AB}$$

$$- 0.173455\ \text{A}^2 + 0.394045\ \text{B}^2 + 0.216545\ \text{C}^2$$

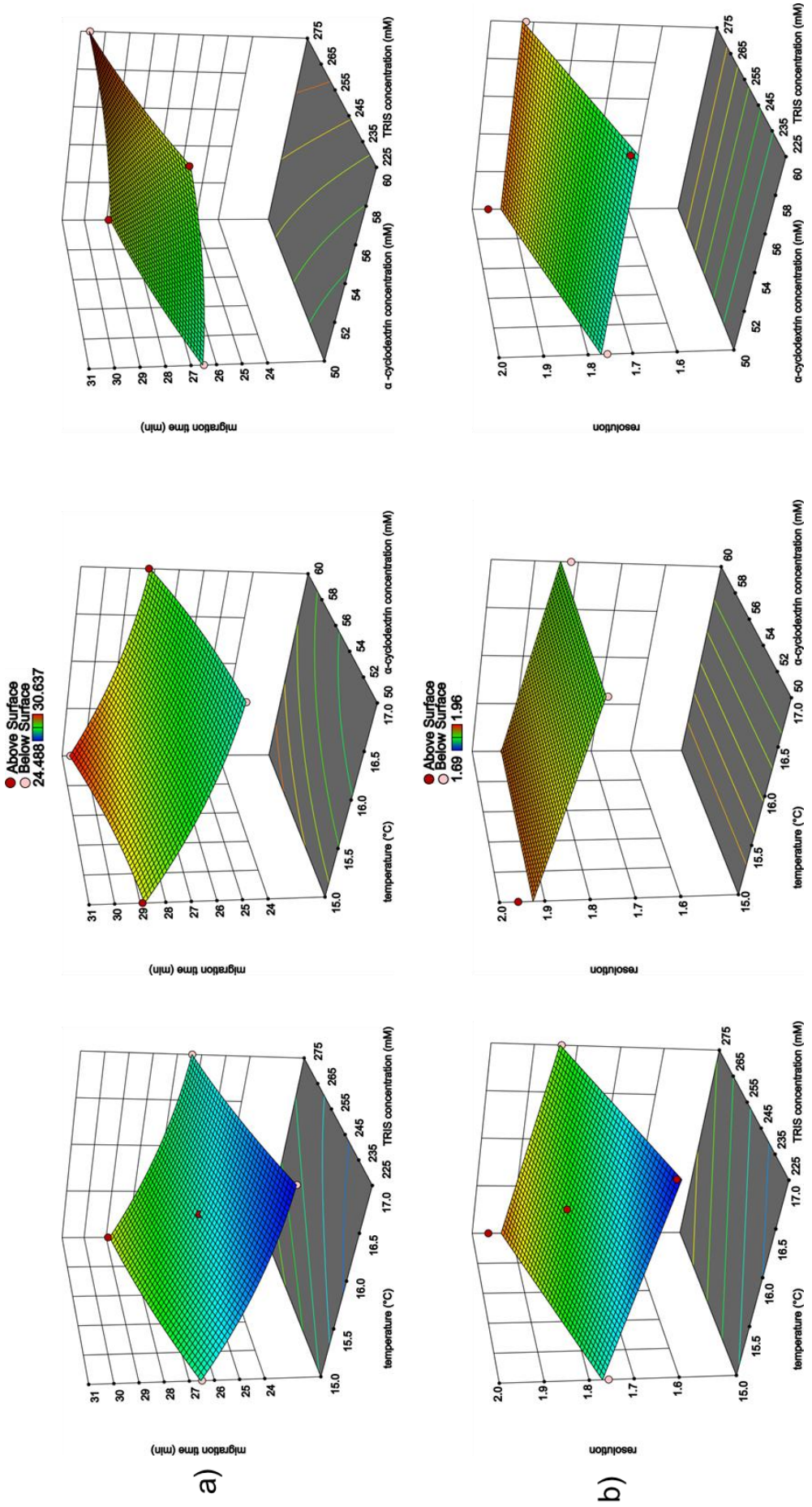

Fig. 1 3D response surface plots for a) migration time and b) resolution

With $R^2 = 0.9204$ and R^2adj. = 0.9111 for the resolution and $R^2 = 0.9991$ and R^2adj. = 0.9986, respectively, for the migration time the data and the model showed a good fit, and an optimization can be carried out. The software´s own optimization function was used. The highest resolution with the shortest migration time should be the goal, while the resolution should be at least 1.9. All conditions were of equal importance. The most optimal condition was found to be a 275 mM TRIS/phosphate buffer with pH 2.5 and 50 mM α-cyclodextrin at a temperature of 15 °C while applying a constant voltage of 30 kV. An electropherogram with the optimized conditions is shown in Fig. 2.

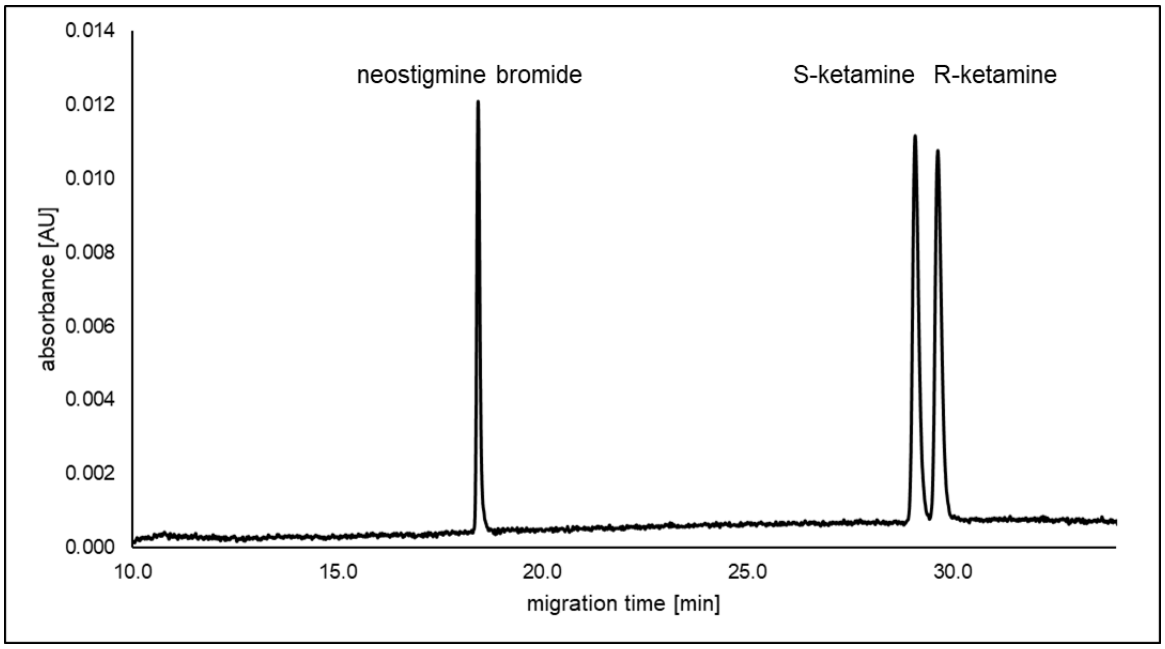

Fig. 2 Electropherogram of racemic ketamine with neostigmine bromide with optimized conditions: 275 mM TRIS buffer adjusted with 85% phosphoric acid to a pH value of 2.50, 50 mM α-cyclodextrin, 15 °C, 30 kV, injection at 1.0 psi for 10 s, fused silica capillary with a total length of 70 cm and an effective length of 60 cm

3.3. Analytical performance/validation

The developed method has been validated according to the ICH Q2 (R1) guideline [26]. The parameters precision, accuracy, specificity, limit of quantification (LOQ), linearity, working range and robustness were evaluated. To determine the precision, three racemic solutions with concentrations of 16.5, 38.4 and 60.3 µg/ml were injected on two different days (n = 3). An additional 35.1 µg/ml neostigmine bromide was added as an internal standard to minimize the influence of UV/Vis detectors fluctuations. The parameters to be tested were the migration time of both enantiomers and their resolution. The accuracy was checked by means of the recovery rate.

For this purpose, three solutions of 8.2 µg/ml racemic ketamine were prepared and spiked with 2.74, 13.7 and 21.9 µg/ml of *R*-ketamine to obtain three different concentration levels (*n* = 3) and an overlay of the electropherograms is shown in Fig. 3.

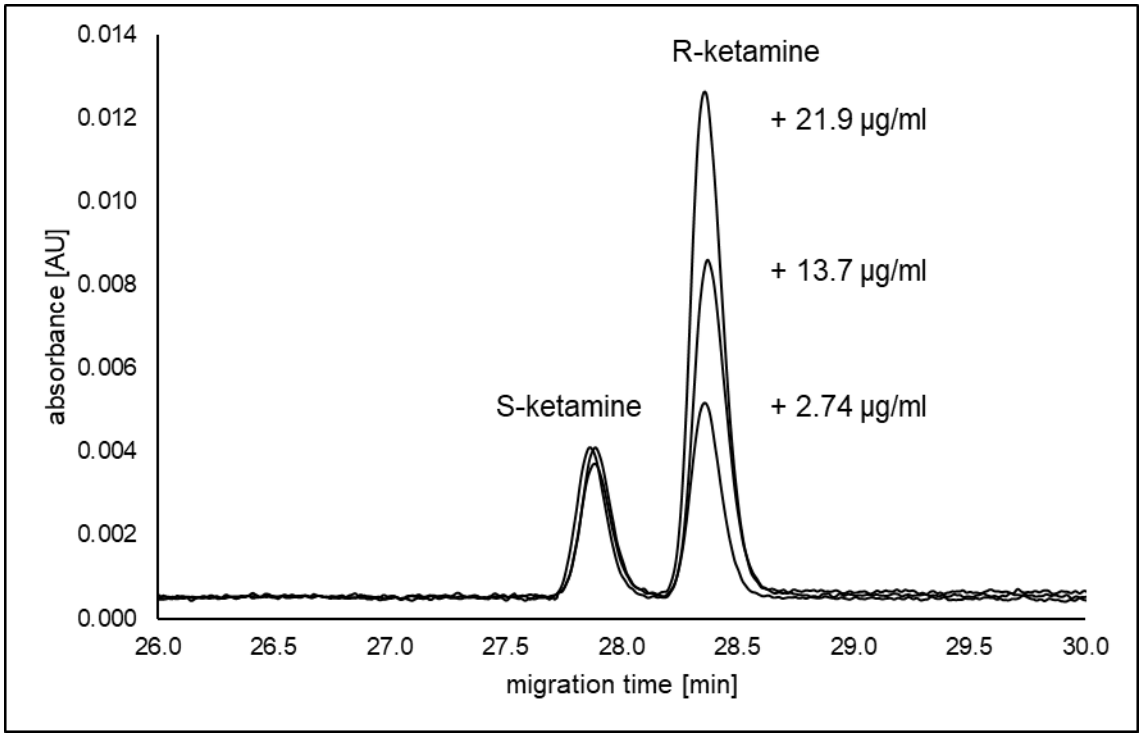

Fig. 3 Overlay of the electropherograms of the 8.2 µg/ml racemic ketamine solutions spiked with 2.74, 13.7, and 21.9 µg/ml of *R*-ketamine under optimized conditions

These solutions were also injected on two different days and quantified. The exact results are listed in Table 3. The solution with additional 21.9 µg/ml *R*-ketamine was used to determine the specificity of the method. The peak of *R*-ketamine is clearly larger than that of the *S*-ketamine. An overlapping of the peaks is also not recognizable. Accordingly, the method is specific for the separation of both ketamine enantiomers and the migration order could be confirmed. For linearity, calibration curves with six different concentration levels of a racemic mixture were measured in triplicate in the range of 5.5 - 32.9 µg/ml per enantiomer. The coefficient of determination of 0.9995 for *S*-ketamine and 0.9994 for *R*-ketamine shows the good linearity of the method. The calibration curves and residual plots are shown in Fig. S2. With these calibration curves, the LOQ was determined according to Eq. (2) with s being the slope of the respective regression line and σ is the standard deviation of the response.

$$\text{Eq. (2) LOQ} = \frac{10 * \sigma}{s}$$

A LOQ of 3.51 µg/ml was determined for *S*-ketamine and a LOQ of 3.98 µg/ml for *R*-ketamine.

To determine the lowest possible content of *S*-ketamine in *R*-ketamine, linearity was determined in the range of 0.1% to 5.0% *S*-ketamine at a constant *R*-ketamine concentration of 500 µg/ml. A coefficient of determination of 0.9996 also indicated good

linearity. The calibration curve and residual plot are shown in Fig. S3. The LOQ of *S*-ketamine was determined again using Eq. (2) and was 2.24 µg/ml which corresponds to 0.45%. Fig. 4 shows an example of an electropherogram of 0.5% *S*-ketamine in *R*-ketamine.

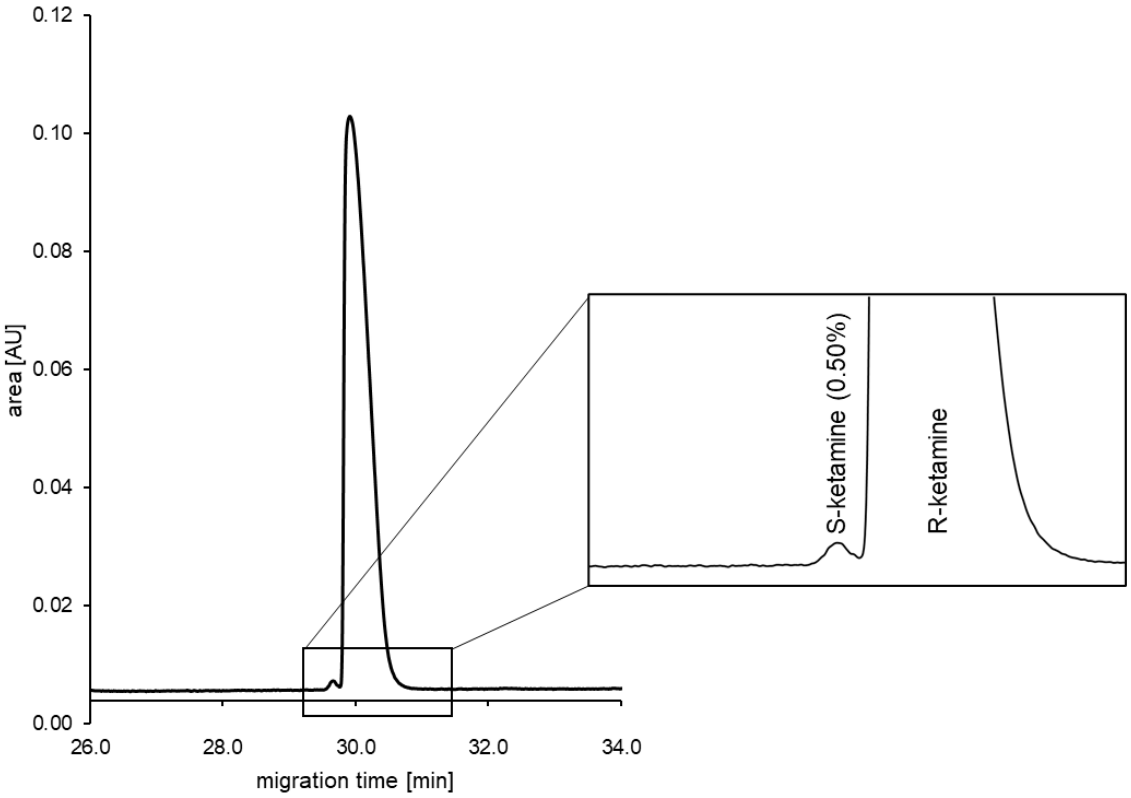

Fig. 4 Electropherogram of 0.50% *S*-ketamine in *R*-ketamine under optimized conditions

Since the resolution according to Eq. (1) should only be used for peaks of equal size, the European pharmacopoeia determines the peak-to-valley ratio according to Eq. (3) for peaks with high concentration differences.

$$\text{Eq. (3)}\quad \frac{\text{p}}{\text{v}} = \frac{\text{Height}_{\text{peak}}}{\text{Height}_{\text{valley}}}$$

The peak-to-valley ratio of 0.5% *S*-ketamine in *R*-ketamine is 4.26 and thus there is still sufficient separation. The two LOQ determined are very similar with the slight difference being explained by the large excess of *R*-ketamine compared to the racemate. To check for accuracy, three samples were measured in triplicate on two different days with 0.75%, 1.5% and 3.0% *S*-ketamine. The recovery rate was in the range of 98.8% to 100.4%. The exact results are listed in Table S1.

A two-level fractional design was again performed to check robustness. pH-value, buffer and cyclodextrin concentration were selected as parameters. Resolution and migration

time were also used as responses, as in screening and optimization. The factor levels and the results can be found in Table 4.

Table 4 Factor A = TRIS concentration [mM], Factor B = pH value, Factor C = α-cyclodextrin concentration [mM], Response 1 = resolution, Response 2 = migration time of the later migrating enantiomer [min]

Run	Factor A	Factor B	Factor C	Response 1	Response 2
1	275	2.5	50	1.93	29.86
2	285	2.6	55	1.98	31.65
3	265	2.6	45	1.82	28.57
4	275	2.5	50	1.92	29.83
5	572	2.5	50	1.97	29.84
6	285	2.4	45	1.95	29.48
7	265	2.4	55	1.89	30.97
8	275	2.5	50	1.96	29.83

Of note, the statistical evaluation showed that the buffer concentration has a significant influence and is therefore not considered a robust parameter. This was foreseeable. However, the responses obtained are within an acceptable range. The worst resolution for racemic ketamine was found 1.82, which still exceeds criteria of the European pharmacopoeia for baseline separation (> 1.5). The migration time increased by two minutes in the worst case. This means that even if a change in buffer concentration has a statistically significant effect on the result, they are still acceptable, and the method can therefore still be regarded as robust [27].

Table 3 Overview of the results and their relative standard deviation [%] of the validation experiments on precision and accuracy

precision				**accuracy**			
day 1							
sample concentration (n=3)		**S-ketamine**	**R-ketamine**	**sample concentration (n=3)**		**S-ketamine**	**R-ketamine**
8.2 µg/ml	*migration time*	29.35 min ± 0.10%	29.91 min ±0.10%	8.2 µg/ml rac. ketamine + 2.74 µg/ml R-ketamine	*recovery rate [%]*	98.17%% ± 1.81%	99.67% ± 1.08%
	resolution	2.00 ± 0.00%					
19.2 µg/ml	*migration time*	29.35 min ± 0.38%	29.91 min ± 0.39%	8.2 µg/ml. ketamine + 13.7 µg/ml R-ketamine		99.45 % ± 1.43%	100.97% ± 2.40%
	resolution	1.99 ± 1.16%					
26.6 µg/ml	*migration time*	29.30 min ± 0.02%	29.97 min ± 0.02%	8.2 µg/ml. ketamine + 21.9 µg/ml R-ketamine		101.86% ± 2.61%	101.61% ± 3.09%
	resolution	1.90 ± 0.30%					
day 2							
8.2 µg/ml	*migration time*	29.45 min ± 0.53%	30.02 min ± 0.53%	8.2 µg/ml ketamine + 2.74 µg/mlR-ketamine	*recovery rate [%]*	100.88% ± 3.94%	102.21% ± 1.66%
	resolution	2.03 ± 0.85%					
19.2 µg/ml	*migration time*	29.03 min ± 0.18%	29.58 min ± 0.13%	8.2 µg/ml. ketamine + 13.7 µg/ml R-ketamine		99.11% ± 2.25 %	100.76% ± 1.0.82%
	resolution	1.97 ± 0.29					
26.6 µg/ml	*migration time*	28.86 min ± 0.23%	29.41 min ± 0.24%	8.2 µg/ml rac. ketamine + 21.9 µg/ml R-ketamine		101.37% ± 1.16%	101.10% ± 1.03%
	resolution	1.91 ± 0.61%					

4. Conclusion

A CE method to separate both ketamine enantiomers with α-cyclodextrin as neutral chiral selector was successfully developed. The resolution could be improved in comparison to existing methods using α-cyclodextrin as chiral selector. The obtained resolution of 2.0 is in the range of methods with charged cyclodextrins (2.2 [13], 2.4 [14]), but the migration time is longer. However, the native cyclodextrin costs significantly less than charged cyclodextrins. Additionally, the separation is not negatively affected by inhomogeneous substitution of charged cyclodextrins as long as non-single isomer cyclodextrins are used. To the best of our knowledge, the presented method is the only CE method for the separation of ketamine enantiomers that has been developed and validated by statistical experimental design. DoE was used for screening and method optimization as well as for the test of robustness. For the first two a FCCC design was used, for robustness a two-level fractional design. The method was optimized for a minimum resolution of 1.9 of racemic ketamine and the fastest possible migration time of the later migrating enantiomer which was the *R*-ketamine. A separation with the optimized parameters was achieved within 30 minutes. The lowest possible quantifiable content of *S*-ketamine in *R*-ketamine was 0.45%.

Upon validation the method was found to be accurate, robust, specific, linear, and reproducible.

Conflict of interests

None of the authors of this paper does have a financial or personal relationship with other people or organizations that could inappropriately influence or bias the content of the paper.

Acknowledgements:

Thanks are due to Karlo Heider for practical support in the lab.

Funding:

The authors declare that no funds, grants, or other support were received during the preparation of this manuscript.

Competing Interests:

The authors have no relevant financial or non-financial interests to disclose.

SUPPLEMENTARY MATERIAL

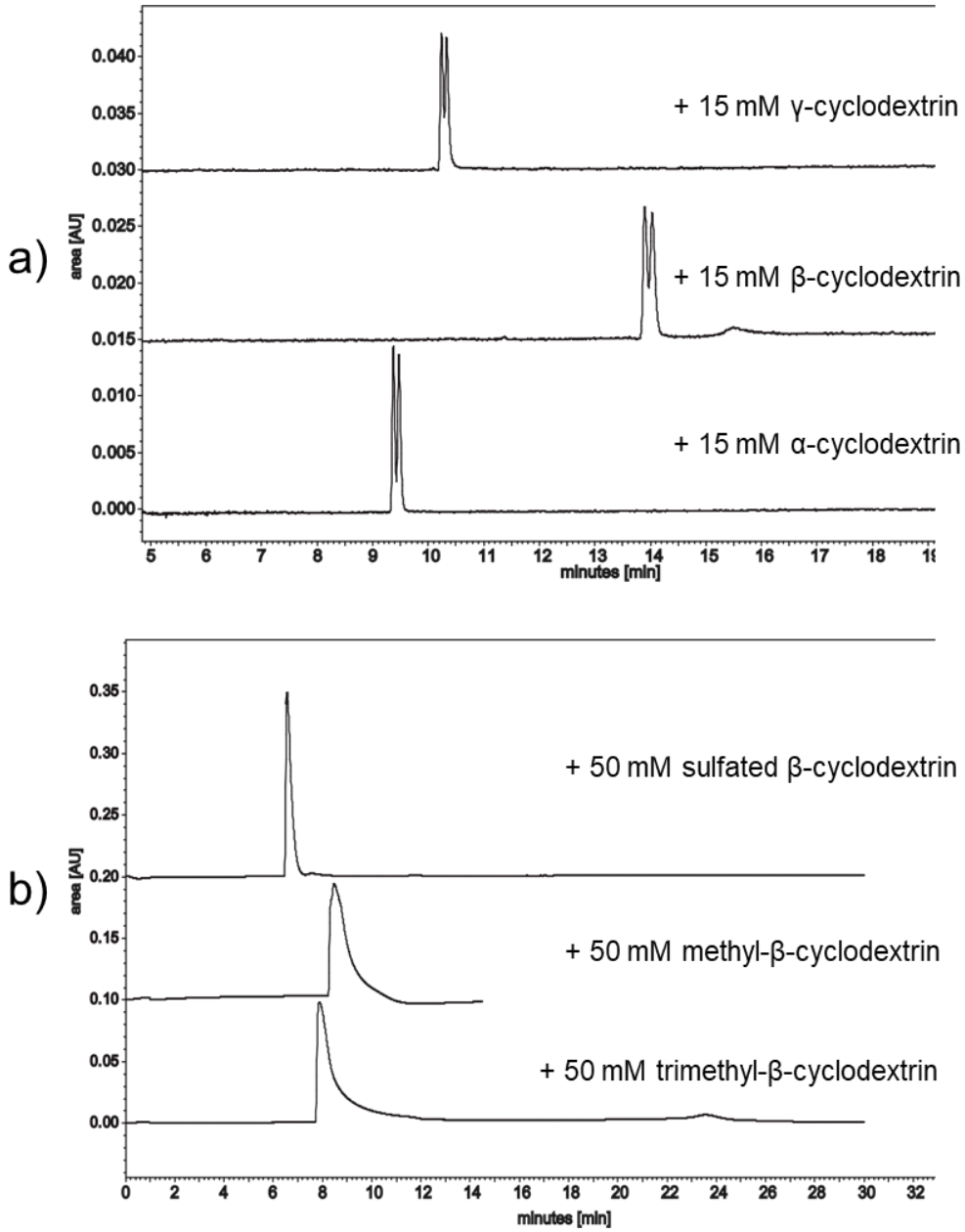

Fig. S1 Electropherograms of the preliminary analysis of native (a) and modified (b) cyclodextrins with the conditions: background electrolyte consisting of 100 mM phosphate, adjusted to pH 3.00 with triethanolamine, 25 °C, 30 kV, injection at 1.0 psi for 10 s, fused silica capillary with a total length of 60 cm and an effective length of 52 cm

.

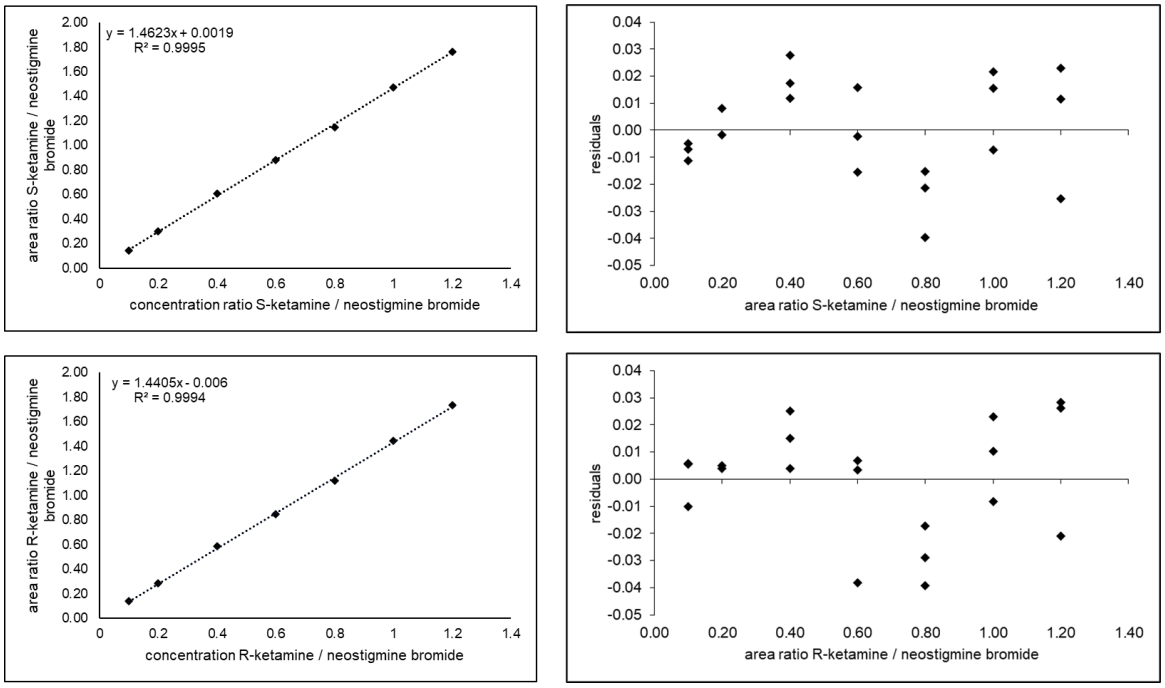

Fig. S2 Calibration curves and residual plots of racemic ketamine for the LOQ determination

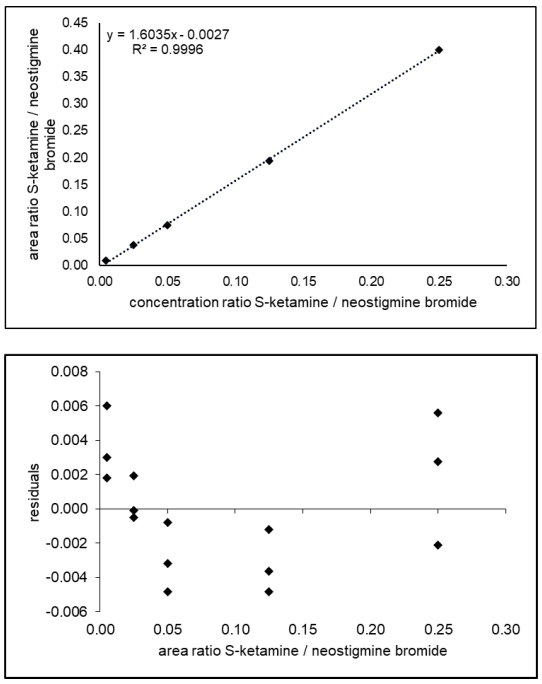

Fig. S3 Calibration curve and residual plot for the determination of the lowest amount of *S*-ketamine in *R*-ketamine

Table S1 Results of the determination of the lowest content of *S*-ketamine in *R*-ketamine

***S*-ketamine [µg/ml]**	***S*-ketamine [%]**	**Recovery [%]**	**RSD [%]**	**Recovery [%]**	**RSD [%]**
		Day 1		**Day 2**	
3.75	0.75	100.4	2.78	100.4	0.87
7.5	1.50	99.5%	0.66	99.5	0.87
15.0	3.00	100.2%	3.20	98.8	1.28

References

[1] Kohtala, S. (2021). Ketamine-50 years in use: from anesthesia to rapid antidepressant effects and neurobiological mechanisms. Pharmacol Rep., 73(2), 323-345. doi:https://doi.org/10.1007/s43440-021-00232-4

[2] Das, J. (2020). Repurposing of Drugs–The Ketamine Story. J Med Chem, 63(22), 13514-13525. doi:https://doi.org/10.1021/acs.jmedchem.0c01193

[3] Domino, E. F., & Warner, D. S. (2010). Taming the ketamine tiger. Anesthesiology, 113(3), 678-684. doi:https://doi.org/10.1097/ALN.0b013e3181ed09a2

[4] Sinner, B., & Graf, B. (2008). Ketamine.

[5] Liu, Y., Lin, D., Wu, B., & Zhou, W. (2016). Ketamine abuse potential and use disorder. Brain Res. Bull., 126, 68-73. doi:https://doi.org/10.1016/j.brainresbull.2016.05.016

[6] White, P., Ham, J., Way, W., & Trevor, A. (1980). Pharmacology of ketamine isomers in surgical patients.

[7] EDQM. (2022). Monograph Esketamine hydrochloride. In: European Pharmacopeia Online 10.8, Council of Europe, Straßbourg, France.

[8] Aboul-Enein, H. Y., & Islam, M. R. (1992). Enantiomeric separation of ketamine hydrochloride in pharmaceutical formulation and human serum by chiral liquid chromatography. J. Liq. Chromatogr. Relat. Technol., 15(18), 3285-3293. doi:https://doi.org/10.1080/10826079208020884

[9] Geisslinger, G., Menzel-Soglowek, S., Kamp, H.-D., & Brune, K. (1991). Stereoselective high-performance liquid chromatographic determination of the enantiomers of ketamine and norketamine in plasma. J. Chromatogr. B Biomed. Appl., 568(1), 165-176. doi:https://doi.org/10.1016/0378-4347(91)80350-L

[10] Svensson, J.-O., & Gustafsson, L. L. (1996). Determination of ketamine and norketamine enantiomers in plasma by solid-phase extraction and high-performance liquid chromatography. J. Chromatogr. B Biomed. Appl., 678(2), 373-376. doi:https://doi.org/10.1016/0378-4347(95)00545-5

[11] Juvancz, Z., & Szejtli, J. (2002). The role of cyclodextrins in chiral selective chromatography. Trends Analyt Chem, 21(5), 379-388. doi:https://doi.org/10.1016/S0165-9936(02)00506-X

[12] Cherkaoui, S., & Veuthey, J.-L. (2002). Use of negatively charged cyclodextrins for the simultaneous enantioseparation of selected anesthetic drugs by capillary electrophoresis–mass spectrometry. J Pharm Biomed Anal, 27(3-4), 615-626.

[13] Kwaterczak, A., Duszczyk, K., & Bielejewska, A. (2009). Comparison of chiral separation of basic drugs in capillary electrophoresis and liquid chromatography using neutral and negatively charged cyclodextrins. Analytica chimica acta, 645(1-2), 98-104. doi:https://doi.org/10.1016/j.aca.2009.04.049

[14] Porpiglia, N., Musile, G., Bortolotti, F., De Palo, E. F., & Tagliaro, F. (2016). Chiral separation and determination of ketamine and norketamine in hair by capillary electrophoresis. Forensic Sci Int, 266, 304-310. doi:https://doi.org/10.1016/j.forsciint.2016.06.017

[15] Sandbaumhüter, F. A., Theurillat, R., & Thormann, W. (2017). Separation of hydroxynorketamine stereoisomers using capillary electrophoresis with sulfated β-cyclodextrin and highly sulfated γ-cyclodextrin. Electrophoresis, 38(15), 1878-1885. doi:https://doi.org/10.1002/elps.201700016

[16] Stalcup, A. M., & Gahm, K. H. (1996). Application of sulfated cyclodextrins to chiral separations by capillary zone electrophoresis. Anal Chem, 68(8), 1360-1368. doi:https://doi.org/10.1021/ac950764a

[17] Theurillat, R., Larenza, M. P., Feige, K., Bettschart-Wolfensberger, R., & Thormann, W. (2014). Development of a method for analysis of ketamine and norketamine enantiomers in equine brain and cerebrospinal fluid by capillary electrophoresis. Electrophoresis, 35(19), 2863-2869. doi:https://doi.org/10.1016/0378-4347(95)00545-5

[18] Ying Kwan, H., & Thormann, W. (2012). Electrophoretically mediated microanalysis for characterization of the enantioselective CYP 3 A 4 catalyzed N-demethylation of ketamine. Electrophoresis, 33(22), 3299-3305. doi:https://doi.org/10.1002/elps.201200127

[19] Lurie, I. S., Odeneal, N. G., McKibben, T. D., & Casale, J. F. (1998). Effects of various anionic chiral selectors on the capillary electrophoresis separation of chiral phenethylamines and achiral neutral impurities present in illicit methamphetamine. Electrophoresis, 19(16-17), 2918-2925. doi:https://doi.org/10.1002/elps.1150191620

[20] Amini, A., Sörman, U. P., Lindgren, B. H., & Westerlund, D. (1998). Enantioseparation of anaestethic drugs by capillary zone electrophoresis using cyclodextrin-containing background electrolytes. Electrophoresis, 19(5), 731-737. doi:https://doi.org/10.1002/elps.1150190522

[21] Bingcheng, L., Yibing, J., Yuying, C., Epperlein, U., & Koppenhoefer, B. (1996). Separation of drug enantiomers by capillary electrophoresis: α-cyclodextrin as chiral solvating agent. Chromatographia, 42(1), 106-110. doi:https://doi.org/10.1007/BF02271064

[22] Chankvetadze, B., Burjanadze, N., Breitkreutz, J., Bergander, K., Bergenthal, D., Kataeva, O., Blaschke, G. (2002). Mechanistic study on the opposite migration order of the enantiomers of ketamine with α-and β-cyclodextrin in capillary electrophoresis. J Sep Sci, 25(15-17), 1155-1166. doi:https://doi.org/10.1002/1615-9314(20021101)25:15/17%3C1155::AID-JSSC1155%3E3.0.CO;2-M

[23] Koppenhoefer, B., Epperlein, U., Christian, B., Lin, B., Ji, Y., & Chen, Y. (1996). Separation of enatiomers of drugs by capillary electrophoresis III. β-cyclodextrin as chiral solvating agent. J Chromatogr A, 735(1-2), 333-343. doi:https://doi.org/10.1016/0021-9673(95)01210-9

[24] Koppenhoefer, B., Epperlein, U., Christian, B., Yibing, J., Yuying, C., & Bingcheng, L. (1995). Separation of enantiomers of drugs by capillary electrophoresis I. γ-cyclodextrin as chiral solvating agent. J Chromatogr A, 717(1-2), 181-190. doi:https://doi.org/10.1016/0021-9673(95)00556-5

[25] Fillet, M., Hubert, P., & Crommen, J. (1998). Method development strategies for the enantioseparation of drugs by capillary electrophoresis using cyclodextrins as chiral additives. Electrophoresis, 19(16-17), 2834-2840. doi:https://doi.org/10.1002/elps.1150191608

[26] ICH. (2005). Guideline Q2(R1), validation of analytical procedures: text and methodology International conference on harmonisation of technical requirements for registration of pharmaceuticals for human use.

[27] Vander Heyden, Y., Nijhuis, A., Smeyers-Verbeke, J., Vandeginste, B., & Massart, D. (2001). Guidance for robustness/ruggedness tests in method validation. J Pharm Biomed Anal, 24(5-6), 723-753. doi:https://doi.org/10.1016/S0731-7085(00)00529-X

3.3. Do the enantiomers of ketamine bind enantioselective to human serum albumin?

Sebastian Schmidt, Ulrike Holzgrabe

Manuscript submitted for publication.

Abstract

The binding of drugs to plasma proteins is an important pharmacokinetic parameter. Human serum albumin (HSA) has the most important function as a transporter protein. The binding of ketamine to HSA has already been described in literature, but only of the racemate. The enantiomerically pure *S*-ketamine is used as injection solution for induction of anesthesia and has been approved by the *Food and Drug Administration* for the therapy of severe depression as a nasal spray in 2019. The question arises if there is enantioselective binding to HSA. Hence, the aim of this study was to investigate whether there is enantioselective binding of *S*-and *R*-ketamine to HSA or not. Ultrafiltration (UF) followed by chiral capillary electrophoretic analysis was used to determine the extent of protein binding. 65-72.0% was observed for the individual enantiomers and the racemate, respectively. Detailed binding properties were studied by Saturation Transfer Difference (STD)-, waterLOGSY- and Carr-Purcell-Meiboom-Gill (CPMG)-NMR spectroscopy. With all three methods, the aromatic ring and the *N*-methyl group could be identified as the structural moieties most strongly involved in binding of ketamine to HSA. pK_{aff} values determined using UF and NMR indicate that ketamine is a weak affinity ligand to HSA and no significant differences in binding behavior were found between the individual enantiomers and the racemate.

Graphical Abstract

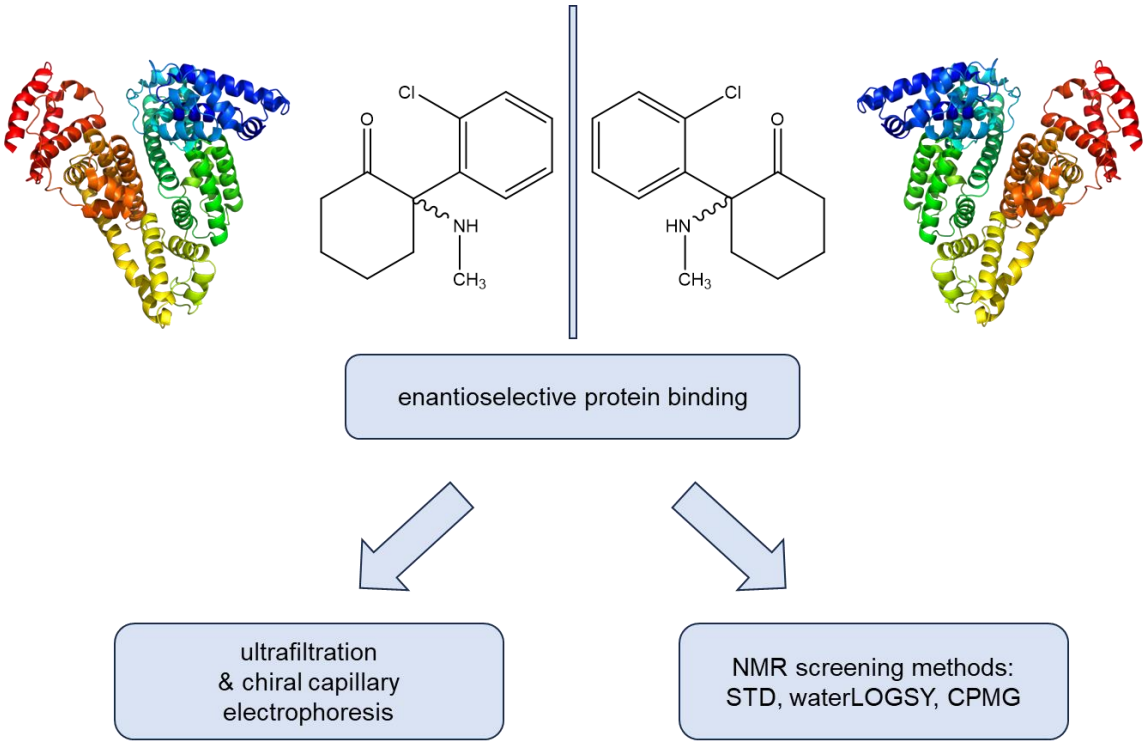

1. Introduction

Binding of drugs to proteins, such as albumin, plays an important role in drug therapy. It can lead to low drug levels in cases of very high binding and interactions between simultaneously administered drugs, if there is competition for the same binding site (Rahman et al., 1993; Wani et al., 2020; Yamasaki et al., 2013). The purpose of protein binding is the transport of xenobiotics and endogenous substances. Human serum albumin (HSA) is the most important plasma protein, with an amount of 60% of total plasma proteins. In addition, it also maintains the colloid osmotic pressure of the blood, has antioxidant and antithrombotic functions, and stabilizes the endothelium (Spinella et al., 2016). HSA is synthetized in the liver, has a molecular weight of 66 kDa and an average serum concentration of 600 µM in healthy adults. HSA concentration may be reduced by diseases such as live cirrhosis leading to hypoalbuminemia which can affect the protein binding of drugs (Doweiko and Nompleggi, 1991; Tillement et al., 1978).

Binding of drugs to HSA is very well described. HSA has two main binding sites, which are known as Sudlow`s site I and Sudlow`s site II according to their discoverer Sudlow (Sudlow et al., 1975, 1976). In addition to these two binding sites, it also has many other sites where xenobiotics and endogenous substances are bound to be transported (Kragh-Hansen, 1981). HSA binds mainly anionic (Sudlow`s site I) and neutral (Sudlow`s site II)

substances but not exclusively (Routledge, 1986). Other plasma proteins such as alpha-1-acid glycoprotein (AGP) bind mainly basic substances.

The anesthetic ketamine that has been on the market for over 50 years (Kohtala, 2021), is of basic structure. It is used as an injection solution for the induction of anesthesia either in racemic form, or as the enantiomerically pure *S*-ketamine. Both enantiomers differ in their anesthetic effect due to different affinity to the NDMA receptor, with *S*-ketamine being the eutomer (White et al., 1980). It also received approval by the Food and Drug Administration in 2019 for the treatment of severe depression as a nasal spray (FDA, 2019).

Protein binding of ketamine to HSA has been described in the past, with an extent of a wide range of 15-80% (Dayton et al., 1983; Hijazi and Boulieu, 2002; Pedraz et al., 1985). Since enantioselective binding of basic drugs such as antihistaminic drugs to HSA has already been described, it is of interest whether ketamine enantioselective binds to HSA or not (Martínez-Gómez et al., 2007).

In this study, protein binding was determined by ultrafiltration (UF) in combination with chiral capillary electrophoresis (CE). CE is ideally suited for the separation of enantiomers, by adding chiral selectors such as cyclodextrins. It is possible to separate enantiomers quickly without waste of resources. Hence, the chiral CE method of Schmidt et al. was applied here (Schmidt and Holzgrabe, 2023). NMR measurements were performed to confirm the results of the UF and to elucidate binding properties. Ligand screening techniques such as Saturation Transfer Difference-NMR spectroscopy (STD-NMR) and waterLOGSY-NMR spectroscopy, both based on the nuclear overhauser effect (NOE), and Carr-Purcell-Meiboom-Gill (CPMG) measurements, applying relaxation filters, were used to characterize binding with two orthogonal principles. A non-linear fit was used for the UF, while an isotherm model was used for the NMR measurements to determine the affinity constant Kaff. The aim of this work was to investigate a possible enantioselective binding of ketamine to HSA and to characterize its binding properties.

2. Materials and methods

2.1. Chemicals

Racemic ketamine hydrochloride, sodium chloride, potassium chloride, albumin from human serum (> 96% agarose gel electrophoresis), disodium hydrogen phosphate, tripotassium phosphate, *R*-ketamine hydrochloride, tris-(hydroxymethyl)-aminomethane (TRIS), and sodium azide were purchased from Sigma Aldrich (Darmstadt, Germany). *S*-Ketamine hydrochloride in form of Ketanest® was obtained from Pfizer (New York City,

US). α-Cyclodextrin was purchased from Wacker Chemie (Munich, Germany), neostigmine bromide from Roche (Grenzach, Germany), 0.1 M sodium hydroxide solution from VWR chemicals (Darmstadt, Germany), 0.1 M hydrochloric acid solution from Bern Kraft (Duisburg, Germany), deuterated water, tetramethyl silane, and deuterated hydrochloric acid from Deutero GmbH (Kastellaun, Germany). 85% Phosphoric acid and potassium dihydrogen phosphate were obtained from Merck (Darmstadt, Germany) as well as an in-house purification system for deionized water.

2.2. Instrumentation

pH measurements were performed using a pH meter from Metrohm (Filderstadt, Germany). Capillary electrophoresis was performed using a P/ACE MDQ system from Sciex (Darmstadt, Germany) equipped with a photodiode array detector. NMR data were acquired on a Bruker III Avance spectrometer operating at 400.1 MHz equipped with a PABBI inverse probe (Karlsruhe, Germany). The samples of the UF were incubated in a thermomixer and centrifuged with a centrifuge 5702, both from Eppendorf (Hamburg, Germany).

2.3. Capillary electrophoresis

The method described by Schmidt et al. was used to separate the ketamine enantiomers by means of CE (Schmidt and Holzgrabe, 2023). Therefore, a fused silica capillary from BGB Analytik Vertrieb (Rheinfelden, Germany) with an internal diameter of 50 µm, a total length of 70 cm and an effective length of 60 cm was chosen. Samples were injected at a pressure of 1.0 psi for 10.0 s. New capillaries were conditioned with 1.0 M sodium hydroxide solution, 2.0 M hydrochloric acid and deionized water at a pressure of 30.0 psi in this order, each for 10 min. Subsequently, the capillary was rinsed with background electrolyte (BGE) for 2 min and a voltage of 20.0 kV for 20 min was applied. Before each sample injection, the capillary was rinsed 1.0 min with a 0.1 M sodium hydroxide solution, 1.0 min deionized water and 2.0 min with BGE at a pressure of 20.0 psi. Analytes were detected at a wavelength of 194 nm. A constant voltage of 30 kV and a temperature of 15 °C was applied. The BGE consisted of 275 mM TRIS dissolved in deionized water, adjusted with 85% phosphoric acid to a pH of 2.50, and 50 mM α-cyclodextrin. Data were analyzed with 32 Karat software 8.0 from Sciex (Darmstadt, Germany).

2.4. Ultrafiltration

A PBS buffer consisting of 12 mM phosphate salts, 137 mM sodium chloride and 2.7 mM potassium chloride was used as the incubation medium, thus representing the physiological properties of the blood well. The pH was adjusted to 7.40 with a 0.1 mM

sodium hydroxide solution. 900 µM HSA, 800 µM neostigmine bromide, 2.5 mM racemic ketamine and 1.25 mM *R*-ketamine stock solutions were prepared by dissolving the required amount in PBS buffer. The drug Ketanest® was diluted with PBS buffer, resulting in a 1.25 mM stock solution for *S*-ketamine. The protein and drug stock solutions were mixed with the respective amount of PBS buffer in 5 ml Eppendorf caps, resulting in six different ratios in the range from 0.2 to 0.5 of drug to protein, based on the respective enantiomer. Both the individual enantiomers and the racemate were incubated for 45 min. The minimum drug concentration was 120 µM and maximum 600 µM. HSA concentration was kept constant at 600 µM. The mixtures were incubated at 37 °C for 45 min. Before being transferred into the Amicon® Ultra 4.0 ml ultracentrifugation unit with a molecular cut-off of 10 kDa (Merck, Darmstadt, Germany), 500 µM neostigmine bromide was added as an internal standard. Subsequently, centrifugation was performed at 4400 rpm for 15 min. The filtrate was diluted in vials and measured by means of CE. Each drug-protein ratio measurement was performed in triplicate. Data fitting was performed with GraphPad Prism 9.5.1 from GraphPad Software (Boston, MA, US).

2.5. NMR conditions

The solvent used was a partially deuterated 30 mM phosphate buffer (90% H2O/10% D2O, V/V) consisting of tripotassium phosphate, 25 mM sodium chloride, 0.02% sodium azide and 100 µM tetramethyl silane. The buffer was adjusted with deuterated hydrochloric acid to a pD of 7.40. 3.125 mM stock solutions of racemic ketamine, *S*-ketamine, *R*-ketamine respectively, and a 125 µM HSA stock solution was prepared by weighing the required amount of substance and dissolving it in the buffer. The samples were prepared by mixing the individual stock solutions with the buffer. For screening, one sample was measured with HSA only (50 µM), one sample with ligand only (1 mM), and a mixture of both (50 µM HSA, 1 mM ligand). The difference in chemical shifts were evaluated for the determination of the pK_{aff}. Therefore, different drug-protein ratios were measured at a constant HSA concentration of 25 µM. Ligand concentration ranged from 25 µM to 2.5 mM.

For STD-NMR measurements, the pulse frequency stddiffesgp.3 was used, coupled with an excitation sculpting pulse frequency to suppress the water signal at 4.703 ppm. The number of scans was 8 with 16 dummy scans. The saturation pulse was 400 Hz and the saturation time 3 s.

The sequence cpmg_esgp2d was applied for the relaxation filter measurements. The CPMG filters were 2 and 20 ms, respectively. The number of scans was 128 and the number of dummy scans was 4.

For the waterLOGSY experiments, the sequence ephogsygopno.2 was used. The number of scans was 256 with 4 dummy scans. The mixing time for the transfer of saturation by the NOE was 1.7 ms.

For K_{aff} determination using the chemical shift, ^{1}H spectra with water signal suppression at 4.703 ppm through excitation sculpting were recorded with a scan number of 1024 and 4 dummy scans. HSA concentration was kept constant at 50 µM and different drug-protein ratios between 1:1 and 50:1 were mixed in the solvent. All measurements were performed at 300 K and a spectral width of 15.98 ppm with an applied loop counter of 1.

NMR data was evaluated with TopSpin 4.0.9 from Bruker (Karlsruhe, Germany). Data fitting was performed with GraphPad Prism 9.5.1 from GraphPad Software (Boston, MA, US).

3. Results and discussion

3.1. Protein binding determination by means of ultrafiltration

UF was performed to determine the extent of protein binding of ketamine to HSA. The experiment was divided into two parts. First, the drug was incubated with the protein and then the drug-protein complex was separated by a membrane filter. Free unbound drug is filtered, which is then analyzed. Using cyclodextrin-modified CE the enantiomers could be separated and individually quantified or as racemate. An example electropherogram is given in Fig. 1.

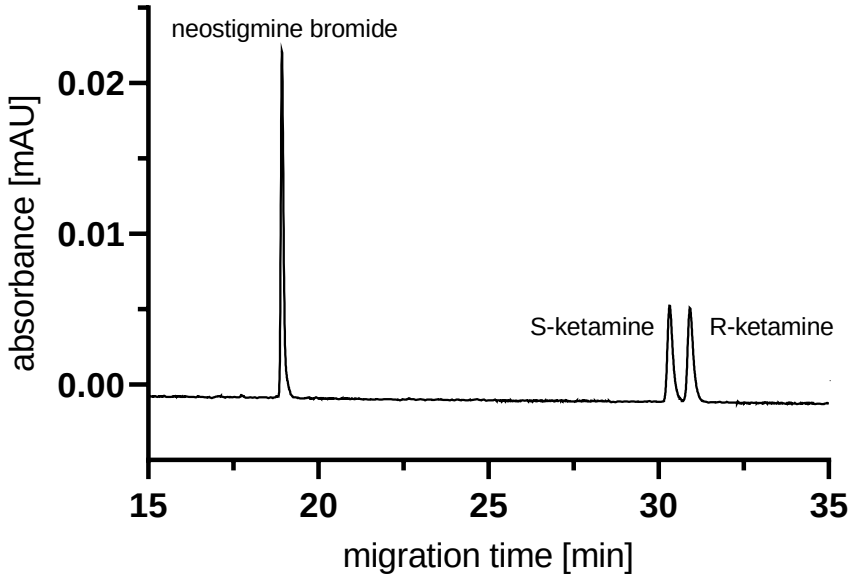

Fig. 1 Electropherogram of racemic ketamine with neostigmine bromide as internal standard after incubation with 600 µM HSA; electrophoretic conditions: 275 mM TRIS buffer adjusted with 85% phosphoric acid to a pH value of 2.50, 50 mM cyclodextrin, 15 °C, 30 kV, injection at 1.0 psi for 10 s, fused silica capillary with a total length of 70 cm and an effective length of 60 cm, internal diameter of 50 µm, wavelength 194 nm

Both ketamine enantiomers and neostigmine could be baseline separated within 30 min. Neostigmine was used as internal standard because no binding to HSA has been reported in the literature (Ammon, 2001). Nevertheless, to avoid unknown binding processes of neostigmine to HSA, the internal standard was not added to the solution until immediately before filtration. A protein normally shows several binding sites of different composition. As already mentioned in the introduction, albumin has the Sudlow`s site I and Sudlow`s site II, mainly to bind anionic and neutral substances. Ligands can either bind to one binding site only, or multiple binding to more binding sites is also possible. In both cases, the greater the extent of ligand, the more binding sites can be occupied. The binding occurs under an equilibrium reaction which can be described by Eq. (1).

$$\text{Eq. (1) ligand} + \text{protein} \rightleftharpoons \text{ligand} - \text{protein complex}$$

To characterize the binding behavior, the affinity constant K_{aff} can be determined from the equilibrium reaction using the law of mass action. For this purpose, different drug-protein ratios were incubated together, and the free, unbound part of the drug is analyzed, using a constant protein concentration and different ligand concentrations. The experimental conditions were kept as physiological as possible: an HSA concentration of 600 µM, incubation at 37 °C and low drug protein ratios of 0.2 to 0.5 were used (Asensi-Bernardi et al., 2010). The extent of protein binding was determined by quantifying the unbound

ligand concentration ($ligand_{free}$). Eq. (2) and Eq. (3) are used to determine the bound fraction (f_{bound}). Results are presented in Table 1.

$$\text{Eq. (2)} \quad \mathrm{ligand_{bound}} = \mathrm{ligand_{total}} - \mathrm{ligand_{free}}$$

$$\text{Eq. (3)} \quad \mathrm{f_{bound}}\ [\%] = \frac{\mathrm{ligand_{bound}}}{\mathrm{ligand_{total}}} * 100$$

The drug bound per mole of protein can be defined as r and is characterized by Eq. (4).

$$\text{Eq. (4)} \quad \mathrm{r} = \frac{\mathrm{ligand_{bound}}}{\mathrm{protein_{total}}}$$

If this term is plotted as r/1-r in logarithmic form against the logarithmic free ligand concentration, information can be obtained about the number of binding sites to which the drug binds. If a straight line is obtained with a slope of 1, the drug binds only to one binding site. The presence of one binding site can also be verified using Eq. (5).

$$\text{Eq. (5)} \quad \mathrm{K_{aff}} = \frac{\mathrm{f_{bound}}}{1 - \mathrm{f_{bound}}} * \frac{1}{\mathrm{protein_{total}}}$$

K_{aff} is constant over all measured drug-protein ratios if the drug binds only to one binding site (Volpp and Holzgrabe, 2019). As shown in Fig. 2 and S1, K_{aff} remains constant, which proves the existence of only one binding site for both enantiomers. For better usability, the pK_{aff} is used, which corresponds to the negative decadic logarithm of the K_{aff}.

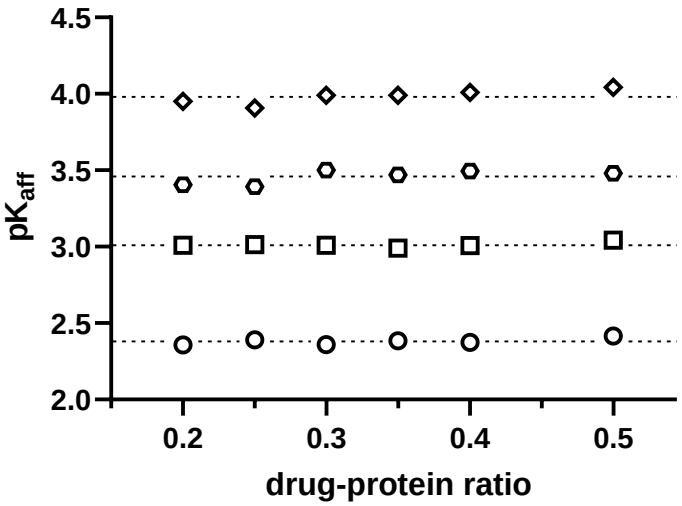

Fig. 2 pK_{aff} of ○ *R*-ketamine (enantiomerically pure), □ *S*-ketamine (enantiomerically pure), ◊ *R*-ketamine (in racemate), ⬡ *S*-ketamine (in racemate) of different drug-protein ratios at a constant HSA concentration of 600 µM; for better presentation, a y-offset of 0.5 was used, the mean value of the respective pK_{aff} is shown in

Table 1; in racemate: incubation of the racemate with HSA; enantiomerically pure: incubation of the respective enantiomer with HSA

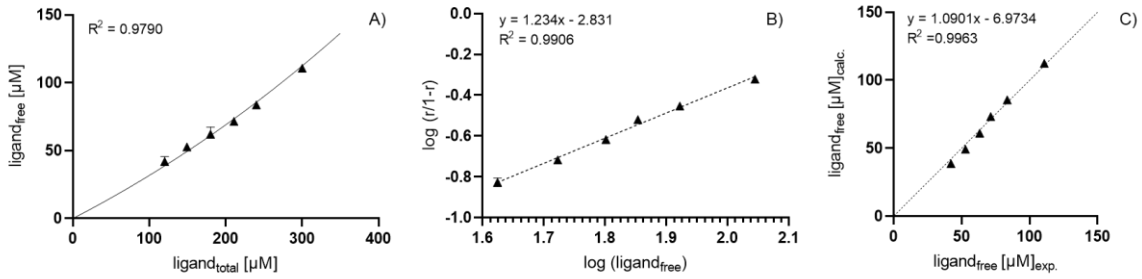

Fig. 3 A) non-linear fit according to Eq. (6) between $ligand_{total}$ and $ligand_{free}$ of ***S*-ketamine** (enantiomerically pure) B) logarithmic check of the presence of one binding site between log (r/1-r) and log ($ligand_{free}$) with r being the quotient between $ligand_{bound}$ and $protein_{total}$ C) correlation between calculated and experimental data of $ligand_{free}$ of the non-linear fit

The confirmation of the presence of one binding site allows the use of a non-linear model according to Asensi-Bernardi (Asensi-Bernardi et al., 2010). In cases where n (number of binding sites) = 1, Eq. (6) can be fitted for Kaff.

$$\text{Eq.}(6)\quad \mathrm{ligand_{free}} = \frac{-(1 - \mathrm{K_{aff}} * \mathrm{ligand_{total}} + \mathrm{n} * \mathrm{K_{aff}} * \mathrm{protein_{total}}) \pm \sqrt{(1 - \mathrm{K_{aff}} * \mathrm{ligand_{total}} + \mathrm{n} * \mathrm{K_{aff}} * \mathrm{protein_{total}})^2 + 4 * \mathrm{K_{aff}} * \mathrm{ligand_{total}}}}{2 * \mathrm{K_{aff}}}$$

The fit for enantiomerically pure *S*-ketamine as well as the correlation between experimental and calculated values of the fit are shown in Fig. 3. The data for *R*-ketamine and the racemic mixtures are shown in Fig. S2, the obtained values are given in Table 1.

Table 1 Comparison of the determined protein binding by means of ultrafiltration, mean value of pK_{aff} calculated according to Eq. (5) and pK_{aff} fitted with the non-linear fit according to Eq. (6); in racemate: incubation of the racemate with HSA; enantiomerically pure: incubation of the respective enantiomer with HSA

	protein binding [%]	pK_{aff} Eq. (5)	pK_{aff} (non-linear fit)
***R*-ketamine (enantiomerically pure)**	71.2 ± 1.2	2.38 ± 0.03	2.25
***S*-ketamine (enantiomerically pure)**	64.9 ± 1.5	2.51 ± 0.03	2.39
***R*-ketamine (in racemate)**	66.4 ± 2.8	2.48 ± 0.06	2.38
***S*-ketamine (in racemate)**	67.5 ± 2.8	2.46 ± 0.06	2.36
ketamine (racemate)	66.5 ± 3.4	2.48 ± 0.07	2.20

The protein binding of all enantiomers, whether enantiomerically pure or in the racemic mixture, and the racemate are between 64.9 and 71.2%. Comparing the enantiomerically pure *R*- and *S*-ketamine, *R*-ketamine shows a slightly, but significantly higher binding. However, a clinically relevant impact is not expected. No significant differences between the enantiomers have been observed in the racemic mixtures as a kind of average was measured. In the literature, binding of ketamine of 15-33% to HSA and human plasma, respectively, and 45% to AGP (Dayton et al., 1983), 60% to HSA (Hijazi and Boulieu, 2002), 30-60% to HSA and 60-80% to human serum (Pedraz et al., 1985) have been reported. Except for Dayton et al., the binding percentages obtained, fall into theses wide ranges. Dayton et al. focused primarily on binding of ketamine to human plasma. Nevertheless, binding of ketamine to bovine serum albumin, HSA, AGP and γ-globulin was also studied. Additionally, enantioselective binding to AGP was investigated, with the result that both *S*- and *R*-ketamine bind equally with 45%. Thus, ketamine does not bind enantioselective to AGP. As our results show, this is also the case for binding to HSA.

pK_{aff} values obtained with Eq. (5) and the non-linear fit are in a similar range, but they are lower than the pK_{aff} value of 3.01 reported by Pedraz et al. (Pedraz et al., 1985). In our work, drug-protein ratios were measured no greater than 0.5, while Pedraz et al. measured

up to twice the amount of drug compared to protein. Hence, a different model was chosen for the data fit resulting in different pK_{aff} values. Asensi-Bernardi et al. demonstrated the advantages of using low-drug protein ratios, which is why we chose this approach (Asensi-Bernardi et al., 2010).

3.2. Characterization of binding properties by means of NMR spectroscopy

NMR is an excellent tool for drug screening in drug development (Stockman and Dalvit, 2002). Different measurement methods can be used to investigate structure-affinity relationships and chemical structures of a drug involved in binding. The main advantage is the possibility to apply lower target concentrations compared to UF. In addition, titration experiments can also be used to determine affinity constants. In this study, STD-NMR, waterLOGSY and CPMG relaxation filters were applied as screening methods. ^{1}H NMR spectra of different drug-protein ratios were used to determine the affinity constant. Fig. 4 shows a ^{1}H NMR spectrum of ketamine and the assignment of the individual protons to their respective signals.

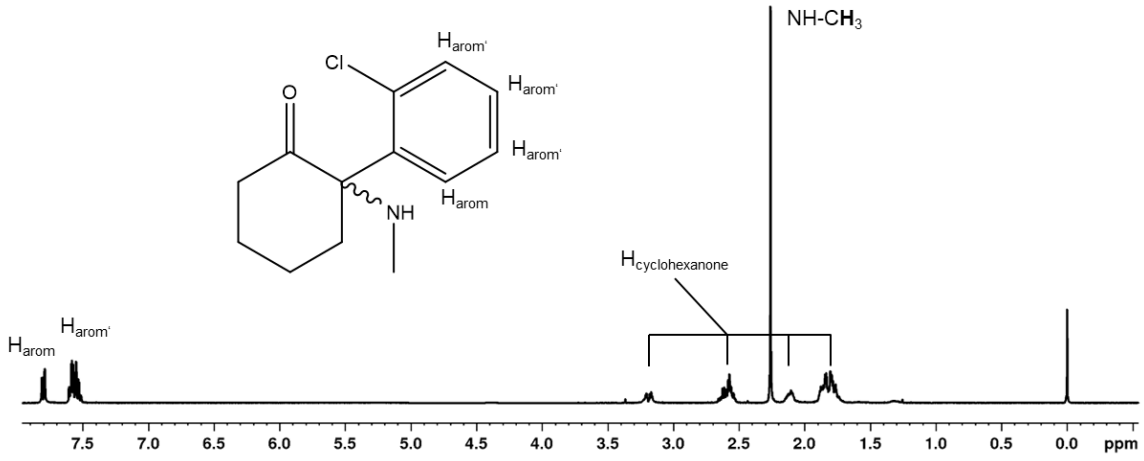

Fig. 4 ^{1}H NMR spectrum of racemic ketamine and the assignment of its protons; spectrum was recorded with water signal saturation at 4.703 ppm by excitation sculpting

STD-NMR is based on the Nuclear Overhauser Enhancement (NOE) effect. When a drug binds to a protein, which is saturated with a pulse frequency, the saturation is transferred to the protons of the drug involved in the protein binding. By comparison of a spectrum recorded with (on-resonance spectrum) and without (off-resonance spectrum) the saturation pulse frequency, a difference spectrum is obtained. Signals that are seen in the difference spectrum are protons of the ligand involved in binding. It is important that no proton of the ligand is hit by the saturation pulse and thus falsifies the measurement. For each protein the appropriate saturation pulse must be found. Fig. S3 shows, that only the NHC**H**$_3$ protons are hit slightly, and HSA is fully saturated by the pulse. This effect was

considered for the evaluation. The obtained STD signal is dependent on saturation time, rebinding processes, binding kinetics, and drug respective protein concentration (Walpole et al., 2019). With shorter saturation times, it can be assumed that complete saturation has not yet been reached and the signal is therefore independent. In this study, a short saturation time of 3 s was chosen to minimize the influence. Fig. 5A shows the difference spectrum (black) and the off-resonance spectrum (red) of *S*-ketamine. In the difference spectrum, the NHC**H**$_3$ protons and the aromatic protons of ketamine are the most intense signals, suggesting that these structure moieties are primarily involved in binding to HSA. The cyclohexanone protons show fewer intensive signals.

Another screening technique based on the NOE is waterLOGSY. The difference here is that the protein is not saturated with a pulse, but the bulk water in the solution is (Claridge, 2016). When a ligand binds to a protein, the saturation is transferred from the bulk water, via various processes such as spin diffusion, to the protein and beyond to the ligand. This transfer leads to a reduction in the intensity of the ligand signals up to negative deflections. It is important that the saturation can also be transferred directly to the ligand, which could distort the result. It is essential to conduct an experiment with only ligand and no protein to include possible intensity changes that are transferred by direct transmission of saturation through the water to the ligand and not the protein. Fig. 5B shows the waterLOGSY spectrum of *S*-ketamine without HSA (black) and with protein (red). The effect of binding and transfer of saturation respectively is so intense that the signals of the ligand are reduced in a way that they change into the negative. Again, the aromatic protons and NHC**H**$_3$ show the most intense signals. The cyclohexanone protons show only weak intensity changes. Hence, the results of the waterLOGSY experiments are in line with those of the STD measurements.

CPMG spin lock filters were used as a third screening option. Large molecules relax much faster than smaller ones (Fernández and Wider, 2006). By setting suitable filter times, the signals of the protein can be attenuated until they are no longer visible. This effect is also transferred to bound ligands. If a ligand binds to a protein that is exposed to a relaxation filter, the signals of the protons involved in the binding are attenuated. First, it must be checked whether the signals of the HSA, are filtered out with a filter time of 200 ms or not. For this purpose, a pure sample of HSA is measured with a filter time of 2 and 200 ms, respectively. Pure ligand is also measured under these conditions to ensure that the ligand is not also attenuated. The results here are shown in Fig. S4. HSA is completely filtered out at a filter time of 200 ms and ketamine remains unaffected. Fig. 5C shows the spectra of the mixture of HSA with *S*-ketamine at a filter time of 2 ms (red) and a filter time of 200 ms (black). The signals of the aromatic protons and of NHC**H**$_3$ are attenuated, while

the signals of the cyclohexanone protons completely disappeared. STD, waterLOGSY, and CPMG spectra of *R*-ketamine and racemic ketamine are presented in Fig. S5 and S6. *S*-ketamine, *R*-ketamine and racemic ketamine show similar results. Aromatic and NHC**H**$_3$ protons are the most intense signals in STD NMR and have largest attenuations in waterLOGSY and CPMG. There was no difference between the individual enantiomers and the racemate. Since all three screening methods show the same result, it can be assumed that the aromatic protons and NHC**H**$_3$ are most strongly involved in the binding. As mentioned before, HSA has two main binding sites (Sudlow`s site I and Sudlow`s site II). Sudlow`s site I is characterized by its ability to bind mainly bulky anionic ligands, while Sudlow`s site II binds aromatic, anionic but also neutral substances (Sudlow et al., 1975, 1976). Since ketamine is still partially uncharged at physiological pH (pK_a 7.5 (Tolksdorf, 1988)) and has an aromatic ring structure, Sudlow`s site II could be a possible binding site for ketamine. However, it must also be mentioned that HSA, as a transporter protein, has many uncharacterized binding sites that could bind ketamine.

To confirm the pK_{aff} determined via UF an orthogonal method was applied. Differences in the chemical shift of individual signals of various drug-protein ratios in the range from 1 to 100 drug to protein were investigated. When a ligand binds to a protein, it experiences a different chemical environment and a change in chemical shift. Since the H_{arom} and NHC**H**$_3$ protons showed the largest difference and were well resolved in the screening, these signals were selected for the determination of K_{aff}. Various drug-protein ratios were measured, with the HSA concentration kept constant at 25 µM and a ligand concentration between 25 µM and 2.5 mM.

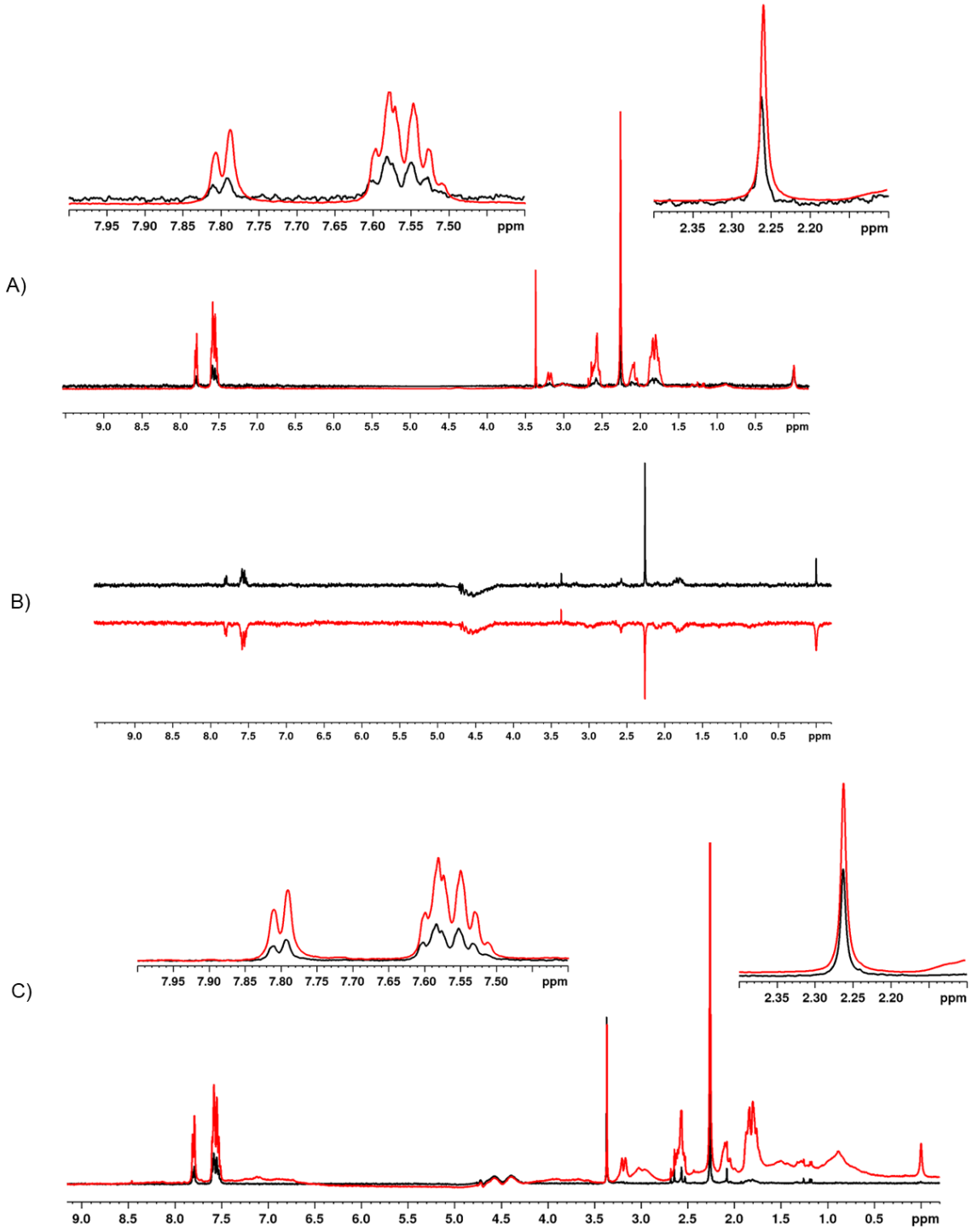

Fig. 5 A) STD-NMR: overlay of the off-resonance spectrum of 1 mM ***S*-ketamine** with 50 µM HSA (red) and the difference spectra (black) with a saturation pulse of 400 Hz and water signal suppression at 4.703 ppm by excitation sculpting **B)**: waterLOGSY: overlay of 1 mM *S*-ketamine (black) with 1 mM *S*-ketamine + 50 µM HSA (red) **C)** CPMG NMR: overlay of the ^{1}H NMR with water signal suppression at 4.703 ppm by excitation sculpting of 1 mM S-ketamine with 50 µM HSA with a relaxation filter of 2 ms (red) and 200 ms (black)

Fig. 6C shows the chemical shifts at different drug-protein ratios of *S*-ketamine. The differences of the chemical shifts were determined according to Eq. (7) with δ being the chemical shift. A sample of 50 µM ligand was used as reference.

$$\text{Eq. (7)} \quad \Delta\delta = \delta_{\text{drug-protein ratios}} - \delta_{\text{reference}}$$

An isotherm is achieved by plotting Δδ against ligand concentration after a double reciprocal data transformation as seen in Fig. 6A. Since the UF showed that the drug binds to one binding site, a model according to Eq. (8) was used for data fitting to determine K_{aff} (Motulsky and Neubig, 2010). Fig. 6B shows the correlation of the experimentally determined and the calculated fits. Fig. S7 and S8 show data for *R*-ketamine and racemic ketamine.

$$\text{Eq. (8)} \quad \Delta\delta = \frac{\Delta\delta_{max} * \text{ligand}}{K_{aff} + \text{ligand}}$$

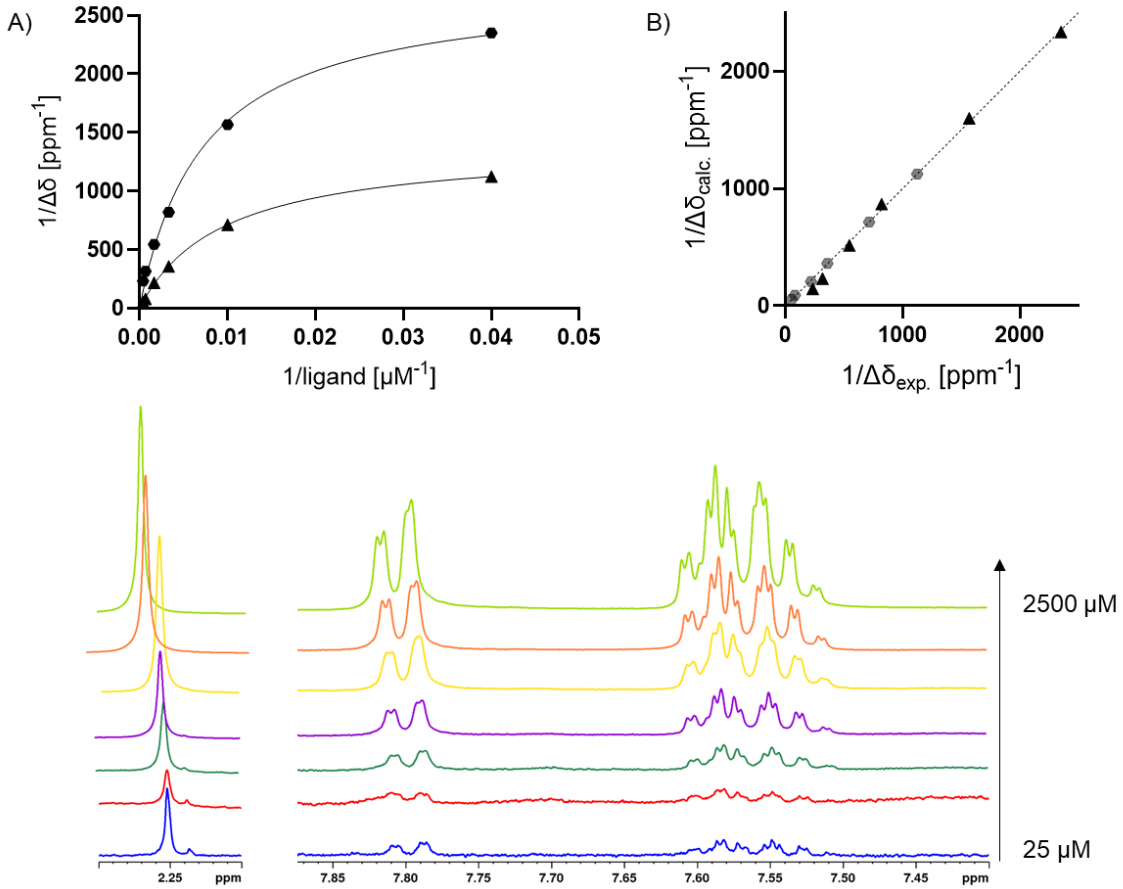

Fig. 6A) double reciprocal fit for pK_{aff} according to Eq. (8) for ▲NHC**H**$_3$ and ●H_{arom} between Δδ and ligand concentration for *S*-ketamine B) correlation between calculated and experimental data of Δδ of the double reciprocal fit C) shift of signal at 2.26 and 7.56-7.80 ppm at different ligand concentration of *S*-ketamine at a constant protein concentration of 25 µM

In Table 2, pK_{aff} values are given as the mean of the individual fits of H_{arom} and NHC**H**$_3$, as well as the coefficients of variation of the fit and the correlation.

Table 2 Comparison of the determined pK_{aff} fitted according to Eq. 8 for NHC**H**$_3$ and H_{arom} and the coefficient of variation of the double reciprocal fit and the correlation of calculated and experimental data of $\Delta\delta$

	pK_{aff}		**R^2 fit**		**R^2 correlation**	
	H_{arom}	NHC**H**$_3$	**H_{arom}**	NHC**H**$_3$	**H_{arom}**	NHC**H**$_3$
***R*-ketamine**	2.08	2.02	0.9971	0.9997	0.9968	0.9997
***S*-ketamine**	2.01	2.09	0.9948	0.9909	0.9991	0.9925
racemic ketamine	2.01	2.04	0.9949	0.9951	0.9970	0.9951

pK_{aff} values obtained with the NMR method are lower than those of the UF, but in the same order of magnitude. No significant difference can be observed between the evaluation of the H_{arom} and NHC**H**$_3$ and between the individual enantiomers and the racemate. However, due to the rather low pK_{aff}, the enantiomers of ketamine can be classified as low affinity ligands to HSA.

4. Conclusion

The extent of protein binding of ketamine was successfully determined and agrees with previously reported values in literature. For the first time, enantioselective binding of *R*- and *S*-ketamine to HSA were investigated, both enantiomerically pure and in racemic mixtures. There was no significant difference between the enantiomers found. Consequently, the drug does not bind enantioselective to HSA. Various NMR methods were used to investigate the structural binding behavior. It was found that mainly the aromatic protons and the protons of the *N*-methyl group are involved in the binding, indicating a hydrophobic binding site like the known Sudlow`s site II binding site. The pK_{aff} values determined were lower than already published ones but confirmed by two orthogonal methods, indicating that ketamine is a weak affinity ligand to HSA.

Declarations of interests

None of the authors of this paper does have a financial or personal relationship with other people or organizations that could inappropriately influence or bias the content of the paper.

Acknowledgements:

Thanks are due to Markus Zehe for the support with the NMR measurements.

Funding:

This research did not receive any specific grant from funding agencies in the public, commercial, or not-for-profit sectors.

SUPPLEMENTARY MATERIAL

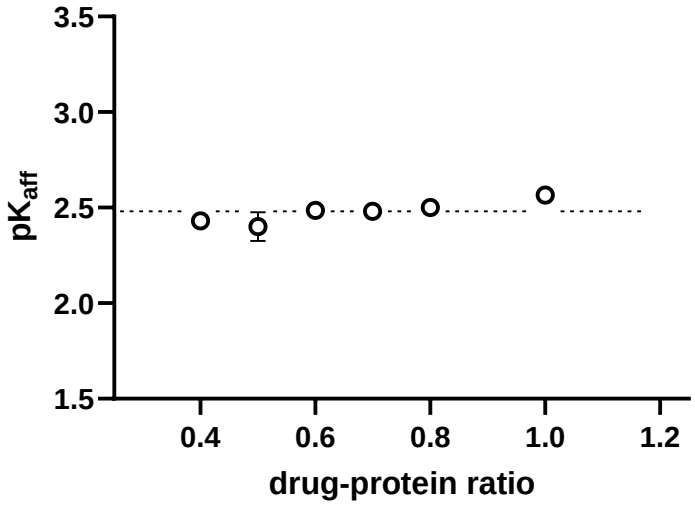

Fig. S1 pK_{aff} of ○ racemic ketamine of different drug-protein ratios at a constant HSA concentration of 600 µM

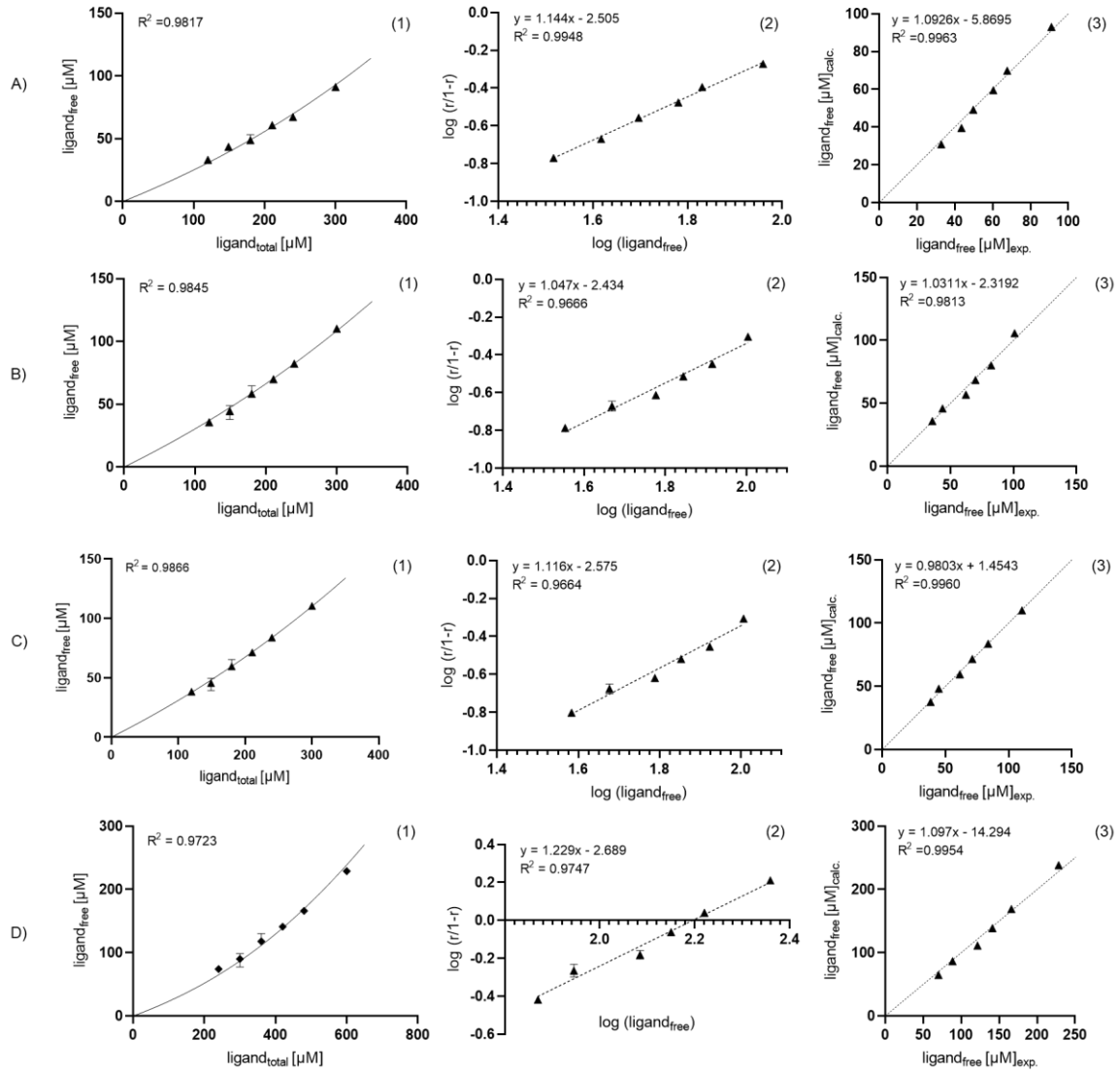

Fig. S2 A) 1) non-linear fit according to Eq. (6) between $ligand_{total}$ and $ligand_{free}$ of ***R*-ketamine (enantiomerically pure)** 2) logarithmic check of the presence of one binding site between log (r/1-r) and log ($ligand_{free}$) with r being the quotient between $ligand_{bound}$ and $protein_{total}$ 3) correlation between calculated and experimental data of $ligand_{free}$ of the non-linear fit **B)** 1) non-linear fit according to Eq. 6 between $ligand_{total}$ and $ligand_{free}$ of ***S*-ketamine (racemic mixture)** 2) logarithmic check of the presence of one binding site between log (r/1-r) and log ($ligand_{free}$) with r being the quotient between $ligand_{bound}$ and $protein_{total}$ 3) correlation between calculated and experimental data of $ligand_{free}$ of the non-linear fit **C)** 1) non-linear fit according to Eq. 6 between $ligand_{total}$ and $ligand_{free}$ **of *R*-ketamine (racemic mixture)** 2) logarithmic check of the presence of one binding site between log (r/1-r) and log ($ligand_{free}$) with r being the quotient between $ligand_{bound}$ and $protein_{total}$ 3) correlation between calculated and experimental data of $ligand_{free}$ of the non-linear fit **D)** 1) non-linear fit according to Eq. 6 between $ligand_{total}$ and $ligand_{free}$ of **racemic ketamine** 2) logarithmic check of the presence of one binding site between log (r/1-r) and log ($ligand_{free}$) with r being the quotient between $ligand_{bound}$ and $protein_{total}$ 3) correlation between calculated and experimental data of $ligand_{free}$ of the non-linear fit

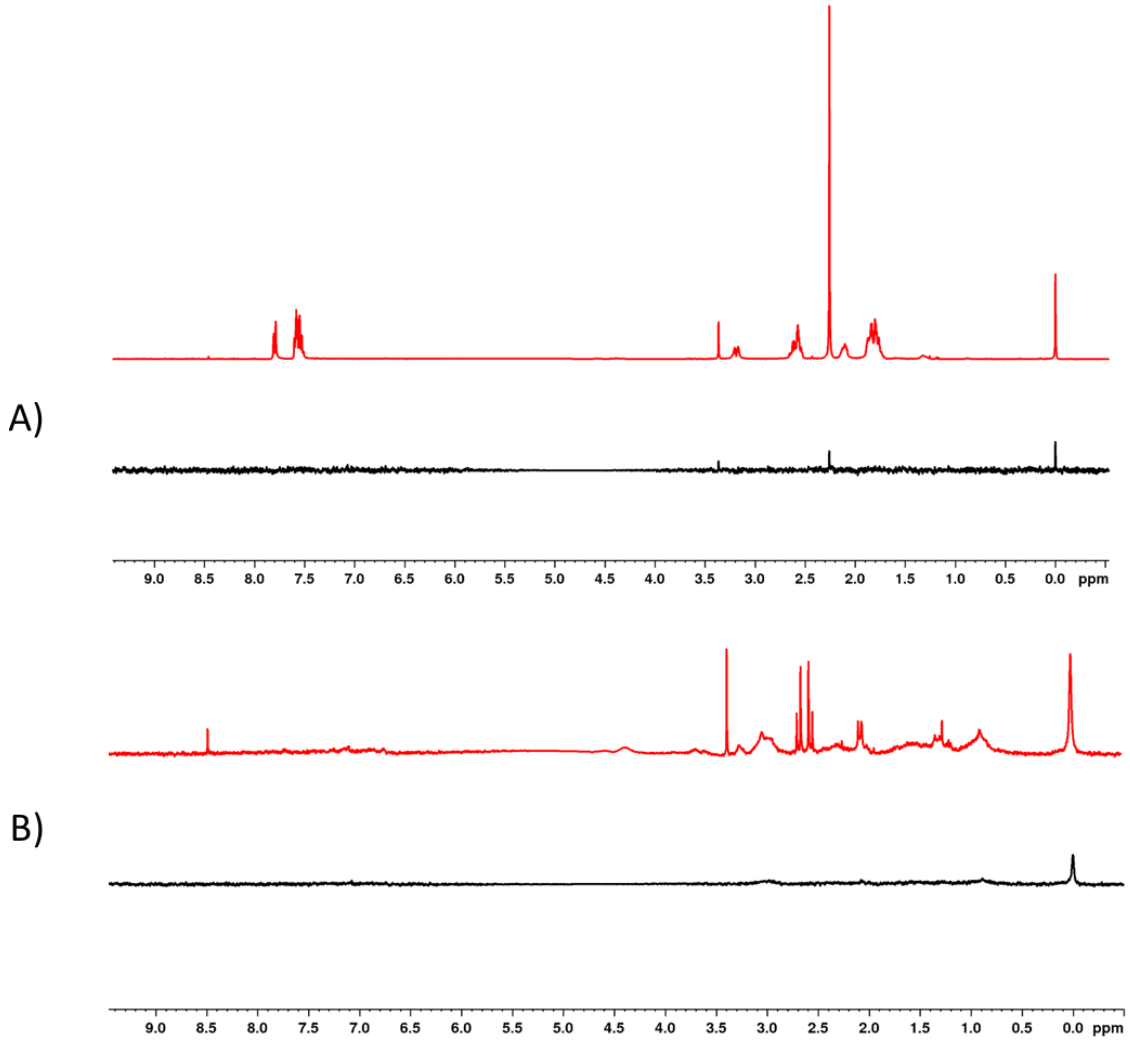

Fig. S3 A) STD NMR: off-resonance spectrum of 1 mM *S*-**ketamine** (red) and the difference spectra (black) with a saturation pulse of 400 Hz and water signal suppression at 4.703 ppm by excitation sculpting **B)** STD-NMR: off-resonance spectrum of 50 µM **HSA** (red) and the difference spectra (black) with a saturation pulse of 400 Hz and water signal suppression at 4.703 ppm by excitation sculpting

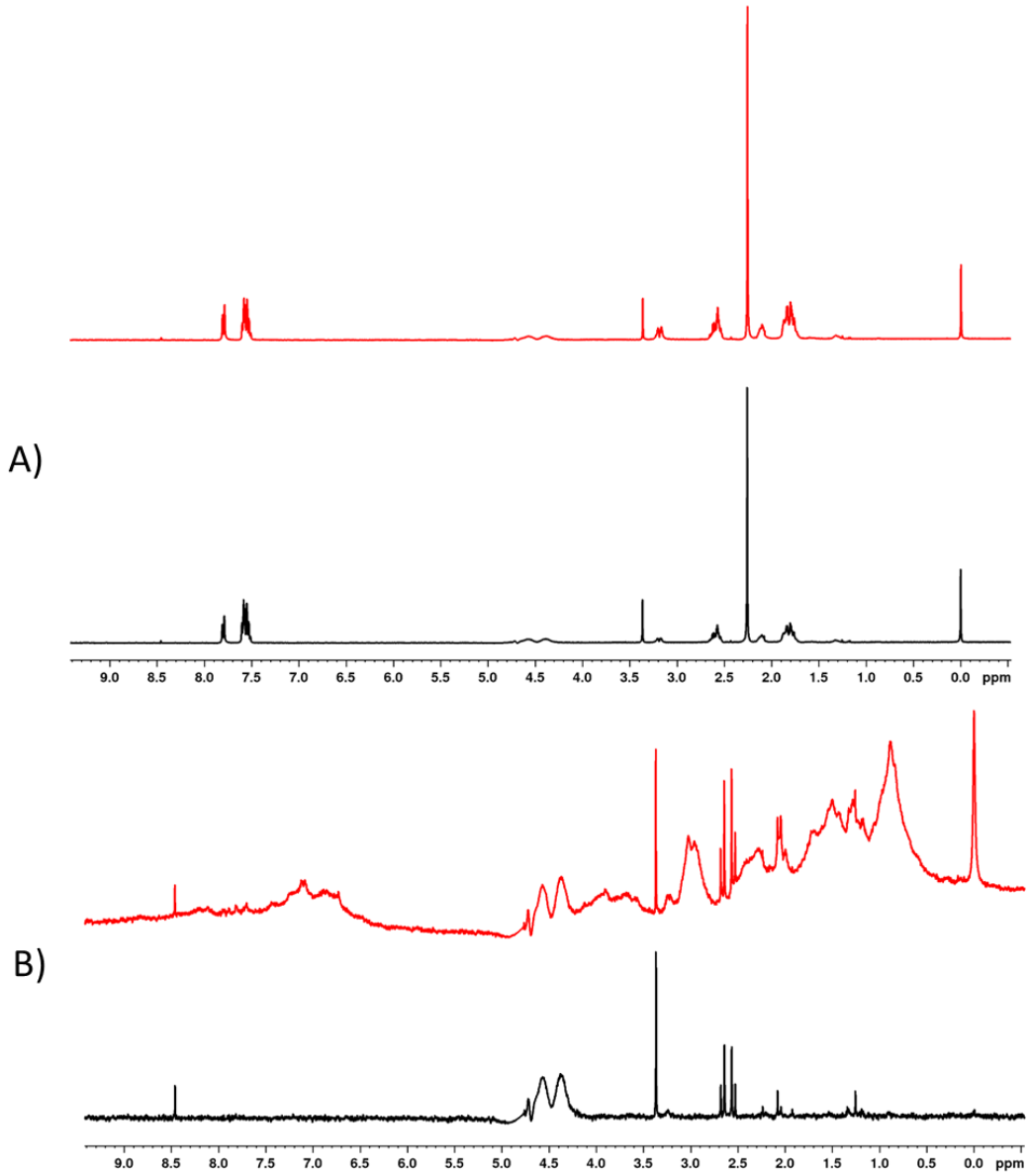

Fig. S4 A) CPMG NMR: spectra of the ^{1}H NMR with water signal suppression at 4.703 ppm by excitation sculpting of 1 mM ***S*-ketamine** with a relaxation filter of 2 ms (red) and 200 ms (black) **B)** spectra of the ^{1}H NMR with water signal suppression at 4.703 ppm by excitation sculpting of 50 µM **HSA** with a relaxation filter of 2 ms (red) and 200 ms (black)

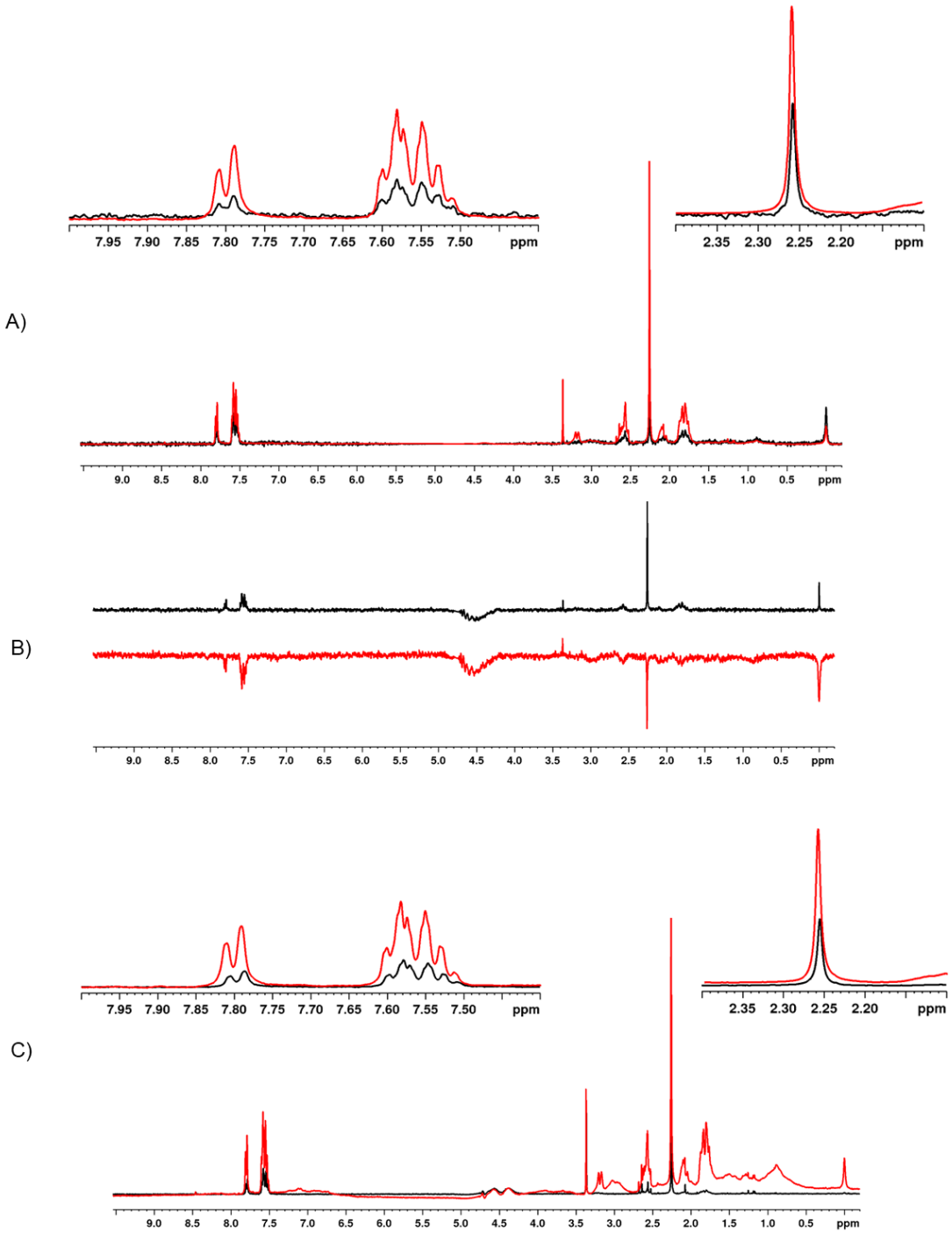

Fig. S5 A) STD NMR: overlay of the off-resonance spectrum of 1 mM ***R*-ketamine** with 50 µM HSA (red) and the difference spectra (black) with a saturation pulse of 400 Hz and water signal suppression at 4.703 ppm by excitation sculpting **B)**: waterLOGSY: overlay of 1 mM R-ketamine (black) with 1 mM *R*-ketamine + 50 µM HSA (red) **C)** CPMG NMR: overlay of the ^{1}H NMR with water signal suppression at 4.703 ppm by excitation sculpting of 1 mM *R*-ketamine with 50 µM HSA with a relaxation filter of 2 ms (red) and 200 ms (black)

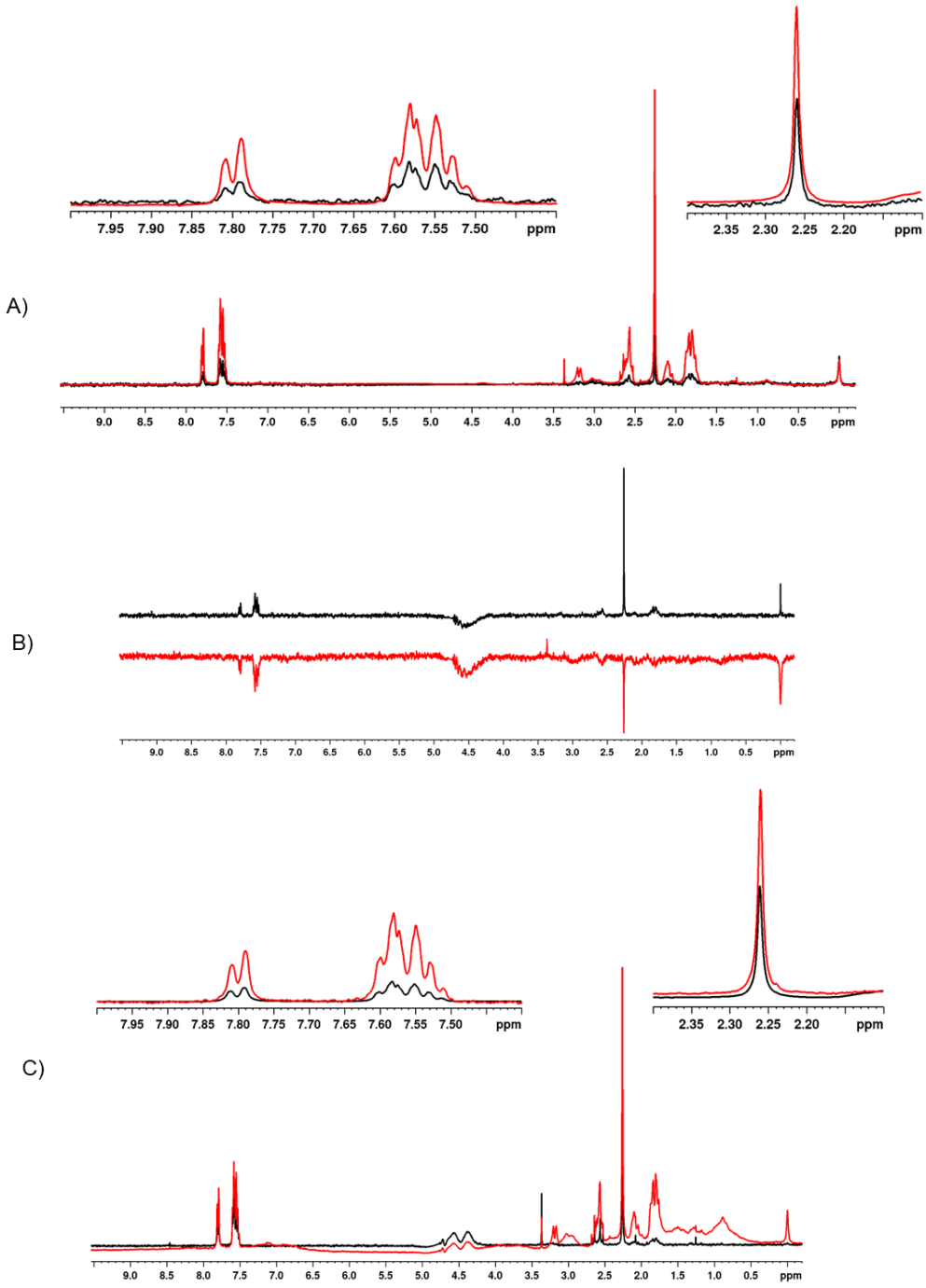

Fig. S6 A) STD NMR: overlay of the off-resonance spectrum of 1 mM **racemic ketamine** with 50 µM HSA (red) and the difference spectra (black) with a saturation pulse of 400 Hz and water signal suppression at 4.703 ppm by excitation sculpting **B):** waterLOGSY: overlay of 1 mM racemic ketamine (black) with 1 mM racemic ketamine + 50 µM HSA (red) **C)** CPMG NMR: overlay of the ^{1}H NMR with water signal suppression at 4.703 ppm by excitation sculpting of 1 mM racemic ketamine with 50 µM HSA with a relaxation filter of 2 ms (red) and 200 ms (black)

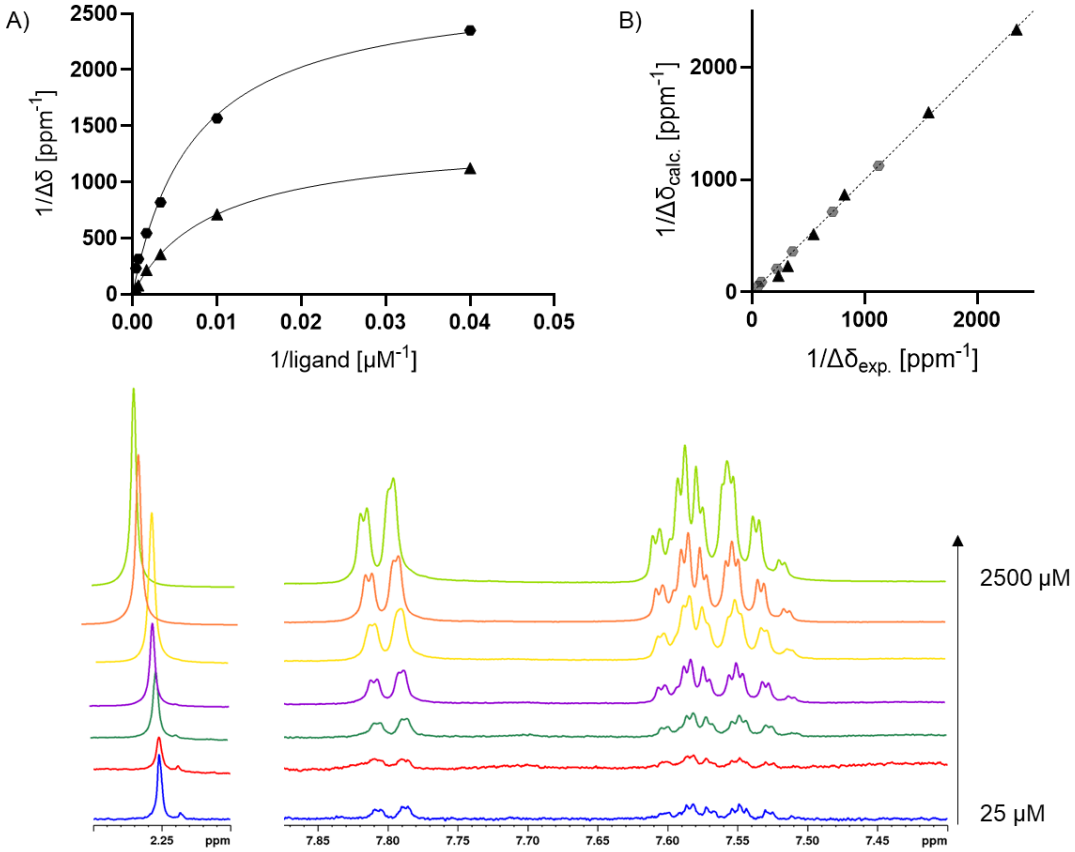

Fig. S7 A) double reciprocal fit for pK_{aff} according to Eq. (8) for ▲$NHCH_3$ and ●$H_{arom'}$ between Δσ and ligand concentration for ***R*-ketamine B)** correlation between calculated and experimental data of Δσ of the double reciprocal fit **C)** shift of signal at 2.26 and 7.56-7.80 ppm at different ligand concentration of *R*-ketamine and constant protein concentration of 25 μM

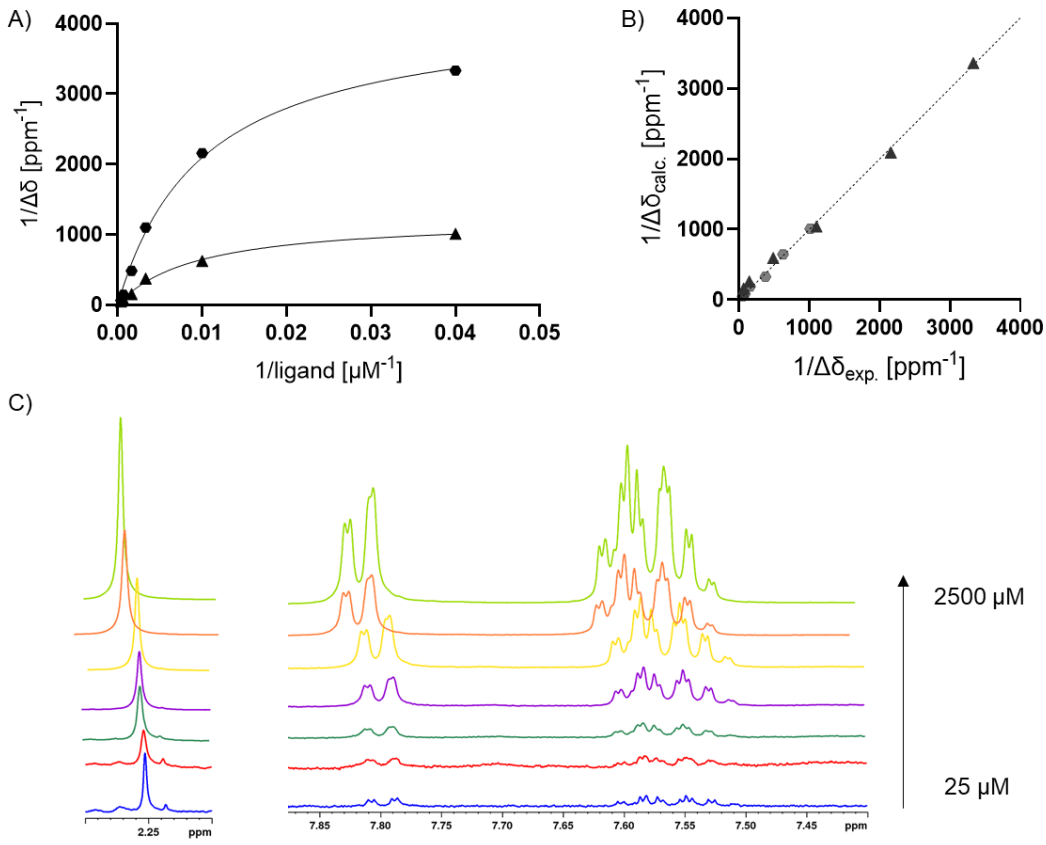

Fig. S8 A) double reciprocal fit for pK_{aff} according to Eq. (8) for ▲NHC**H**$_3$ and ●H_{arom}, between Δσ and ligand concentration for **racemic ketamine B)** correlation between calculated and experimental data of Δσ of the double reciprocal fit **C)** shift of signal at 2.26 and 7.56-7.80 ppm at different ligand concentration of racemic ketamine and constant protein concentration of 25 μM

References:

Ammon, H.P.T., 2001. Arzneimittelneben- und -wechselwirkungen, 4th ed. Wissenschaftliche Verlagsgesselschaft GmbH Stuttgart.

Asensi-Bernardi, L., Martin-Biosca, Y., Villanueva-Camañas, R.M., Medina-Hernández, M.J., Sagrado Vives, S., 2010. Evaluation of enantioselective binding of fluoxetine to human serum albumin by ultrafiltration and CE–experimental design and quality considerations. Electrophoresis 31, 3268-3280.

Claridge, T.D., 2016. High-resolution NMR techniques in organic chemistry, 3rd ed. Elsevier.

Dayton, P., Stiller, R., Cook, D., Perel, J., 1983. The binding of ketamine to plasma proteins: emphasis on human plasma. Eur. J. Clin. Pharmacol. 24, 825-831.

Doweiko, J.P., Nompleggi, D.J., 1991. The role of albumin in human physiology and pathophysiology, Part III: Albumin and disease states. J. Parenter. Enteral Nutr. 15, 476-483.

FDA, 2019. FDA approves new nasal spray medication for treatment-resistant depression; available only at a certified doctor´s office or clinic. FDA News Release.

Fernández, C., Wider, G., 2006. Advanced Techniques in Biophysics. Springer Berlin, Heidelberg

Hijazi, Y., Boulieu, R., 2002. Protein binding of ketamine and its active metabolites to human serum. Eur. J. Clin. Pharmacol. 58, 37-40.

Kohtala, S., 2021. Ketamine - 50 years in use: from anesthesia to rapid antidepressant effects and neurobiological mechanisms. Pharmacol. Rep. 73, 323-345.

Kragh-Hansen, U., 1981. Molecular aspects of ligand binding to serum albumin. Pharmacol. Rev. 33, 17-53.

Martínez-Gómez, M.A., Villanueva-Camañas, R.M., Sagrado, S., Medina-Hernández, M.J., 2007. Evaluation of enantioselective binding of antihistamines to human serum albumin by ACE. Electrophoresis 28, 2635-2643.

Motulsky, H.J., Neubig, R.R., 2010. Analyzing binding data. Curr Protoc Neurosci 52, 7.5. 1-7.5. 65.

Pedraz, J., Marino, E., Burguillo, F., Dominguez-Gil, A., 1985. In vitro binding of ketamine to human serum albumin. Int. J. Pharm. 25, 147-153.

Rahman, M.H., Maruyama, T., Okada, T., Imai, T., Otagiri, M., 1993. Study of interaction of carprofen and its enantiomers with human serum albumin—II: stereoselective site-to-site displacement of carprofen by ibuprofen. Biochem. Pharmacol. 46, 1733-1740.

Routledge, P., 1986. The plasma protein binding of basic drugs. Br. J. Clin. Pharmacol. 22, 499-506.

Schmidt, S., Holzgrabe, U., 2023. Method Development, Optimization, and Validation of the Separation of Ketamine Enantiomers by Capillary Electrophoresis Using Design of Experiments. Chromatographia 86, 87-95.

Spinella, R., Sawhney, R., Jalan, R., 2016. Albumin in chronic liver disease: structure, functions and therapeutic implications. Hepatol. Int. 10, 124-132.

Stockman, B.J., Dalvit, C., 2002. NMR screening techniques in drug discovery and drug design. Prog Nucl Magn Reson Spectrosc. 41, 187-231.

Sudlow, G., Birkett, D., Wade, D., 1975. The characterization of two specific drug binding sites on human serum albumin. Mol. Pharmacol. 11, 824-832.

Sudlow, G., Birkett, D., Wade, D., 1976. Further characterization of specific drug binding sites on human serum albumin. Mol. Pharmacol. 12, 1052-1061.

Tillement, J.-P., Lhoste, F., Giudicelli, J., 1978. Diseases and drug protein binding. Clin. Pharmacokinet. 3, 144-154.

Tolksdorf, W., 1988. Neue Aspekte zu Ketamin in der Anaesthesie, Intensiv-und Notfallmedizin. Springer.

Volpp, M., Holzgrabe, U., 2019. Determination of plasma protein binding for sympathomimetic drugs by means of ultrafiltration. Eur. J. Phar. Sci. 127, 175-184.

Walpole, S., Monaco, S., Nepravishta, R., Angulo, J., 2019. STD NMR as a technique for ligand screening and structural studies. Methods Enzymol. 615, 423-451.

Wani, T.A., Bakheit, A.H., Zargar, S., Rizwana, H., Al-Majed, A.A., 2020. Evaluation of competitive binding interaction of neratinib and tamoxifen to serum albumin in multidrug therapy. Spectrochim. Acta A Mol. Biomol. Spectrosc. 227, 117691.

White, P., Ham, J., Way, W., Trevor, A., 1980. Pharmacology of ketamine isomers in surgical patients. Anesthesiology.

Yamasaki, K., Chuang, V.T.G., Maruyama, T., Otagiri, M., 2013. Albumin–drug interaction and its clinical implication. Biochim. Biophys. Acta - Gen. 1830, 5435-5443.

3.4. Stability assessment: ketamine

Sebastian Schmidt, Ulrike Holzgrabe

Unpublished manuscript.

1. Introduction

The control of impurities in drugs and medicinal products has always been a major challenge for authorities and the pharmaceutical industry. Such impurities can be starting products, products of side reactions, impurities of reagents, solvents, catalysts, and degradation products. Various guidelines of the International Council for Harmonization of Technical Requirements for Pharmaceuticals for Human Use (ICH) specify how to classify, control, and analyze impurities. Guidelines ICH-Q3A-Q3E deal with impurities in the active pharmaceutical ingredient (API), in drug products, as well as residual solvents, elemental impurities, and extractables and leachables [1-5]. The control of mutagenic substances is described in guideline ICH-M7 “assessment and control of DNA reactive (mutagenic) impurities in pharmaceuticals to limit potential carcinogenic risk” [6]. How exactly an impurity must be characterized is categorized based on the maximum daily intake of the API. The reporting threshold describes the limit above which an impurity must be named. Above the identification threshold, the structure of the impurity must be elucidated and above the qualification threshold a full biological and toxicological investigation must be carried out. To assess the stability of the API, stability studies must be performed, and possible degradation products must be characterized. Guideline ICHQ1A(R2) describes the procedure for stability testing of API and drugs [7]. In addition to intermediate, accelerated, and long-term studies (cf. Table 1), stress tests must be also carried out. Long term stability can be performed under two different conditions depending on the applicant´s choice. In option B, temperature is increased to 30 °C and relative humidity to 65%, compared to option A, where temperature is set at 25 °C and 60%. If option B is selected, no intermediate tests need to be performed.

Table 1 Overview of storage conditions of stability test according to ICH Q1A (R2) [7], temp. = temperature, RH = relative humidity

study	storage condition		minimum time covered by data at submission
long term	A) temp.:25 °C ± 2 °C, RH: 60% ± 5%	B) temp.:30 °C ± 2 °C, RH: 65% ± 5%	12 months
intermediate	temp.:30 °C ± 2 °C, RH: 65% ± 5%		6 months
accelerated	temp.:40 °C ± 2 °C, RH: 75% ± 5%		6 months

Stress testing is characterized by forcing the degradation of the API under harsh conditions such as high temperature or pH values [8]. This provides information on possible degradation products that may be formed during storage. Typical stress test conditions are detailed in Table 2.

Table 2 Overview of common conditions of stress tests, modified according to Blessy et al. [8], RH = relative humidity

degradation investigated	experimental conditions	typical storage conditions	sampling time
hydrolysis	0.1 M HCl 0.1 M NaOH pH: 2, 4, 6, 8	40 °C, 60 °C	1-5 days
oxidation	3% H_2O_2	25 °C, 60 °C	1-5 days
thermal	heat chamber	60 °C; 60 °C, 75% RH; 80 °C; 80 °C, 75% RH; room temperature	1-5 days
photolytic	light 1 light 3	--	1-5 days
All experiments are performed with respective control (API and solutions)			

In a stress test, a yellow discoloration of an aqueous solution at 85 °C of the drug ketamine of a cooperating partner was reported. The monograph of ketamine in the European pharmacopoeia (PhEur) lists three related substances: one is a synthesis intermediate (impurity A) and the other two products of a side reaction of impurity A (impurity B and C). Under high temperatures and pH values, ketamine can degrade to impurity A and consequently impurity B and C can also be formed [9]. A mass spectrometric analysis of 150 ketamine samples revealed seventeen additional impurities that are mainly formed by side reactions [10]. In the wake of the emergence of nitroso contaminants in recent

years [11], *N*-nitrosoketamine would also be a conceivable impurity. Fig. 1 shows the structural formulas of possible impurities for ketamine and ketamine itself.

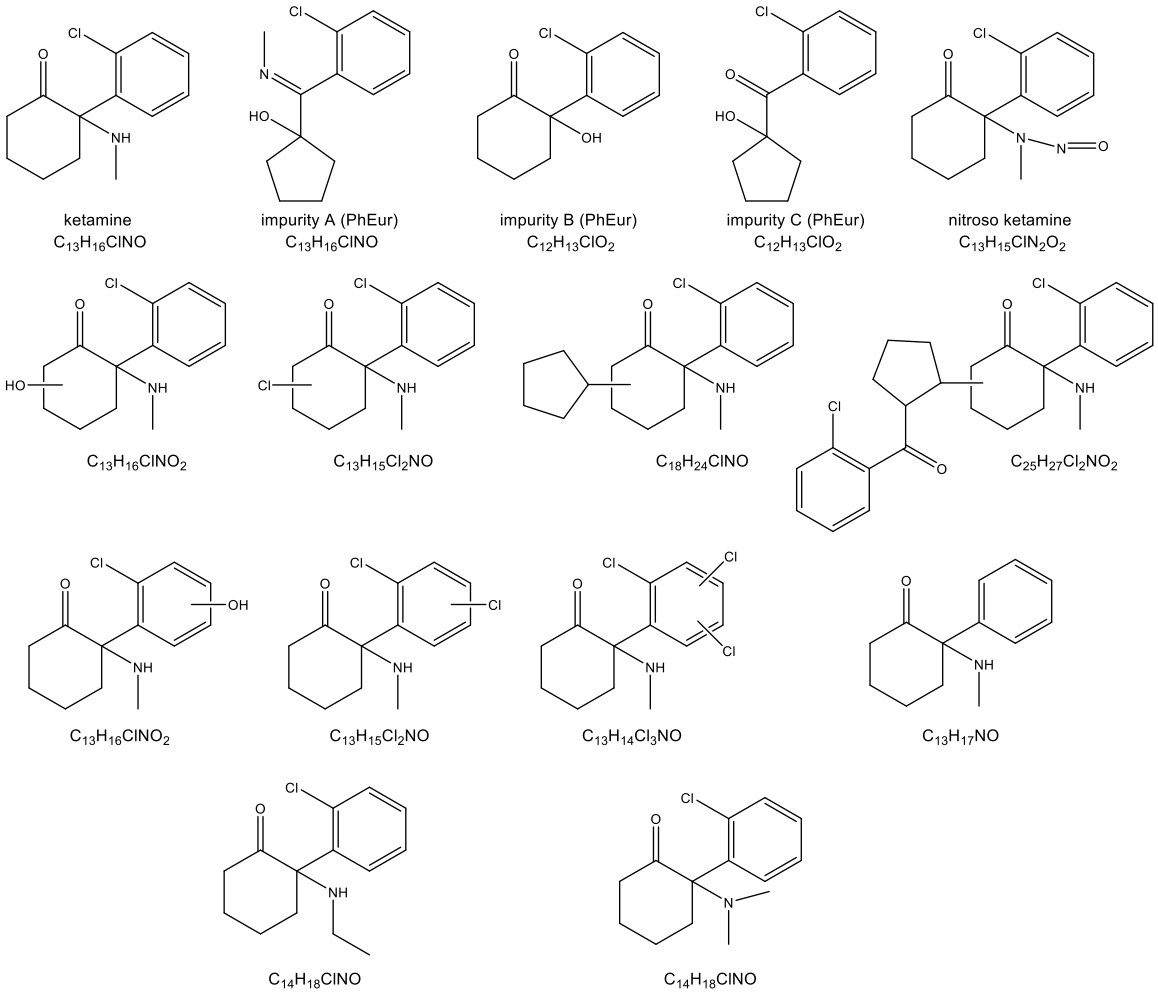

Fig. 1. Structural formulas of ketamine and its known impurities

Some stability studies have been conducted in the past, but no yellow discoloration has been reported [12-35]. Focus of these studies was primarily on drug mixtures in injection solutions and storage at 4 °C or at room temperature. The aim of this study was to elucidate the root cause of the yellow discoloration and to characterize a possible degradation of ketamine. For this purpose, a non-targeted general unknown comparative screening (GUCS) and information dependent acquisition (IDA) by means of high-resolution mass spectrometry (HRMS) was applied.

2. Material and methods

2.1. Chemicals

Ketamine hydrochloride, ketamine impurity A, sodium sulphate anhydrous, acetic acid 99%, Methanol HPLC grade were purchased from Sigma Aldrich (Taufkirchen, Germany).

Water and methanol MS grade were used from Merck Millipore (Darmstadt, Germany) as well as an inhouse water purification system. Formic acid 99% MS grade, 30% ammonium hydroxide were obtained from VWR chemicals (Darmstadt, Germany), concentrated hydrochloric acid 37% (V/V) and dichloromethane from Fisher Scientific (Schwerte, Germany) and sodium nitrite from Grüssing GmbH (Filsum, Germany). Ketamine as a solid as well as a yellow stressed solution of ketamine was provided by the cooperation partner.

2.2. Materials

For solid phase extraction (SPE) a Chromabond® C18 ec 6 ml column from Machery Nagel (Düren, Germany), strata SCX column 3 ml and screen C 3 ml columns, both from Phenomenex (Aschaffenburg, Germany) were used.

2.3. Instrumentation

ultra high-performance liquid chromatography-UV (UHPLC-UV) measurements were performed on a Vanquish™ Flex modular chromatographic system from Thermo Fisher Scientific (Germering, Germany) consisting of a dual pump with an online vacuum degaser, a thermostatted split sampler, a thermostatted column compartment with an active pre-heater and a diode array detector. UHPLC-HRMS spectra were measured on an Agilent Infinity II system 1290 series (Waldbronn, Germany), consisting of a quaternary pump, a thermostatted autosampler and column compartment, coupled to a Sciex X500R QTOF mass spectrometer (Concord, Ontario, Canada) equipped with a Turbo V™ Ion source with electrospray ionization (ESI) probe. X-ray powder diffraction (XRPD) was measured on a silicon single crystal holder and analyzed with a Bruker Discover D8 powder diffractometer (Karlsruhe, Germany). Melting point was measured on a MP70 melting point system from Mettler Toledo (Gießen, Germany).

2.4. Chromatographic conditions

Mobile phase A consisted of 95% water, 5% methanol and 0.1% formic acid, while mobile phase B contained 95% methanol, 5% water and 0.1% formic acid. The same gradient elution was used for UHPLC-UV and UHPLC-HRMS measurements. The gradient started after an initial isocratic step of 5% B for 0.2 min. B was raised to 40% for the next 2.4 min and then to 90% for 5.3 min. System was rinsed back to the initial condition of 5% B within 0.1 min and re-equilibrated for 3 min. Flow rate was 0.4 ml/min and the injection volume was 1 µl. UV detection was performed at 269 nm, using a diode array detector. A Kinetex® XB-C18 (2.6 µm,100 Å, 100 x 2.1 mm) column from Phenomenex (Aschaffenburg, Germany) was used and the temperature was set at 40 °C. UHPLC-UV data was analyzed with Chromeleon 7.3 from Thermo Fisher Scientific (Karlsruhe, Germany).

2.5. Mass spectrometry

Source parameters of the IDA methods used are shown in Table 3. ESI positive mode was used. An autocalibration was done after every fifth injection. UPHLC-HRMS data were evaluated using Sciex OS 2.1. By the non-targeted GUCS algorithm, a mass-to-charge-ratio (m/z) was assigned to the respective peaks, which were picked and integrated automatically. A peak was classified as hit when the area ratio of comparison between sample and reference was > 10. Structural formulas were developed based on the m/z of the precursor ion with a mass error < 5 ppm, isotope patterns with a tolerance < 20%, ring double bound equivalents and detected fragments.

Table 3 Parameters of mass spectrometry measurements

Parameter	ESI +
Gas 1 (psi)	50
Gas 2 (psi)	50
Temperature (°C)	600
Spray voltage (V)	5500
Mass range (Da)	50-500
Curtain gas (psi)	30
Declustering potential ± spread (V)	80
MS (TOF)	
Accumulation time (s)	0.25
Collision energy ± spread (V)	10
IDA	
Accumulation time (s)	0.1
Collision energy ± spread(V)	35 ± 15
Maximum candidate ions	10
Intensity threshold (counts/s)	10
Dynamic background subtraction	true

2.6. XRPD parameter

Scan run was from 3 ° to 50 ° 2θ. A step size of 0.020 ° was adjusted with a counting time of 2.00 s for each step. XRPD spectra were measured with DIFFRAC.Measurement Center and evaluated with DIFFRAC.EVA from Bruker (Karlsruhe, Germany)

2.7. Extraction

Liquid-Liquid extraction (LLE): 20 ml sample of the yellow stressed solution were acidified with 0.1 M HCl and then extracted three times with 10 ml dichloromethane.

SPE: Strata SCX and Screen C columns were first conditioned with 1 ml methanol and then equilibrated with 1 ml of 0.1 M HCl. 5 ml sample of the yellow stressed solution were acidified with 0.1 M HCl to a concentration of 100 mg/ml and loaded on the column. The column was washed with 1 ml 0.1 M HCl (aqueous) and 1 ml 0.1 M HCl (methanolic) and dried in vacuo for 5 min. Solutions were discarded and the analyte was eluted with 1 ml 5% ammonium hydroxide (methanolic). The Chromabond® C18 ec column was conditioned with 6 ml methanol and afterwards with 6 ml water. 5 ml sample of the yellow stressed solution was acidified with 0.1 M HCl to a concentration of 100 mg/ml and loaded on the column. Column was washed with 3 ml methanol/water (5/95 V/V). Analytes were eluted with 4 ml methanol.

Eluted SPE samples were diluted with water to a concentration of 0.01 mg/ml and LLE samples with methanol.

2.8. Sample preparation

Stock solutions of ketamine, (1 mg/ml), *N*-nitrosoketamine (1 mg/ml) and impurity A (0.4 mg/ml) were prepared by weighing the required amount of substance and by dissolving in water. For *N*-nitrosoketamine a 50/50 (V/V) mixture of water and methanol was used as solvent. A mixture of all substances was prepared as well as reference solutions by diluting stock solutions to a concentration of 0.01 mg/ml each for UHPLC-HRMS. As stress solutions 10 g of ketamine was weighed and dissolved in 50 ml water, 0.1 M sodium hydroxide and 0.1 M hydrochloric acid, respectively (200 mg/ml). After heating at 85 °C and stirring for 10 h, stress solutions were diluted with water to a concentration of 0.01 mg/ml. Sample concentrations for UHPLC-UV were 0.2 mg/ml respectively.

2.9. Synthesis of *N*-nitrosoketamine

1 g ketamine was dissolved in 20 ml acetic acid (20%, V/V). An equimolar amount of sodium nitrite was added to the solution and stirred. After 15 min of stirring 10 ml of ice-cold water was poured into the solution. Subsequently, *N*-nitrosoketamine was extracted with 3 x 30 ml chloroform. Organic phase was dried with anhydrous sodium sulphate, filtered, and evaporated. A yellow solid remained with a yield of 74%. No further purification was performed.

3. Results and discussion

3.1. Investigation of polymorphism

Polymorphs differ in their physical properties, such as solubility and melting point. Additionally, it has already been shown that different polymorphs tend to form different degradation products [36]. Hence, it was checked whether the different samples of ketamine show polymorphism since the yellow discoloration did not occur in every batch.

First, the melting point of ketamine from another manufacturer (SA) was measured as a reference and then compared with the “polluted” batch (18M). According to the monograph of ketamine hydrochloride of the PhEur [37], the API melts under decomposition at a temperature around 260 °C. Both SA and 18M showed a melting point of 258 °C and decomposed, making polymorphism unlikely. XRPD measurements were performed to confirm this. The diffraction patterns are shown in Fig. 2. Since no differences between the batches was found, no polymorphism could be detected.

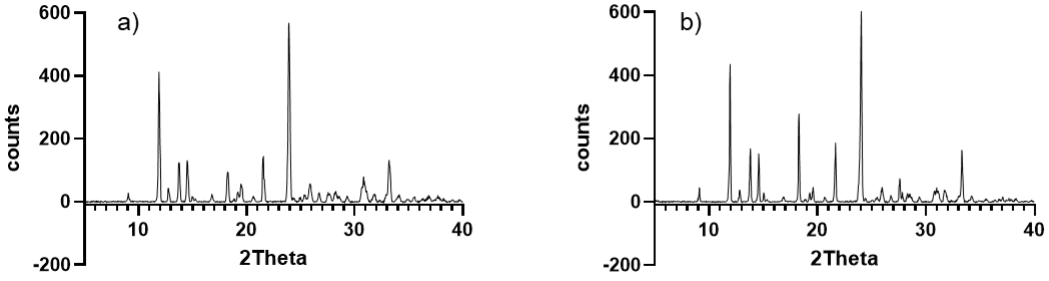

Fig. 2. XRPD measurements of a) ketamine (SA) b) ketamine (18M)

3.2. UHPLC-HRMS

IDA measurements which simultaneously record MS and MS/MS spectra withing one analysis run were performed [38]. Fragmentation of specific precursors is based on predefined criteria such as signal intensity. Ring and double bond equivalents (RDB) were used for structural elucidation, as well as fragments and their respective fragmentation pattern. Structural formulas were derived from detected m/z of the precursor mass with a mass tolerance error of < 5 ppm and isotopic pattern with an intensity tolerance of 20%. A proposed fragmentation pattern of ketamine is shown in Fig. 3.

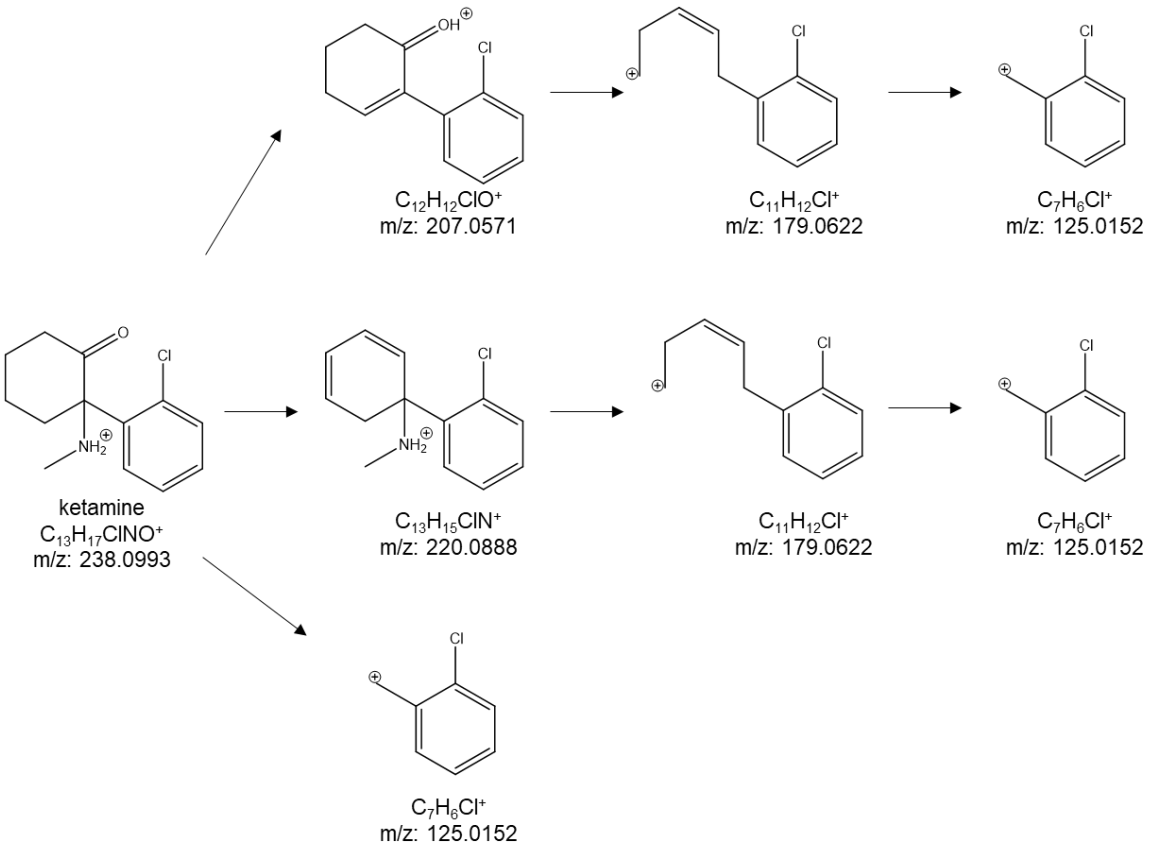

Fig. 3. Proposed fragmentation pattern of ketamine

Since GUCS is a non-targeted approach, possible impurities may not be detected due to non-suitable parameters for ionization. Liu et al. were able to detect 17 different ketamine impurities with their ionization parameters, which is why they were used for this study [10]. To confirm the usability of these ionization parameters, a mixture consisting of ketamine and two other ketamine related substances was prepared. *N*-nitrosoketamine was synthesized according to Toyama et al. [39]. Ketamine impurity A of the PhEur is commercially available as a reference substance. An UHPLC-UV analysis of an aqueous solution of impurity A showed another impurity besides impurity A. The solution was measured again after two days of storage in the refrigerator: interestingly the peak of the unknown impurity increased while the peak of impurity A decreased compared to the first measurement. Therefore, impurity A is degraded in aqueous solution to an unknown impurity. Sass and Fusari presented a mechanism for impurity A to form impurity B and C in aqueous solution [9]. The mechanism is shown in Fig. 4.

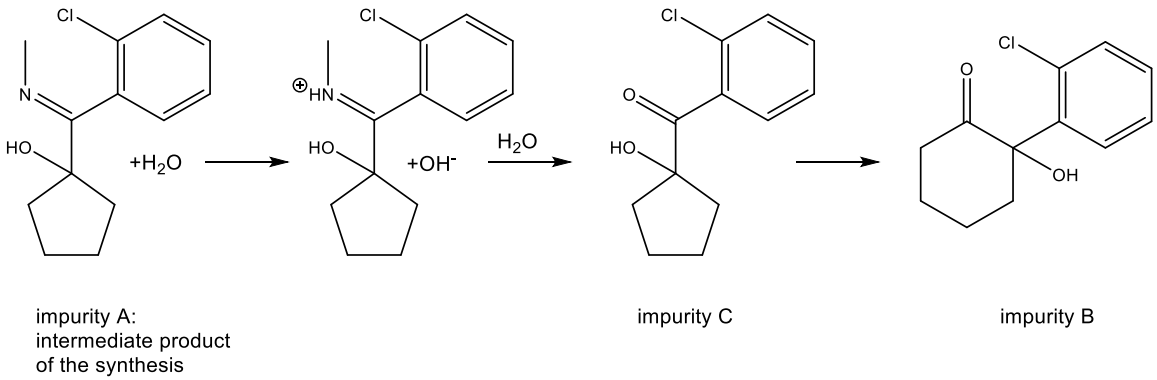

Fig. 4. Presented mechanism of formation of impurity B and C of the European pharmacopoeia by Sass and Fusari [9]

To determine the identity of the unknown impurity, an aqueous solution of impurity A was measured by UHPLC-HRMS. IDA measurements determine up to the 10 most intense m/z depending on previously defined settings and fragment them automatically in the same measurement. A m/z of 247.0497 was detected. The signal is a sodium adduct to the m/z of 225.0677, which corresponds to impurity B. The m/z of impurity B itself could not be detected. However, the most intense signal was the m/z of 207.0512. This signal is also the main fragment of ketamine (cf. Fig. 3), which corresponds to the cleaved chlorophenyl residue. It is highly probable that this fragment is also generated by impurity B, since the chlorophenyl moiety is also present. It appears that impurity B is a) very strongly fragmented by the selected ionization parameter to the m/z of 207.0512 and b) preferentially forms a sodium adduct. Therefore, no m/z of 225.0677 is detected. However, since the sodium adduct was detected, it can be assumed that the unknown impurity is impurity B. Nevertheless, without a reference substance, the structure can only be assumed. The mixture therefore consisted of ketamine, *N*-nitrosoketamine, impurity A and probably impurity B. Fig. 5 shows an extraction ion chromatogram (XIC) of the mixture which confirms the suitable ionization parameters and the usability for GUCS.

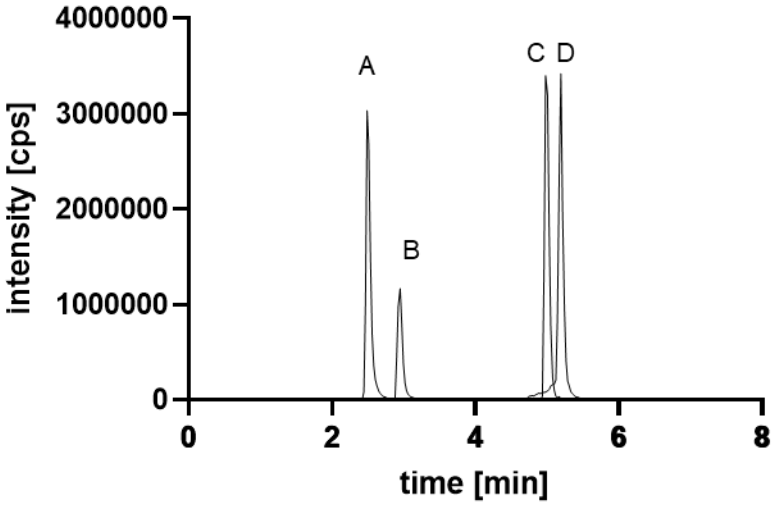

Fig. 5. Extracted ion chromatogram (XIC) of ketamine (A), impurity A (B), probably impurity B (C) and *N*-nitrosoketamine (D), each 0.01 mg/ml

3.3. General unknown comparative screening

GUCS is an excellent tool for impurity profiling of APIs. It is based on the comparison between a sample and a reference. Such a reference can be for example a blank sample without API, an API of another batch or sampling after different points in time. Peak areas and retention time are used to calculate the factor in which a peak occurs in the sample compared to the reference. A peak is indicated as a hit if the area ratio of comparison between sample and reference is at least 10.0. An area ratio of comparison of 1.00 indicates no difference between reference and sample. Small differences may be due to different weights.

GUCS was divided into three categories: 1. Stress testing of the “polluted” batch; 2. Extraction of a yellow stressed solution (YS); 3. Comparison with another manufacturer´s API and water as blank sample.

Stress conditions were set according to the description of the collaborator. 10 g of solid API was dissolved in 50 ml water and heated for 85 °C for 10 h. In addition, preparations with 0.1 M hydrochloric acid and 0.1 M sodium hydroxide were studied. In a sodium hydroxide solution, the API did not completely dissolve. Every two hours, a sample was drawn from the respective stress solution. In contrast to the observations made by the collaborator, none of the solutions turned yellow. Nevertheless, GUCS was performed with the stressed samples. As reference, a sample taken just before temperature rise was set and compared with a sample taken after 10 h of heating. The area ratio of comparison of acidic and aqueous conditions is very close to 1.00, indicating that no API has been

degraded. Evaporation of solvent during stressing could account for the slightly elevated values of the sample after 10 h. Lower value for basic conditions can be explained by the poorly dissolved API in the solvent. In all stress conditions, only ketamine was shown as a hit and no other impurities were found. Therefore, ketamine is stable in water, acid, and base at temperature of 85 °C for 10 h.

SPE and LLE were used to isolate the impurity responsible for the yellow discoloration. For the SPE, three columns with different column materials and thus different retention mechanism were used. Two of the columns were cation exchangers and one was a reversed phase column. Visually, during the procedure of SPE and LLE, an extraction of the yellow color could be observed. As reference a blank sample of water was set. Only ketamine, the ketamine fragment (m/z: 207.0573) and the chlorine isotope (m/z: 240.0965) were detected as a hit. Due to sample preparation, API was hardly extracted, which is reflected in a small area ratio of comparison.

In the last GUCS, YS was compared with a water blank and a ketamine API from another manufacturer as a reference. The result obtained is equal to the previous ones. Only ketamine, ketamine fragments (m/z: 125.0151, 207.0573) and the chlorine isotope (m/z: 240.0967) and no impurities were detected. Table 4 shows the results of the respective GUCS lists.

3.4. UHPLC-UV measurements

Mass detectors are very sensitive and operate at lower concentration to avoid detector overload. In case, the yellow impurity is characterized by a high absorption coefficient, it might not be detected by mass spectrometry because of a low concentration. Therefore, additional UHPLC-UV measurements were performed to be able to measure the samples at much higher concentrations. Fig. 6 shows chromatograms of pure solutions of SA and YS, a mixture of SA, *N*-nitrosoketamine and impurity A and a mixture, where ketamine from SA and YS were mixed in a 1:1 ratio, *N*-nitrosoketamine and impurity A. No differences were seen between the pure solutions of SA and YS as well as between both mixtures. No impurities were detected. Since the peak area is almost identical at the same concentration (0.2 mg/ml), it can be assumed that the yellow discoloration does not result from the degradation of the API. UHPLC-UV data thus confirm the results of the UHPLC-HRMS measurements that ketamine is stable under the stress conditions mentioned.

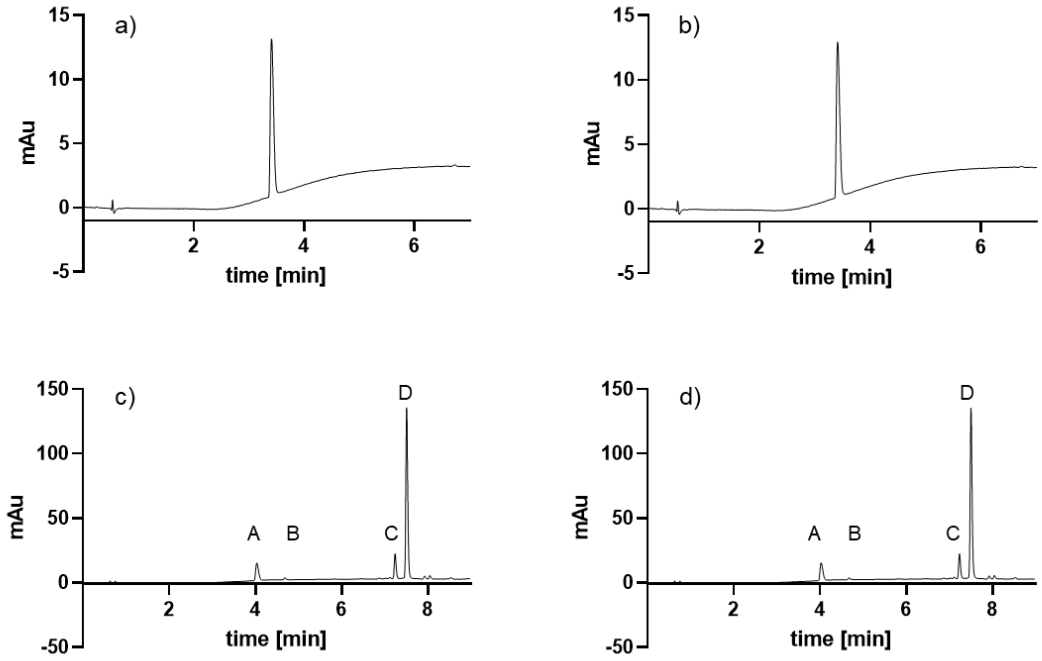

Fig. 6. UHPLC-UV measurements: a) ketamine (SA) b) ketamine (YS) c) mixture of ketamine SA (A), impurity A (B), possibly impurity B (C) and *N*-nitrosoketamine (D) d) mixture of ketamine SA and ketamine YS (A), impurity A (B), possibly impurity B (C) and *N*-nitrosoketamine (D), each 0.2 mg/ml

3.5. Assessment of other influencing factors

Upon further risk evaluation, the water used was identified as a possible factor for the discoloration, as water of different quality was used by our laboratory and the collaborator. The water used of the collaborator was tap water (A), while our water was deionized water with a resistivity of 18.2 Ωm (B). The further planned procedure was to exchange water batches and to carry out the stress tests again with the water of the respective other.

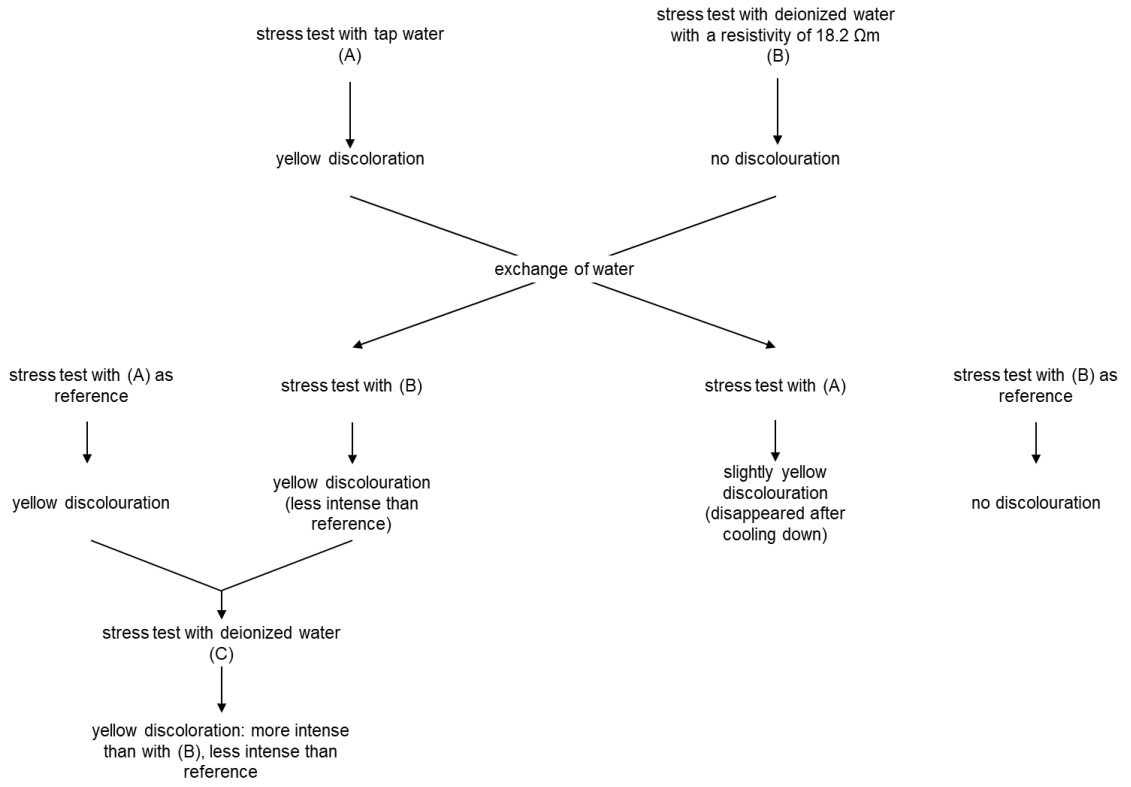

Fig. 7. Chronicle of the performed stress tests; (A) = tap water, (B) = deionized water with a resistivity of 18.2 Ωm, (C) = deionized water

Fig. 7 shows the chronicle of the stress tests. In our laboratory a slight yellowish discoloration was observed after 10 h using (A), which disappeared again after cooling down. Even though the yellow color disappeared, it could be reproduced for the first time. The reference stress test with (B) showed no discoloration However, a stress test, performed by the collaborator with (B), showed a yellow discoloration. This was not as intensely colored as their reference test with (A). In addition, the collaborator stressed the API with their own deionized water (C). A yellowish discoloration that was more intense than the stress test with (B), but less intense than the reference with (A) was observed.

Consequently, the quality of the used water seems to have an influence on the yellow discoloration, as different quality showed different intensity of discoloration. How exactly this influence works has not yet been clarified. It is tempting to speculate that an equilibrium reaction depending on time of heating, temperature, and water quality might shift the equilibrium to the “colored” or the “colorless” side. This could be the reason why the yellow color disappeared once after the reaction solution cooled down and reproducibility was difficult. Further investigations need to be carried out.

Table 4 General unknown comparative screening (GUCS) list of the UHPLC-MS measurements; N/A = not applicable

GUCS reference vs. sample	m/z of found hits	retention time	adduct	precursor mass	area ratio of comparison	assignment
blank vs YS	ketamine	2.50	[M+H]+	238.0991	325.297	API
	125.0151	2.50	[M+H]+	125.0151	511.208	fragment: API
	207.0573	2.50	[M+H]+	207.0573	552.942	fragment: API
	240.0965	2.50	[M+H]+	240.0965	388.588	chlorine isotope: API
SA vs YS	ketamine	2.50	[M+H]+	238.0991	0.944	API
	125.0154	N/A	[M+H]+	125.0154	N/A	fragment: API
	240.0967	N/A	[M+H]+	240.0967	N/A	chlorine isotope: API
18M 0h vs 18M 10h: H_2O	ketamine	2.48	[M+H]+	238.0991	1.007	API
18M 0h vs 18M 10h: HCl	ketamine	2.48	[M+H]+	238.0991	1.031	API
18M 0h vs 18M 10h: NaOH	ketamine	2.50	[M+H]+	238.0991	0.794	API
blank vs LLE	ketamine	2.48	[M+H]+	207.0573	0.079	API
	207.0573	N/A	[M+H]+	240.0965	N/A	fragment: API
	240.0965	N/A	[M+H]+	207.0573	N/A	chlorine isotope: API
blank vs SPE: Screen C	ketamine	2.48	[M+H]+	238.0991	0.022	API
	207.0573	N/A	[M+H]+	207.0573	N/A	fragment: API
	240.0965	N/A	[M+H]+	240.0965	N/A	chlorine isotope: API
blank vs SPE: C18	ketamine	2.48	[M+H]+	238.0991	0.040	API
	207.0573	N/A	[M+H]+	207.0573	N/A	fragment: API
	240.0965	N/A	[M+H]+	240.0965	N/A	chlorine isotope: API
blank vs SPE: SCX	ketamine	2.47	[M+H]+	238.0991	0.002	API

However, the yellow discoloration is not due to a degradation of the API, which is stable under the tested stress conditions, as UHPLC-HRMS/UV data show. Additionally, it can be stated, that the impurity causing the yellow color, occurs below the reporting threshold.

4. Conclusion

The root cause of the yellow discoloration could not be found. Stress tests performed did not show any discoloration and could not be reproduced. However, it was shown that ketamine remains stable in aqueous, acidic, and basic solutions at 85 °C and does not decompose. Therefore, the yellow discoloration cannot be simply attributed to the API. However, there must be other influences, like water quality. Other factors influencing the process of the collaborator must be considered.

References

[1] ICH Guideline Q3A(R2) on Impurities in New Drug Substances 2006.

[2] ICH Guideline Q3B(R2) on Impurities in New Drug Products 2006.

[3] ICH guideline Q3E EWG on Assessment and Control of Extractables and Leachables for Pharmaceuticals and Biologics. 2019.

[4] ICH Guideline Q3C(R8) on Residual Solvents. 2021.

[5] ICH Guideline Q3D(R2) on Elemental Impurities. 2022.

[6] ICH Guideline M7(R2) on Assessment and Control of DNA Reactive (Mutagenic) Impurities in Pharmaceuticals to Limit Potential Carcinogenic Risk 2023.

[7] ICH Guideline Q1A(R2) on Stability Testing of New Drug Substances and Products. 2003.

[8] Blessy, M., R.D. Patel, P.N. Prajapati, and Y. Agrawal, Development of forced degradation and stability indicating studies of drugs - A review. J. Pharm. Anal., 2014. 4(3): p. 159-165.

[9] Sass, W.C. and S.A. Fusari, Ketamine, in Analytical profiles of drug substances. 1977, Elsevier. p. 297-322.

[10] Liu, C.-M., Z.-D. Hua, W. Jia, P.P. Liu, and Y. Xu, Characterization of 17 unknown ketamine manufacturing by-product impurities by UHPLC-QTOF-MS. Drug. Test. Anal., 2022. Special Issue: p. 1-11.

[11] Holzgrabe, U., Nitrosated active pharmaceutical ingredients–lessons learned? J. Pharm. Sci., 2023. 112(5): p. 1210-1215.

[12] Ancedy, D., M. Sebti, M. Postaire, F. Vidal, S. Cisternino, and J. Schlatter, Stability of 10-mg/mL and 50-mg/mL ketamine oral solutions. Am. J. Health-Syst. Pharm., 2021. 78(9): p. 825-831.

[13] Anderson, C. and M. MacKay, Stability of fentanyl citrate, hydromorphone hydrochloride, ketamine hydrochloride, midazolam, morphine sulfate, and pentobarbital sodium in polypropylene syringes. Pharm., 2015. 3(4): p. 379-385.

[14] Bedocs, P., D.L. Evers, and C.C. Buckenmaier III, Predosing chemical stability of admixtures of propofol, ketamine, fentanyl, and remifentanil. Anesth. Analg., 2019. 129(1): p. e13-e15.

[15] Beiler, B., D. Barraud, J. Vigneron, and B. Demoré, Physicochemical stability of an admixture of lidocaine and ketamine in polypropylene syringe used in opioid-free anaesthesia. Eur. J. Hosp. Pharm., 2020. 27(e1): p. e79-e83.

[16] Bourdon, F., N. Simon, D. Lannoy, C. Berneron, B. Décaudin, L. Reumaux, A. Duhamel, P. Richart, and P. Odou, Quality control and stability of ketamine, remifentanil, and sufentanil syringes in a pediatric operating theater. Pediatric Anesthesia, 2019. 29(2): p. 193-199.

[17] Chen, F., H. Xiong, J. Yang, B. Fang, J. Zhu, and B. Zhou, Butorphanol and ketamine combined in infusion solutions for patient-controlled analgesia administration: a long-term stability study. Med. Sci. Monit., 2015. 21: p. 1138.

[18] Closset, M., J. Hecq, E. Gonzalez, B. Bihin, J. Jamart, and L. Galanti, Does an interaction exist between ketamine hydrochloride and Becton Dickinson syringes? Eur. J. Hosp. Pharm., 2017. 24(4): p. 230-234.

[19] Colsoul, M., J. Hecq, L. Soumoy, L. Defrene, and N. Goderniaux, Long-Term Stability of an Infusion Containing Morphine, Ketamine and Lorazepam in Syringe at 5±3 C. J Pharma Pharma Sci: JPPS-182. DOI, 2019. 10: p. 2574-7711.100082.

[20] Daouphars, M., C.-H. Hervouët, P. Bohn, D. Martin, J. Rouvet, F. Basuyau, and R. Varin, Physicochemical stability of oxycodone-ketamine solutions in polypropylene syringe and polyvinyl chloride bag for patient-controlled analgesia use. Eur. J. Hosp. Pharm., 2018. 25(4): p. 214-217.

[21] Donnelly, R.F., Physical compatibility and chemical stability of ketamine–morphine mixtures in polypropylene syringes. Can. J. Hosp. Pharm., 2009. 62(1): p. 28.

[22] Donnelly, R.F., Stability of diluted ketamine packaged in glass vials. Can. J. Hosp. Pharm., 2013. 66(3).

[23] Donnelly, R.F., E. Willman, and G. Andolfatto, Stability of ketamine–propofol mixtures for procedural sedation and analgesia in the emergency department. Can. J. Hosp. Pharm., 2008. 61(6): p. 426-430.

[24] Ensom, M.H., D. Decarie, K. Leung, and C. Montgomery, Stability of hydromorphone–ketamine solutions in glass bottles, plastic syringes, and IV bags for pediatric use. Can. J. Hosp. Pharm., 2009. 62(2): p. 112.

[25] Fang, B., L. Wang, J. Gu, F. Chen, and X.-y. Shi, Physicochemical stability of ternary admixtures of butorphanol, ketamine, and droperidol in polyolefin bags for patient-controlled analgesia use. Drug. Des. Devel. Ther., 2016: p. 3873-3878.

[26] Foertsch, M.J., J.T. McMullan, N.J. Harger, D. Rodriquez Jr, A. Salvator, E.W.M. PharmD, and C.A. Droege, Ketamine stability over six months of exposure to moderate and high temperature environments. Preshosp. Emerg. Care, 2022. 26(3): p. 422-427.

[27] Gu, J., W. Qin, F. Chen, and Z. Xia, Long-term stability of tramadol and ketamine solutions for patient-controlled analgesia delivery. Med. Sci. Monit., 2015. 21: p. 2528.

[28] Hamdi, M., C. Lentschener, C. Bazin, Y. Ozier, and L. Havard, Compatibility and stability of binary mixtures of acetaminophen, nefopam, ketoprofen and ketamine in infusion solutions. Eur. J. Anaesthesiol., 2009. 26(1): p. 23-27.

[29] Hijazi, Y., M. Bolon, and R. Boulieu, Stability of ketamine and its metabolites norketamine and dehydronorketamine in human biological samples. Clin. Chem., 2001. 47(9): p. 1713-1715.

[30] Huvelle, S., M. Godet, J.-D. Hecq, P. Gillet, B. Bihin, J. Jamart, and L. Galanti. Long-term stability of ketamine hydrochloride 50 mg/ml injection in 3 ml syringes. in Annales pharmaceutiques francaises. 2016. Elsevier.

[31] Izgi, M., B. Basaran, A. Muderrisoglu, A. Ankay Yilbas, M.S. Uluer, and B. Celebioglu, Evaluation of the stability and stratification of propofol and ketamine mixtures for pediatric anesthesia. Pediatric Anesthesia, 2018. 28(3): p. 275-280.

[32] Schenkel, L., I. Vogel Kahmann, and C. Steuer, Opioid-free anesthesia: physico chemical stability studies on multi-analyte mixtures intended for use in clinical anesthesiology. Hosp. Pharm., 2022. 57(2): p. 246-252.

[33] Schmid, R., G. Koren, J. Klein, and J. Katz, The stability of a ketamine-morphine solution. Anesth. Analg., 2002. 94(4): p. 898-900.

[34] Walker, S.E., S. Law, and C. DeAngelis, Stability and compatibility of hydromorphone and ketamine in normal saline. Can. J. Hosp. Pharm., 2001. 54(3).

[35] Watson, D.G., M. Lin, A. Morton, C.G. Cable, and D.A. McArthur, Compatibility and stability of dexamethasone sodium phosphate and ketamine hydrochloride subcutaneous infusions in polypropylene syringes. J. Pain Symptom Manag., 2005. 30(1): p. 80-86.

[36] Raijada, D.K., S. Singh, and A.K. Bansal, Influence of microenvironment pH, humidity, and temperature on the stability of polymorphic and amorphous forms of clopidogrel bisulfate. AAPS PharmSciTech, 2010. 11: p. 197-203.

[37] ketamine monograph. 2017, European Pharmacopeia 11th edition: Strasburg, France.

[38] Zhu, X., Y. Chen, and R. Subramanian, Comparison of information-dependent acquisition, SWATH, and MSAll techniques in metabolite identification study employing ultrahigh-performance liquid chromatography–quadrupole time-of-flight mass spectrometry. Anal. Chem., 2014. 86(2): p. 1202-1209.

[39] Toyama, Y., H. Shimizu, Y. Suzuki, Y. Miyakoshi, and H. Yoshioka, Genotoxic effects of N-nitrosoketamine and ketamine as assessed by in vitro micronucleus test in Chinese hamster lung fibroblast cell line. Environmental health and preventive medicine, 2006. 11(3): p. 120-127.

4. FINAL DISCUSSION

The aim of the thesis was to characterize old established drugs regarding the extent of protein binding and stability. The ephedra alkaloids were tested for possible stereoselective protein binding to AGP, while ketamine was tested to albumin. Ultrafiltration followed by CE analysis were used for the determination of the extent of the plasma protein binding and NMR spectroscopy ligand screening methods for insights about structural moieties involved in binding. A suitable CE method for the separation of the ketamine enantiomers and testing of their enantiomerical purity was developed by means of statistical design of experiments and validated according to established guidelines. In addition, various stability studies were carried out with ketamine as part of a collaboration with a pharmaceutical company. Possible impurities formed were evaluated by means of high-resolution mass spectrometry using an untargeted GUCS approach.

4.1. Enantioselective protein binding

Processes in the body that may be subject to stereoselective mechanisms, such as protein binding, have a major role on the pharmacokinetics of drugs. For older drugs, which have been on the market for a long time, the extent of protein binding with respect to stereoselectivity has hardly been investigated. However, Volpp et al. showed that the extent of plasma protein binding of the ephedra alkaloids ephedrine and pseudoephedrine in serum is significantly increased compared to isolated albumin and there are differences between their individual enantiomers [1]. AGP is the most important binding protein besides albumin and was used for the binding experiments of ephedra alkaloids. Furthermore, the enantioselective binding of ketamine to albumin was investigated since data were only available for racemic ketamine in literature. Both the binding of the ephedra alkaloids to AGP and the binding of ketamine to albumin showed no stereoselectivity. Table 1 shows the results of both experiments in comparison to some selected drugs that bind enantioselectively to the respective protein. The enantiomers of ketamine showed a similar percentage binding to racemic ketamine reported in the literature. The decrease in the binding of ephedra alkaloids is related to their basicity: the less the drugs are protonated at physiological pH, the weaker the drugs are bound. Conversely, the more basic the drug, the higher is the affinity to AGP.

Many ligands that are bound to AGP have a similar chemical structure. They are characterized by an aromatic, as well as a basic, moiety - usually an amine. In contrast, albumin binds many different types of substances that are of different chemical structure. NMR spectroscopy ligand screening methods offer great opportunities not only in drug discovery to identify lead structures, but also to study binding properties of proteins and

drugs to get more insights over the structural moieties involved in the binding process [2]. STD-NMR spectroscopy experiments were performed with the ephedra alkaloids and ketamine, while CPMG- and waterLOGSY-NMR spectroscopy experiments were measured only with ketamine.

Table 1 Results of the binding experiments as well as a selection of drugs with enantioselective binding; UF = ultrafiltration, CE = capillary electrophoresis, LSC = liquid scintillation counter, HPLC = high performance liquid chromatography, ACE = affinity capillary electrophoresis; ED = equilibrium dialysis, CD-EKC = cyclodextrin modified-electrokinetic chromatography, n/a = not applicable

drug	binding		protein	method
pseudoephedrine [3]	(+): 29.1%	(-): 27.6%	AGP	UF, CE
ephedrine [3]	(+): 25.0%	(-): 26.5%		
methylephedrine [3]	(+): 14.9%	(-): 17.3%		
norephedrine [3]	(+): 6.8%	(-): 7.7%		
propranolol [4]	S: 77.2%	R: 74.2%		UF, LSC
mexiletine [5]	S: 22.0%	R: 31.0%		UF, chiral HPLC
ketamine (not yet published)	S: 67.5%	R: 66.4%	HSA	UF, CE
thalidomide [6]	S: 55.0%	R: 65.0%		n/a
chlorpheniramine [7]	S: 82.0%	R: 76.0%		UF, ACE
bupivacaine [7]	S: 98.0%	R: 84.0%		
amlodipine [8]	S: 97.5%	R: 91.8%		ED, CE
verapamil [9]	S: 63.4%	R: 78.8%		UF, HPLC
zopiclone [10]	(+): 79.1%	(-): 87.9%		ED, fluorescence spectroscopy
catechin [5]	(+): 53.0%	(-): 64.0%		UF, CD-EKC

So far, only the binding of propranolol and lidocaine to AGP by STD-NMR spectroscopy has been studied with AGP as binding protein [11, 12]. These two studies confirm the observations made for the binding of ephedra alkaloids to AGP, where the aromatic protons are most strongly bound, followed by the protons of the substituents of the basic amin.

An additional molecular docking of the ephedra alkaloids to AGP provided further insights of similar binding interactions: π-π and van der Waals interactions of the phenyl ring with the hydrophobic binding pocket, a salt bridge of the amine to Glu92 as well as a cationic interaction with His97, and hydrogen bonds of the hydroxyl group to Arg90 and Glu92 were observed. Since propranolol has a naphthalene backbone as an aromatic moiety and not just a phenyl residue, this could explain the significantly stronger binding percentage of

propranolol to AGP compared to the ephedra alkaloids (cf. Table 1), as more hydrophobic interactions can take place.

Ketamine is partially uncharged at physiologically pH and can be considered as a possible ligand for the Sudlow`s site II of albumin since aromatic and neutral substances are bound at this binding site. Fluorescence experiments (data not shown) showed no fluorescence quenching when ketamine was added to albumin. Since tryptophane is found in Sudlow`s site I, ketamine does not bind at this binding site, moreover, binding to another binding site does not lead to a conformational change that attenuates the fluorescence. This and the fact that the aromatic protons, as well as the protons of the substituent of the basic amine, are most strongly bound as all NMR measurements showed, leads to the assumption that ketamine is bound to the Sudlow`s site II. Additionally, pK_{aff} and binding sites were determined graphically through established plots as well as mathematically for both the ephedra alkaloids and ketamine. Both showed to be low affinity ligands for their respective binding protein while binding to one main binding site.

Sensitive methods such as ITC provide data that are difficult to evaluate for low affinity ligands. NMR spectroscopy ligand screening methods, on the other hand, are also suitable for low-affinity ligands to characterize their binding properties and offer great potential for studying protein binding as the performed experiments demonstrated.

4.2. Stability testing

Impurities of API or pharmaceuticals can have different origins. They can be starting products, products of side reactions, impurities of reagents, solvents, catalysts, degradation products or stereoisomers such as enantiomers. Quality assurance of pharmaceutical products is the most important process of drug manufacturing. Due to the “Quality by Design” (QbD) approach, this is done from the first idea of a product to the market launch and beyond. A big part of this is to develop and validate methods by means of statistical procedures, perform stability testing and impurity profiling [11].

The separation of enantiomers is a major analytical challenge [12]. Due to the same physical and chemical properties in an achiral environment, enantiomers can only be separated from each other by derivatization to diastereomers or by introducing a chiral environment. Chiral CE offers a cost-efficient, resource-saving and very versatile possibility to separate enantiomers from each other. Many parameters of the CE can have an influence on the separation, which makes method development very demanding. After a preliminary analysis, screening, and optimization of the method by means of statistical design of experiments, a robust, precise, and efficient method was validated according to ICH Q2(R1) guideline [13]. The optimized method achieved a good resolution, which met

the requirements of the PhEur. Additionally, the enantiomeric purity of ketamine can be determined excellently with this method. The lowest quantifiable amount of *S*-ketamine in *R*-ketamine was 0.45%. Even though that CE is a very good instrumental method to separate enantiomers effectively, it finds only little acceptance in the PhEur. As of today, the enantiomeric purity of only ropivacaine hydrochloride and galantamine hydrochloride are tested with CE in the PhEur, while 51 more monographed drugs are testing for enantiomeric purity with liquid chromatography [14, 15]. Furthermore, it was shown that design of experiments is excellently suited to develop fast, robust, and efficient methods for the quality control of API and drug products and is a good, cost-efficient alternative to chiral liquid chromatography when testing for enantiomeric purity.

Heating of an aqueous solution of ketamine to 85 °C led to the occurrence of a yellowish discoloration after five hours. Since this discoloration was not attributable to any known impurity of ketamine, various batches of ketamine were subjected to stability tests and comprehensive analysis using XRPD and LC-HRMS. Using the GUCS approach, an impurity profile was created [16]. However, no impurity or degradation product of ketamine could be detected implicating the stability of ketamine under the stress conditions used. Since the occurrence of the yellow discoloration was difficult to reproduce, a further risk analysis of possible influencing factors, as it is done within QbD, was performed. Stability test with different water qualities were carried out with the result that the higher the water quality, the less yellow discoloration appeared. Water quality is usually referred to microbiological stability in stability issues and not as a direct influence on possible degradation. Fu et al. already showed that a different ion content or total amount of organic compounds can have an influence on degradation of NSAID by UV/Vis-spectroscopy in combination with persulfate [17]. It is possible, that if degradation follows an equilibrium reaction, the influence of water quality may determine whether and to what extent degradation occurs. Water quality should therefore be monitored in stability studies, not only in microbiological contamination, but also in stress testing.

References

[1] Volpp, M. and U. Holzgrabe, Determination of plasma protein binding for sympathomimetic drugs by means of ultrafiltration. Eur. J. Phar. Sci., 2019. 127: p. 175-184.

[2] Claridge, T.D., High-resolution NMR techniques in organic chemistry. Vol. 27. 2016: Elsevier

[3] Schmidt, S., M. Zehe, and U. Holzgrabe, Characterization of binding properties of ephedrine derivatives to human alpha-1-acid glycoprotein. Eur. J. Phar. Sci., 2023. 181: p. 106333.

[4] Walle, U., T. Walle, S. Bai, and L. Olanoff, Stereoselective binding of propranolol to human plasma, α1‐acid glycoprotein, and albumin. Clin. Pharmacol. Ther., 1983. 34(6): p. 718-723.

[5] Shen, Q., L. Wang, H. Zhou, H.-d. Jiang, L.-s. Yu, and S. Zeng, Stereoselective binding of chiral drugs to plasma proteins. Acta Pharmacol Sin, 2013. 34(8): p. 998-1006.

[6] Teo, S.K., W.A. Colburn, W.G. Tracewell, K.A. Kook, D.I. Stirling, M.S. Jaworsky, M.A. Scheffler, S.D. Thomas, and O.L. Laskin, Clinical pharmacokinetics of thalidomide. Clin. Pharmacokinet., 2004. 43: p. 311-327.

[7] Martínez‐Gómez, M.A., R.M. Villanueva‐Camañas, S. Sagrado, and M.J. Medina‐Hernández, Evaluation of enantioselective binding of basic drugs to plasma by ACE. Electrophoresis, 2007. 28(17): p. 3056-3063.

[8] Maddi, S., M.R. Yamsani, A. Seeling, and G.K. Scriba, Stereoselective plasma protein binding of amlodipine. Chirality, 2010. 22(2): p. 262-266.

[9] Ohara, T., A. Shibukawa, and T. Nakagawa, Capillary electrophoresis/frontal analysis for microanalysis of enantioselective protein binding of a basic drug. Anal. Chem., 1995. 67(19): p. 3520-3525.

[10] Fernandez, C., F. Gimenez, A. Thuillier, and R. Farinotti, Stereoselective binding of zopiclone to human plasma proteins. Chirality, 1999. 11(2): p. 129-132.

[11] Becker, B.A. and C.K. Larive, Probing the binding of propranolol enantiomers to α1-acid glycoprotein with ligand-detected NMR experiments. J. Phys. Chem. B, 2008. 112(43): p. 13581-13587.

[12] Cui, Y., G. Bai, C. Li, C. Ye, and M. Liu, Analysis of competitive binding of ligands to human serum albumin using NMR relaxation measurements. J Pharm Biomed Anal, 2004. 34(2): p. 247-254.

[13] Roge, A., P. Tarte, M. Kumare, G. Shendarkar, and S. Vadvalkar, Forced Degradation Study: An Important Tool in Drug Development. AJRC, 2014. 7(1): p. 8.

[14] Maier, N.M., P. Franco, and W. Lindner, Separation of enantiomers: needs, challenges, perspectives. J. Chromatogr. A, 2001. 906(1-2): p. 3-33.

[15] ICH, Guideline Q2(R1), validation of analytical procedures: text and methodology International conference on harmonisation of technical requirements for registration of pharmaceuticals for human use, 2005.

[16] EDQM, Monograph ropivacaine hydrochloride. 2023, European Pharmacopeia Online 11.0, Council of Europe, Straßbourg, France

[17] EDQM, Monograph galantamine hydrobromide. 2023, European Pharmacopeia Online 11.0, Council of Europe, Straßbourg, France

[18] Wohlfart, J., Analysis of Drug Impurities by Means of Chromatographic Methods: Targeted and Untargeted Approaches. 2022, Universität Würzburg.

[19] Fu, Y., X. Gao, J. Geng, S. Li, G. Wu, and H. Ren, Degradation of three nonsteroidal anti-inflammatory drugs by UV/persulfate: degradation mechanisms, efficiency in effluents disposal. Chemical Engineering Journal, 2019. 356: p. 1032-1041.

[17] Fu, Y., X. Gao, J. Geng, S. Li, G. Wu, and H. Ren, Degradation of three nonsteroidal anti-inflammatory drugs by UV/persulfate: degradation mechanisms, efficiency in effluents disposal. Chemical Engineering Journal, 2019. 356: p. 1032-1041.

5. SUMMARY

The aim of this work was to investigate older, established drugs. The extent of the protein binding of chiral ephedra alkaloids to AGP and of ketamine to albumin was determined. Since enantiomers of these drugs are individual available, the focus was on possible enantioselective binding and structural moieties involved in the binding.

Previously published work suggested that ephedrine and pseudoephedrine can bind stereoselectively to proteins other than albumin in serum. For the determination of the extent of protein binding, the established ultrafiltration with subsequent chiral CE analysis was used. To determine the influence of basicity on binding, the drugs methylephedrine and norephedrine were also analyzed. Drug binding to AGP increased with increasing basicity as follows: norephedrine < methylephedrine < ephedrine < pseudoephedrine. pK_{aff} was determined both graphically using the Klotz plot and mathematical indicating a low affinity of the ephedra alkaloids to AGP. Using STD-NMR spectroscopy experiments the aromatic protons and the C-C**H**$_3$ side chain were shown to be most strongly involved in binding, which could be confirmed by molecular docking experiments in more detail. For all drugs, van der Waals-, π-π -, cationic interactions, hydrogen bonds, and a formation of a salt bridge were observed. The individual enantiomers showed no significant differences and thus the binding of ephedra alkaloids to AGP is not significant.

In contrast to the ephedra alkaloids, the possible enantioselective binding to albumin was investigated for *R*- and *S*-ketamine. Again, ultrafiltration followed by CE analysis was performed. The binding of ketamine to one main binding site could be identified. A non-linear fit was used for the determination of pK_{aff}. Using the NMR methods STD-NMR, waterLOGSY-NMR, and CPMG-NMRspectroscopy: the aromatic protons as well as the protons of the NC**H**$_3$ methyl group showed the largest signal intensity changes, while the cyclohexanone protons showed the smallest changes. pK_{aff} was also determined by the change in the chemical shift at different drug-protein ratios. These obtained values confirm the values obtained from ultrafiltration. Based on this, ketamine is classified as a low-affinity ligand to albumin. There were no significant differences between the individual enantiomers and thus the binding of ketamine to albumin is not a stereoselective process.

Using statistical design of experiments an efficient chiral CE method for determining the extent of protein binding of *R*-and *S*-ketamine to albumin was developed and validated according to ICH Q2 (R1) guideline.

The stability of ketamine was also investigated because a yellowish discoloration of an aqueous solution of ketamine developed under heat. XRPD investigations showed the

same crystal structure for all batches examined. An untargeted screening using LC-HRMS as well as LC-UV measurements showed no degradation of ketamine or the presence of impurities in stress and non-stressed ketamine solutions, confirming the stability of ketamine under the stress conditions investigated. The lower the quality of the water used in the stress tests, the more intense the yellow discoloration occurred. The impurity or the mechanism that causes the yellow discoloration could not be identified.

6. ZUSAMMENFASSUNG

Ziel dieser Arbeit war es ältere, etablierte Arzneistoffe zu untersuchen. Das Ausmaß der Proteinbindung von chiralen Ephedra-Alkaloiden an AGP und von Ketamin an Albumin wurde bestimmt. Da Enantiomere dieser Wirkstoffe individuell verfügbar sind, lag der Fokus auf möglichen enantioselektiven Bindungen und strukturellen Funktionalitäten, die an der Bindung beteiligt sind.

Zuvor veröffentlichte Arbeiten deuteten darauf hin, dass Ephedrin und Pseudoephedrin stereoselektiv an andere Proteine als Albumin im Serum binden können. Zur Bestimmung des Ausmaßes der Proteinbindung wurde die etablierte Ultrafiltration mit anschließender chiraler CE-Analyse eingesetzt. Um den Einfluss der Basizität auf die Bindung zu bestimmen, wurden auch die Wirkstoffe Methylephedrin und Norephedrin analysiert. Die Bindung des Wirkstoffs an AGP nahm mit zunehmender Basizität wie folgt zu: Norephedrin < Methylephedrin < Ephedrin < Pseudoephedrin. pK_{aff} wurde sowohl grafisch mit Hilfe des Klotz-Plots als auch mathematisch bestimmt, was auf eine geringe Affinität der Ephedra-Alkaloide zu AGP hinweist. Mittels STD-NMR Spektroskopie Experimenten konnte gezeigt werden, dass die aromatischen Protonen und die C-C**H**$_3$-Seitenkette am stärksten an der Bindung beteiligt sind, was durch molekulare Docking-Experimente detailliert bestätigt werden konnte. Für alle Wirkstoffe wurden van-der-Waals-, π-π-, kationische Wechselwirkungen, Wasserstoffbrückenbindungen und die Bildung einer Salzbrücke beobachtet. Die einzelnen Enantiomere zeigten keine signifikanten Unterschiede, so dass die Bindung von Ephedra-Alkaloiden an AGP nicht signifikant ist.

Im Gegensatz zu den Ephedra-Alkaloiden wurde die mögliche enantioselektive Bindung an Albumin für *R*- und *S*-Ketamin untersucht. Auch hier wurde eine Ultrafiltration mit anschließender CE-Analyse durchgeführt. Die Bindung von Ketamin an eine Hauptbindungsstelle konnte identifiziert werden. Für die Bestimmung von pK_{aff} wurde eine nichtlineare Anpassung verwendet. Mit den NMR-Methoden STD-NMR, waterLOGSY-NMR und CPMG-NMR Spektroskopie zeigten sowohl die aromatischen Protonen als auch die Protonen der NC**H**$_3$-Methylgruppe die größten Änderungen der Signalintensität, während die Cyclohexanon-Protonen die geringsten Änderungen afuwiesen. pK_{aff} wurde auch durch die Änderung der chemischen Verschiebung bei verschiedenen Wirkstoff-Protein-Verhältnissen bestimmt. Die Werte bestätigen die durch die Ultrafiltration erhaltenen Werte. Auf dieser Grundlage wird Ketamin als Ligand mit niedriger Affinität zu Albumin eingestuft. Es zeigten sich keine signifikanten Unterschiede

zwischen den einzelnen Enantiomeren und somit ist die Bindung von Ketamin an Albumin kein stereoselektiver Prozess.

Mit Hilfe der statistischen Versuchsplanung wurde eine effiziente chirale CE-Methode zur Bestimmung des Ausmaßes der Proteinbindung von *R*- und *S*-Ketamin an Albumin entwickelt und gemäß der ICH Q2 (R1) Richtlinie validiert.

Die Stabilität von Ketamin wurde ebenfalls untersucht, da sich unter Hitze eine gelbliche Verfärbung einer wässrigen Ketaminlösung entwickelte. XRPD-Untersuchungen zeigten für alle untersuchten Chargen die gleiche Kristallstruktur. Ein nicht zielgerichtetes Screening mittels LC-HRMS sowie LC-UV-Messungen zeigte keinen Abbau von Ketamin oder das Vorhandensein von Verunreinigungen in Stress- und nicht gestressten Ketaminlösungen, was die Stabilität von Ketamin unter den untersuchten Bedingungen bestätigt. Je schlechter die Qualität des in den Stresstests verwendeten Wassers war, desto intensiver trat die Gelbverfärbung auf. Die Verunreinigung oder der Mechanismus, der die gelbe Verfärbung verursacht, konnte nicht identifiziert werden.

7. APPENDIX

7.1. List of publications

Research papers

Schmidt, S., Zehe, M., & Holzgrabe, U. (2023). Characterization of binding properties of ephedrine derivatives to human alpha-1-acid glycoprotein. European Journal of Pharmaceutical Sciences, 181, 106333

Schmidt, S., & Holzgrabe, U. (2023). Method Development, Optimization, and Validation of the Separation of Ketamine Enantiomers by Capillary Electrophoresis Using Design of Experiments. Chromatographia, 86(1), 87-95.

Schmidt, S., & Holzgrabe, U. Do the enantiomers of ketamine bind enantioselective to human serum albumin? Manuscript submitted for publication.

7.2. Documentation of authorship

In this section, the individual contribution for each author to the publications reprinted in this thesis is specified. Unpublished manuscripts are handled accordingly.

Julius-Maximilians-
UNIVERSITÄT
WÜRZBURG

Fakultät für
CHEMIE UND
PHARMAZIE

Erklärung zur Autorenschaft

A closer look at long-established drugs: enantioselective protein binding and stability studies

Characterization of binding properties of ephedrine derivatives to human alpha-1-acid glycoprotein
Sebastian Schmidt, Markus Zehe, Ulrike Holzgrabe
European Journal of Pharmaceutical Sciences, 181, 106333.

Sebastian Schmidt (SeS), Markus Zehe (MZ), Ulrike Holzgrabe (UH)

Autor	SeS	MZ	UH	∑ in Prozent
Studiendesign	5		5	10
Experimentelle Arbeit: UF, CE, NMR	20			20
Experimentelle Arbeit: Docking		5		5
Datenanalyse und Interpretation	20	5	5	30
Verfassen der Veröffentlichung	17.5	2.5		20
Korrektur der Veröffentlichung		2.5	7.5	10
Koordination der Veröffentlichung			5	5
Summe	62.5	15	22.5	100

Erklärung zur Autorenschaft

A closer look at long-established drugs: enantioselective protein binding and stability studies

Characterization of binding properties of ephedrine derivatives to human alpha-1-acid glycoprotein

Sebastian Schmidt, Markus Zehe, Ulrike Holzgrabe

European Journal of Pharmaceutical Sciences, 181, 106333.

Die Mitautoren der in dieser (teil-)kumulativen Dissertation verwendeten Manuskripte sind sowohl über die Nutzung als auch über die angegebenen Eigenanteile informiert und stimmen dem zu.

Sebastian Schmidt	Markus Zehe	Ulrike Holzgrabe
Hauptautor/in	**Koautor/in**	**Korrespondenzautor/in**
☒ Verweis: E-Mail hinterlegt	☒ Verweis: E-Mail hinterlegt	☒ Verweis: E-Mail hinterlegt

Würzburg,29.09.2023 _____

Prof. Dr. Ulrike Holzgrabe

Julius-Maximilians-
UNIVERSITÄT
WÜRZBURG

Fakultät für
CHEMIE UND
PHARMAZIE

Erklärung zur Autorenschaft

A closer look at long-established drugs: enantioselective protein binding and stability studies

Method Development, Optimization, and Validation of the Separation of Ketamine Enantiomers by Capillary Electrophoresis Using Design of Experiments
Sebastian Schmidt, Ulrike Holzgrabe
Chromatographia, 86(1), 87-95.

Sebastian Schmidt (SeS), Ulrike Holzgrabe (UH)			
Autor	**SeS**	**UH**	**∑ in Prozent**
Studiendesign	10	2.5	12.5
Experimentelle Arbeit	30		30
Datenanalyse und Interpretation	20	2.5	22.5
Verfassen der Veröffentlichung	15		15
Korrektur der Veröffentlichung		12.5	12.5
Koordination der Veröffentlichung		7.5	7.5
Summe	75.0	25.0	100

Erklärung zur Autorenschaft

A closer look at long-established drugs: enantioselective protein binding and stability studies

Method Development, Optimization, and Validation of the Separation of Ketamine Enantiomers by Capillary Electrophoresis Using Design of Experiments

Sebastian Schmidt, Ulrike Holzgrabe

Chromatographia, 86(1), 87-95.

Die Mitautoren der in dieser (teil-)kumulativen Dissertation verwendeten Manuskripte sind sowohl über die Nutzung als auch über die angegebenen Eigenanteile informiert und stimmen dem zu.

Sebastian Schmidt	Ulrike Holzgrabe
Hauptautor/in	**Korrespondenzautor/in**
☒ Verweis: E-Mail hinterlegt	☒ Verweis: E-Mail hinterlegt

Würzburg, 29.09.2023 _____

Prof. Dr. Ulrike Holzgrabe

Julius-Maximilians-
UNIVERSITÄT
WÜRZBURG

Fakultät für
CHEMIE UND
PHARMAZIE

Erklärung zur Autorenschaft

A closer look at long-established drugs: enantioselective protein binding and stability studies

Do the enantiomers of ketamine bind enantioselective to human serum albumin?
Sebastian Schmidt, Ulrike Holzgrabe
Manuscript submitted for publication.

Sebastian Schmidt (SeS), Ulrike Holzgrabe (UH)			
Autor	**SeS**	**UH**	**∑ in Prozent**
Studiendesign	5	5	10
Experimentelle Arbeit	30		30
Datenanalyse und Interpretation	20	10	30
Verfassen der Veröffentlichung	20		20
Korrektur der Veröffentlichung		5	5
Koordination der Veröffentlichung		5	5
Summe	75	25	100

Erklärung zur Autorenschaft

A closer look at long-established drugs: enantioselective protein binding and stability studies

Do the enantiomers of ketamine bind enantioselective to human serum albumin?

Sebastian Schmidt, Ulrike Holzgrabe

Manuscript submitted for publication.

Die Mitautoren der in dieser (teil-)kumulativen Dissertation verwendeten Manuskripte sind sowohl über die Nutzung als auch über die angegebenen Eigenanteile informiert und stimmen dem zu.

Sebastian Schmidt	Ulrike Holzgrabe
Hauptautor/in	**Korrespondenzautor/in**
☒ Verweis: E-Mail hinterlegt	☒ Verweis: E-Mail hinterlegt

Würzburg,29.09.2023 _____

Prof. Dr. Ulrike Holzgrabe

Julius-Maximilians-
UNIVERSITÄT
WÜRZBURG

Fakultät für
CHEMIE UND
PHARMAZIE

Erklärung zur Autorenschaft

A closer look at long-established drugs: enantioselective protein binding and stability studies

Stability assessment: ketamine?
Sebastian Schmidt, Ulrike Holzgrabe
Unpublished manuscript.

Sebastian Schmidt (SeS), Ulrike Holzgrabe (UH)			
Autor	**SeS**	**UH**	**∑ in Prozent**
Studiendesign	5	5	10
Experimentelle Arbeit	30		30
Datenanalyse und Interpretation	20	15	35
Verfassen des Manuskripts	15		15
Korrektur der Veröffentlichung		10	10
Summe	70	30	100

Erklärung zur Autorenschaft

A closer look at long-established drugs: enantioselective protein binding and stability studies

Stability assessment: ketamine

Sebastian Schmidt, Ulrike Holzgrabe

Unpublished manuscript

Die Mitautoren der in dieser (teil-)kumulativen Dissertation verwendeten Manuskripte sind sowohl über die Nutzung als auch über die angegebenen Eigenanteile informiert und stimmen dem zu.

Sebastian Schmidt	Ulrike Holzgrabe
Hauptautor/in	**Korrespondenzautor/in**
☒ Verweis: E-Mail hinterlegt	☒ Verweis: E-Mail hinterlegt

Würzburg,29.09.2023 _____

Prof. Dr. Ulrike Holzgrabe